AN ACCEPTANCE TEST FOR CHIP SEAL PROJECTS BASED ON IMAGE ANALYSIS

By

Ugurcan Ozdemir

A THESIS

Submitted to
Michigan State University
in partial fulfillment of the requirements
for the degree of

Civil Engineering – Master of Science

2016

ABSTRACT

AN ACCEPTANCE TEST FOR CHIP SEAL PROJECTS BASED ON IMAGE ANALYSIS

By

Ugurcan Ozdemir

Chip seal is one of the most popular preventive maintenance techniques performed by many DOTs, county road departments and cities. One of the most important parameters affecting performance of a chip seal is the percent aggregate embedment depth into the binder. Depending on the percent embedment of aggregates in chip seals, they may be susceptible to distresses such as aggregate chip loss and bleeding. In this study, a standard test procedure was developed to directly calculate aggregate embedment depth via digital image processing techniques. Two image-based algorithms were developed to calculate embedment depth, and another algorithm was developed to compute the percentage of the aggregate surface coverage area with binder. The statistical analysis results indicated that there is a good correlation between embedment depth obtained from image-based algorithms and sand patch test results. Analyses of chip seal samples collected from limited number of 'good-performing' field chip seal sections revealed that the aggregate percent embedment ranged from 50% to 70%, which is the typical desired range to minimize bleeding and chip loss. However, more research is needed to investigate the 'poor-performing' field sections. Various laboratory chip seal samples were also prepared to investigate the variation of percent embedment in chip seals made with the minimum and maximum binder and aggregate application rates specified in MDOT's special provisions. The results revealed that the average percent embedment ranged from 55% to 70%.

To My Family

ACKNOWLEDGEMENTS

I would like to express my deepest gratitude to my advisor Dr. M. Emin Kutay for his continuous support, guidance, and encouragement and friendship throughout my research study at Michigan State University. I would not have gotten this far without his priceless advices and suggestions. I am also thankful to the Department of Civil and Environmental Engineering at the Michigan State University for providing all the resources needed for me to complete my M.S. study.

I also would like to thank my committee members, Dr. Karim Chatti and Dr. Neeraj Buch for their participation and valuable comments. Dr. Syed Waqar Haider is also greatly acknowledged for his valuable opinions about asphalt chip seal performance.

This research was co-funded by Michigan Department of Transportation and the Center for Highway Pavement Preservation (CHPP), which is a Tier-1 University Transportation Center (UTC) funded by U.S. Department of Transportation. These supports are greatly acknowledged.

I am thankful to my colleagues, Salih Kocak, Sudhir Varma, Sepehr Soleimani and Derek Hibner for their endless support, motivation and friendliness. I also would like to thank my dear friends from Turkey, Kadri, Osman and Yezdan for their friendly conversations and their support during the research study. I am very grateful to my friends, Bihter Zeytuncu and Semra Cavus for their support and sincere talk.

This study is dedicated to my dear family, my father Nazim Ozdemir, my mother Melek Ozdemir, my brother Yavuz Ozdemir. I would like to thank to them for supporting me morally throughout my life.

DISCLAIMER

"This publication is disseminated in the interest of information exchange. The Michigan Department of Transportation (hereinafter referred to as MDOT) expressly disclaims any liability, of any kind, or for any reason, that might otherwise arise out of any use of this publication or the information or data provided in the publication. MDOT further disclaims any responsibility for typographical errors or accuracy of the information provided or contained within this information. MDOT makes no warranties or representations whatsoever regarding the quality, content, completeness, suitability, adequacy, sequence, accuracy or timeliness of the information and data provided, or that the contents represent standards, specifications, or regulations."

TABLE OF CONTENTS

LIST OF TABLES

LIST OF FIGURES

CHAPTER 1

INTRODUCTION

1.1 Background

Chip seal is one of the most popular preventive maintenance technique performed by many DOTs, county road departments and cities. The procedure involves binder application (asphalt emulsions, or sometimes cutback asphalt) on the surface a deteriorated pavement, followed by spreading aggregates such that one-stone-height is achieved. After spreading, aggregates are compacted. After curing of the emulsion, the loose aggregates are removed by sweeping via rotary power brooms. The primary role of the asphalt binder in the chip seal application is to provide a waterproof membrane that protects the pavement surface from sun, oxidation and moisture infiltration (Wood et al., 2006). Aggregates act as a 'bridge' and provide sufficient skid resistance.

Asphalt chip seal is preferably constructed at lower traffic volumes since structural capacity of asphalt chip seals is very low compared to typical pavements (HMA or concrete pavements). Therefore, while existing pavement underlying the asphalt chip seal provides structural capacity, chip seal seals fine cracks and deteriorations, prevents moisture infiltration and enhances skid resistance. Therefore, asphalt chip seal is not a good maintenance option for heavily distressed roads.

Embedment depth is one of the most important parameters related to the quality of chip seals. Embedment depth is defined as the average height of the binder divided by the average height of the aggregate as shown in Figure 1.1. Asphalt chip seal applications can achieve their

service lives if proper embedment and aggregate orientation are provided. There are several

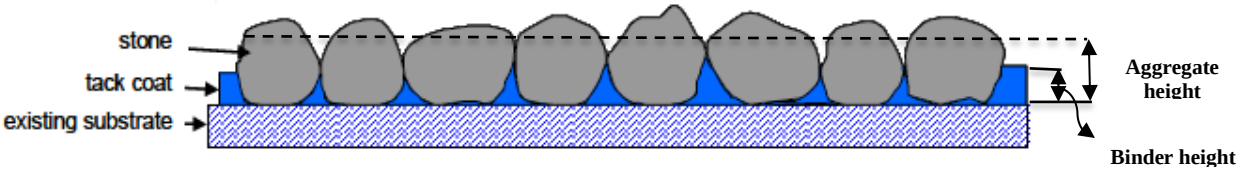

Figure 1.1: Asphalt chip seal

opinions about selecting desired embedment depth right after the construction; however, all design methods have agreed that design criteria of embedment depth should be between 50% and 70% after construction (Gransberg and James, 2005).

McLeod et al. (1969) pointed out the relationship between embedment depth and chip seal aggregate loss and bleeding. Asphalt chip seals having the embedment depth less than 50% are more susceptible to aggregate loss due to insufficient bonding between binder and aggregate; whereas, asphalt chip seals having the aggregate embedment higher than 70% may cause bleeding problems on the surface of the pavement. Therefore, it is very important to achieve desired aggregate embedment into the binder.

Determination of the embedment depth is typically achieved by pulling the aggregates out from the chip seal binder and visually examining the aggregate embedment depth into the binder. This method is difficult to implement and subjective, especially when angular and flat/elongated aggregates are used. Another method suggested by NCHRP Report 680 (2011) is spreading a certain volume of glass beads over the chip seal surface, followed by measurement of its diameter. The aggregate size and texture height calculated from volume of glass beads are used to estimate embedment depth.

Current ways for obtaining embedment depth are so subjective and contains assumptions during calculation; therefore, there is a need for a way to directly calculate aggregate embedment depth into the binder. Obtaining embedment depth via image processing techniques can be reliable and objective method, as compared to current methods.

1.2 Objectives

The main objective of the research study is to develop a standard test procedure to directly calculate aggregate embedment depth into the asphalt binder in a chip seal project via digital image analysis.

1.3 Research Plan

1.3.1 Task 1: Sample Preparation and Image Acquisition

One of the significant tasks of this study was to develop a practical procedure to prepare chip seal samples for image acquisition and to investigate the most appropriate imaging approach before image analysis. For this purpose, the following tasks have been undertaken:

- Chip seal core samples were taken from the field with the help from Michigan DOT crew.
- Chip seal core samples were fabricated with a new methodology in the laboratory based on the concept of NCHRP 680 (2011) recommendation.
- Desired chip seal cross sections were obtained for imaging.
- Different imaging and lighting conditions were investigated and the best method was used to take digital images of the chip seal cross sections.

1.3.2 Task 2: Development of Image Processing Algorithms

The scope of this task included development of image-based algorithms to directly measure percent embedment depth (ED) of chip seal samples. In addition to percent embedment depth, other concepts such as percent of aggregate surface coverage (ASC) by the binder, were studied and image-based algorithms were developed. This task consisted of the following major parts:

- Two different image processing algorithms were developed to calculate percent embedment depth (ED).
- One algorithm was developed to obtain percent of aggregate surface coverage (ASC) by the binder.
- Verification of the algorithms was performed by using idealized images which have particular embedment depth (ED) and aggregate surface coverage (ASC) by the binder.

1.3.3 Task 3: Laboratory Testing & Validation of Algorithms & Data Analysis

As part of this task, the algorithms were validated through laboratory tests, Also, the effect of binder application rate on the chip seal performance was investigated through both laboratory testing and image-based algorithms. This task included the following components:

- Both sand patch test and laser texture scans were conducted on field cores.
- Sand patch test was performed on laboratory-fabricated samples.
- Image analyses were completed on laboratory-fabricated samples and field cores.

- Statistical analysis of embedment depths obtained from image-based algorithms, sand patch test, laser texture scan, and the effect of binder application rate on the chip seal performance were performed.

1.4 Outline

This thesis is arranged as follows: Chapter 2 consists of a literature review of asphalt chip seal design and analysis, including embedment depth concept, chip seal design procedures and their relations with embedment depth and performance tests conducted on chip seals both in the laboratory and in the field. A description of the procedures developed in this study to obtain field cores and to fabricate chip seal samples in the laboratory are described in Chapter 3. Chapter 4 includes descriptions of the sample preparation techniques for image acquisition and the algorithms for calculation of percent embedment depth (ED) and aggregate surface coverage (ASC) by the binder. In Chapter 5, details of the traditional laboratory tests such as the sand patch test, laser scanning and sweep test are given. Chapter 6 includes the results and discussion of the analyses of the field and the laboratory samples. Finally, Chapter 7 includes the major conclusions from this study.

CHAPTER 2

LITERATURE REVIEW

2.1 Asphalt Chip Seal Surface Treatment and Embedment Depth

Asphalt chip seal was first constructed as a main pavement for low volume roads in 1920s. With time, chip seal applications evolved to be used for preservation techniques on deteriorated hot mix asphalt pavements, primarily because of low initial costs (Gransberg and James, 2005). Main primary purposes of asphalt chip seal surface treatments can be summarized as follows: (1) to prevent from existing surface from water and air infiltration by sealing small surface cracks on the surface, (2) to improve surface texture and skid resistance, (3) to reduce oxidation of existing pavement due to temperature and air, and (4) to provide anti-glare surface when the pavement is wet. NCHRP synthesis 342 (Gransberg and James, 2005) defined seven different types of chip seal applications: (i) single chip seal, (ii) double chip seal, (iii) racked-in seal, (iv) cape seal, (v) inverted seal, (vi) sandwich seal, and (vii) geotextile-reinforced seal. However, the focus of this master thesis is only the single chip seal, which consists of a single layer binder application followed by one stone thick aggregate application to provide protective surface wearing. The single chip seal diagram is illustrated in Figure 2.1.

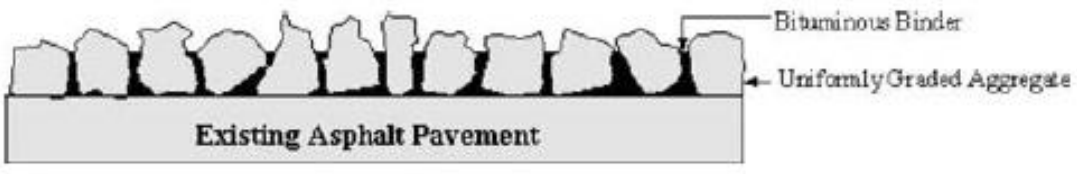

Figure 2.1: Single chip seal diagram (source: Gransberg and James, 2005)

Depth of aggregate embedment into the binder plays an important role to determine whether asphalt chip seal is properly constructed or not. There are two main distresses that occur in chip seal applications: (i) aggregate chip loss and (ii) bleeding. Aggregate chip loss is simply debonding of aggregates from the binder due to the effect of sweeping or traffic. Bleeding on the other hand refers to the condition where almost entire aggregates submerge into the. Embedment depth is a parameter that is related to both of these distresses.

In addition to binder and aggregate application rate, embedment depth depends on several parameters including aggregate size and shape, emulsion type, hardness of existing pavement, rolling patterns and numbers and traffic. (Schuler et al., 2011).

2.2 Design Procedures

Chip seal designs have been based typically on either past experience or certain engineering concepts. Due to the continuous change of material characteristics, construction equipment, climate and most importantly the changes of the existing surface condition in different regions, contractors have generally designed chip seals based on experiences in the field (Gransberg and James, 2005). However, there are also engineering concepts used to design chip seals, which are described in the following subsections.

2.2.1 Hanson Method

First attempt to develop a design procedure for asphalt chip seals was made by F.M Hanson (1935). He stated that voids between the aggregates after spreading over the pavement, rolling and traffic condition becomes nearly 50%, 30% and 20%, respectively (see Figure 2.2). He also stated that after opening to traffic, due to aggregate shapes, aggregates tend to be lying

on their flattest side and therefore, average least dimension (ALD) is nearly equal to the average thickness of the aggregates after the construction.

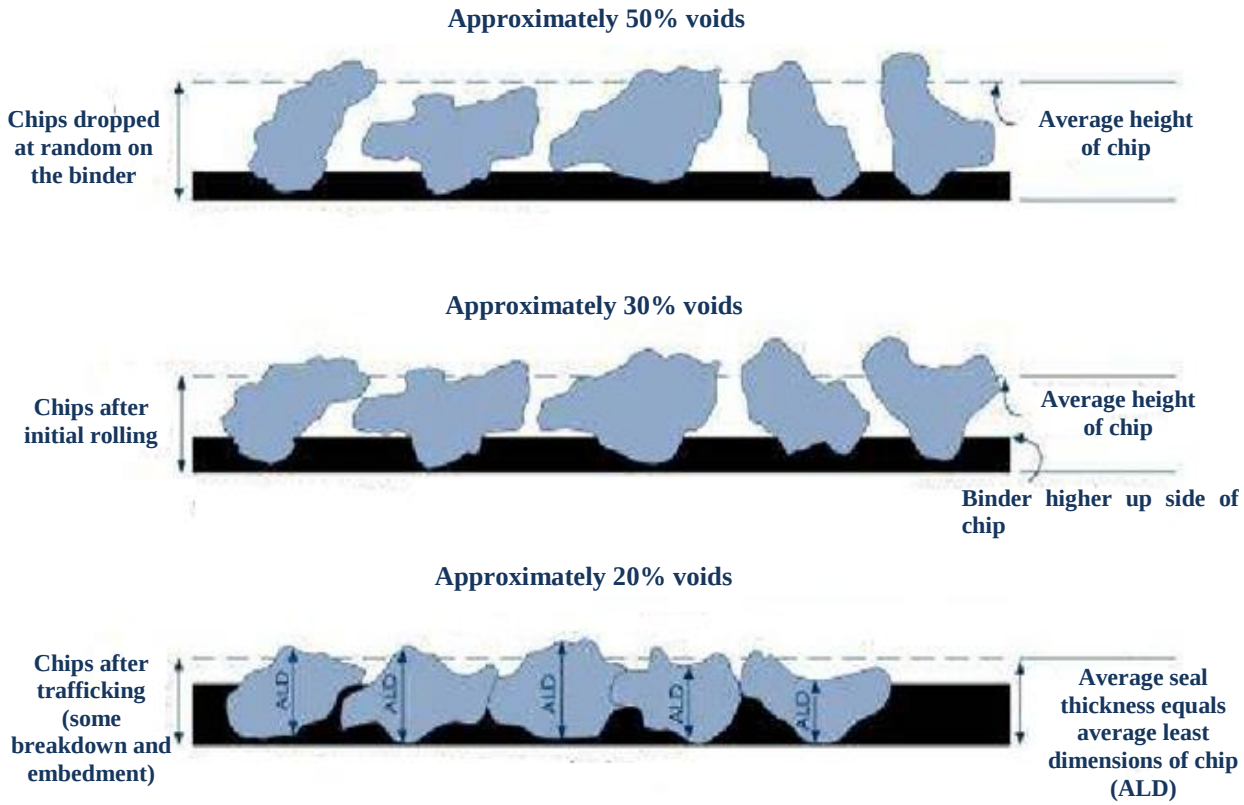

Figure 2.2: States of chip seal embedment (source: New Zealand Road Division, 1968)

Hanson focused on the void percentage in his design method. He did not include embedment depth criteria; however, he pointed out that void area between aggregates should be filled with 60% to 75% residual binder which actually means 60% to 75% embedment depth.

2.2.2 Kearby Method

Kearby (1953) was the first engineer to develop asphalt chip seal design method with respect to determining material application rates. He developed a nomograph, which uses average size of aggregates, percent embedment depth and voids percentage between aggregates

as inputs to obtain asphalt cement rate (in gallons per square yard). One of the drawbacks of Kearby design method is that void percentage and percentage embedment depth range is limited; and also aggregate size range varies between 1/8" and 1". Another drawback according to Kearby (1953) is that traffic effect and aggregate toughness are not included in the nomograph.

2.2.3 McLeod Design Method

After Hanson's work (1935) on asphalt chip seal, N. McLeod created a new design procedure for chip seal based on Hanson's study. McLeod's goal was to find aggregate and binder application rates which should be applied at the construction (McLeod, 1969).

Aggregate size (gradation), shape and specific gravity play a significant role in calculation of aggregate application rate. However, for binder application rate, there are different types of parameters needed to be considered, including aggregate gradation and shape, traffic condition, residual percent of asphalt binder, binder leakage through existing pavement surface condition and binder absorption by aggregates.

McLeod used Hanson's theory and accepted that inter-particle voids in loose condition is about 50%, after rolling and trafficking, it becomes nearly 30% and 20%, respectively. Voids between aggregates after certain volume of traffic is 20% which means that cover aggregates take place 80% of seal application.

Embedment depth is not a direct input for both the binder and aggregate application rate calculation. However, it is actually hidden in the traffic correction during binder application rate calculation. In other words, traffic factor, which depends upon the anticipated traffic volume, is adjusted so that percent embedment depth after trafficking gives 70%.

2.2.4 Modified Kearby Method

First attempt for modification of Kearby Method was Epps et al. study (1974). They tried to change Kearby design monograph so that synthetic aggregates having high porosity can be used in the design. Then, in a different research activity, Epps et al. (1981) tried to adjust Kearby design method so that the design was consistent with field performances. Holmgreen et al. (1985) studied the performance of chip seal sections designed according to Kearby method by using data collected from previous two studies and they found that calculated asphalt application rate was not sufficient to hold aggregates.

Aggregate application rate for modified Kearby method is calculated by using the measurement of a new laboratory test method "Board Test" which is used for finding aggregate quantity in one-thick stone position over one square yard. This test finds aggregate quantity in lb/yd^2 by dividing the weight of aggregate to the aggregate application area (half square yard is generally used). The asphalt rate was modified by adding traffic and existing pavement surface condition. The other modification was shifting the curve in relationship between average mat depth and percentage of embedment (Epps and Gallaway, 1974).

Percent embedment depth can be obtained by using average mat thickness; in other words, average aggregate height. At the same time, percent embedment depth can be chosen manually without suggestion of the method according to average mat depth. In the design, it was suggested that 30±10% and 70±10% embedment depth should be achieved just after the construction and after two years of service, respectively.

2.2.5 Road Note 39 (Sixth Edition)

The design procedure Road Note 39 was developed by The United Kingdom's Transport Research Laboratory in the United Kingdom (Roberts and Nicholls 2008). This design procedure was developed by designing different kinds of systems based on different parameters simulating different conditions and traffics on the pavement (Colwill et al. 1995). The design steps can be put in order as following: selection of dressing type (such as single chip seal, double chip seal etc.); selection of binder and aggregate type, determination of binder and aggregate rate.

Traffic level, existing pavement hardness and size of aggregates are primary inputs for determining binder application rate. Aggregate type and shape, existing surface condition, climate, geometry of pavement and speed of traffic are secondary inputs used for determining binder application rate. On the other hand, aggregate application rate determined by BS EN 12272-1, aggregate shape, size and relative density have role.

In Road Note 39 (Sixth Edition), although embedment depth is mentioned while stating the effect of some parameters such as the road stiffness and climate on the embedment depth, there is no direct specification of embedment depth.

2.2.6 Austroads Design Method

The Austroads method (Sprayed Seal Design Project Group 2001) considers many factors during calculation of binder and aggregate application rate. This design procedure is also selected by the NCHRP 680 report as a recommended design method for chip seal applications in the U.S.

Austroads method is based on certain assumptions on aggregate, traffic and embedment consideration (Schuler et al. 2011). Aggregates are assumed to be one stone layer thick with a flakiness index between 15% and 25%. This design procedure is valid for less than 10% heavy traffic and about 2 years after construction, percent embedment depth is assumed to range from 50% to 60%.

In this design method, basic binder application rate is calculated by percentage of void between aggregates filled with asphalt (VFA), void content between aggregates (VMA), traffic volume and type. In addition to basic binder application rate, design binder application rate is calculated by adding other modifications depending on texture of existing surface, aggregate embedment into existing surface (substrate), binder absorption into substrate and aggregate. The aggregate application rate is determined by considering traffic level, aggregate size and shape and loose unit weight. In Austroads design method, aggregate rate is only calculated in unit of square meter per cubic meter (m^2/m^3) whereas NCHRP 680 also derived aggregate application rate in unit of pound per square yard (lb/yd^2) depending traffic level and loose unit weight.

2.2.7 South African Method, TRH3

South African design method was developed for designing different kind of sealing types such as single and double chip seal (with either conventional or modified binder), cape seal, slurry seal and sand seal. South African designs for different seal types are mostly based on Hanson's design concept, where asphalt binder fills the voids between aggregates and average least dimension determines these voids (The South African National Roads Agency 2007). One of the assumptions this design method made is that, in order to prevent from aggregate loss,

approximately 42% of voids between aggregates which is equivalent about 30% of height should be filled by the binder.

There are two different binder rates described in South African design method; cold and hot binder application rates. Hot binder application rate is the net binder application rate used in construction; whereas, the cold binder application rate is the application rate before subtracting extra part such as water in the emulsions before evaporation. Residual binder application rate is referred to as the net cold binder rate. Aggregate size in terms of average least dimension, traffic level, road stiffness measured by ball penetration test and desired texture at the end are necessary input parameters in order to calculate cold binder application rate. Climate, existing surface condition determined by sand patch test, road geometry in terms of slope are secondary inputs for adjusting cold binder application rate. At the end, hot binder application rate used in construction is calculated by multiplication of net cold binder rate and conversion factor depending on binder type. The aggregate spread rate is obtained by design chart in which average least dimension, flakiness index and type of chip seal information are taken as input.

2.2.8 Discussion of Chip Sealing Design Methods

The factors affecting both aggregate and binder application rate for each chip seal design method is summarized in Table 2.1:

Table 2.1: Parameters for chip seal design methods

DESIGN METHODS	FACTORS	Voids between aggregates	Aggregate Size and Shape	Aggregate Dry Unit Weight	Percent Embedment Depth	Traffic Level	Residual Binder Content	Existing Pavement Cond.	Absorption of Aggregate	Existing Pavement Hardness	Climate	Geometry of Road
Hanson		✓										
Kearby		✓	✓		✓							
McLeod		✓	✓	✓	✓	✓	✓	✓	✓			
Modified Kearby			✓	✓	✓	✓		✓				
Road Note 39			✓	✓		✓		✓		✓	✓	✓
Austroads		✓	✓	✓		✓	✓	✓	✓	✓		✓
South African, TRH3			✓	✓		✓	✓	✓		✓	✓	✓

Although embedment depth criteria is not a direct input in design equations at these chip seal design methods, all design methods mention that embedment depth is one of the most significant criteria that should be achieved at a certain level. Also, all design methods propose certain percent embedment depth just after construction and some years of service.

2.3 Seal Surfacing Performance Tests

Chip seal applications experience two main distresses: aggregate chip loss and bleeding/flushing. Embedment depth is one of the main parameters that affect chip seal's susceptibility to bleeding and aggregate chip loss. Therefore, all design methods mentioned earlier suggests specific percent embedment depths at different time periods after construction. Another concept that has a direct relationship with embedment depth is texture depth (macro

texture) of the chip seal. Texture depth (macro texture) of the sealing treatments is the main indicator of performance (Abdul-Malak et al. 1993 and Roque et al. 1991) since this parameter is related to the embedment depth.

Typically, as embedment depth decreases, the probability of losing aggregate chips increases. However, at a given embedment depth, two different chip seal applications may exhibit different performance. For instance, embedment depth can be similar for two different type of binders, with polymer modified binder and plain binder, however aggregate loss of chip seal prepared with polymer modified binder may be less than the aggregate loss of chip seal prepared with plain binder. Therefore, aggregate mass loss and embedment depth should be studied together to assess performance of chip seal.

In this subsection, two different test procedures recommended by NCHRP 680 (2011) is examined. These methods are "Standard Method of Test for Embedment Depth of Chip Seal Aggregates in the Lab and the Field" and "Recommended Standard Method of Test for Laboratory Chip Loss from Emulsified Asphalt Chip Seal Samples" based on ASTM D7000. The former method is for calculating embedment depth; whereas, the latter method is for finding percentage aggregate mass loss. In addition to these test methods, a summary of few other methods for assessing performance of chip seal asphalts in both laboratory and field is provided. Also, this subsection includes that several image analysis techniques that have been developed to examine performance in terms of aggregate chip loss and bleeding. Lastly, numerical studies such as finite element analysis are discussed.

2.3.1 Embedment Depth Calculation Using NCHRP 680 Procedure

NCHRP Report 680 (2011) recommends two procedures that are applicable to both field and laboratory studies. These two approaches estimate embedment depth via spreading and submerging procedures. For both of them, the goal is to find texture height, and then the aggregate embedment is calculated by subtracting available texture height from average aggregate height.

For spreading procedure, a known volume of glass beads is poured onto chip seal sample in a way that all voids are filled by glass beads. It is assumed that the cross section is similar to the idealized cross section shown in Figure 2.3. Average height of the aggregate particles (H) is equal to texture height of glass beads (T) plus the height of binder (E) (Schuler et al., 2011). Texture height (T) is calculated as dividing volume of beads and aggregate above the asphalt surface by plan area of beads and aggregate. Since the average height of the aggregate (H) is known from the size of the agregate chips, height of the binder (E) is obtained subtracting texture height (T) from the average particle height. Percent embedment depth is calculated by using the following formulas:

$$E = H - T \quad [2.1]$$

$$PE\ (\%) = \frac{E}{H}\ x\ 100 \quad [2.2]$$

where E = embedment depth, H = height of aggregate particles and T = texture height of glass beads, PE = percent embedment depth

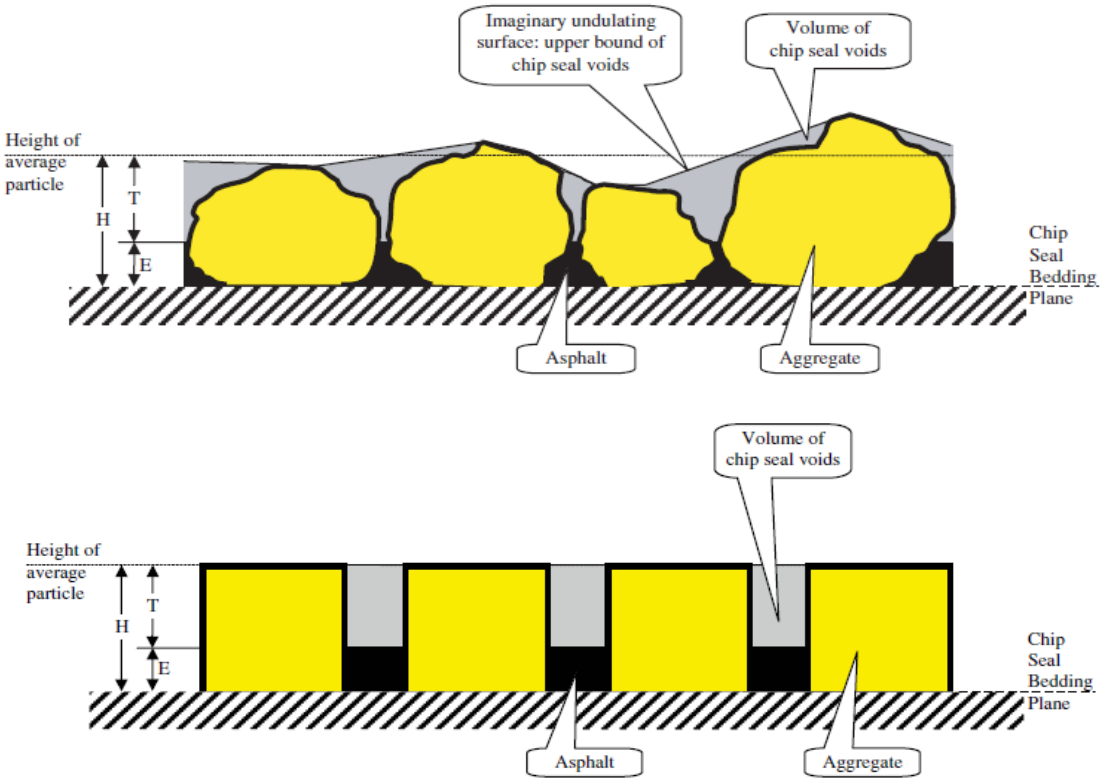

Figure 2.3: Normal and equivalent chip seal (Spreading method) (source: Schuler et al., 2011)

For submerging procedure, chip seal sample surface is completely covered with variable volume of glass beads at the fixed height above average particle height as illustrated in Figure 2.4.

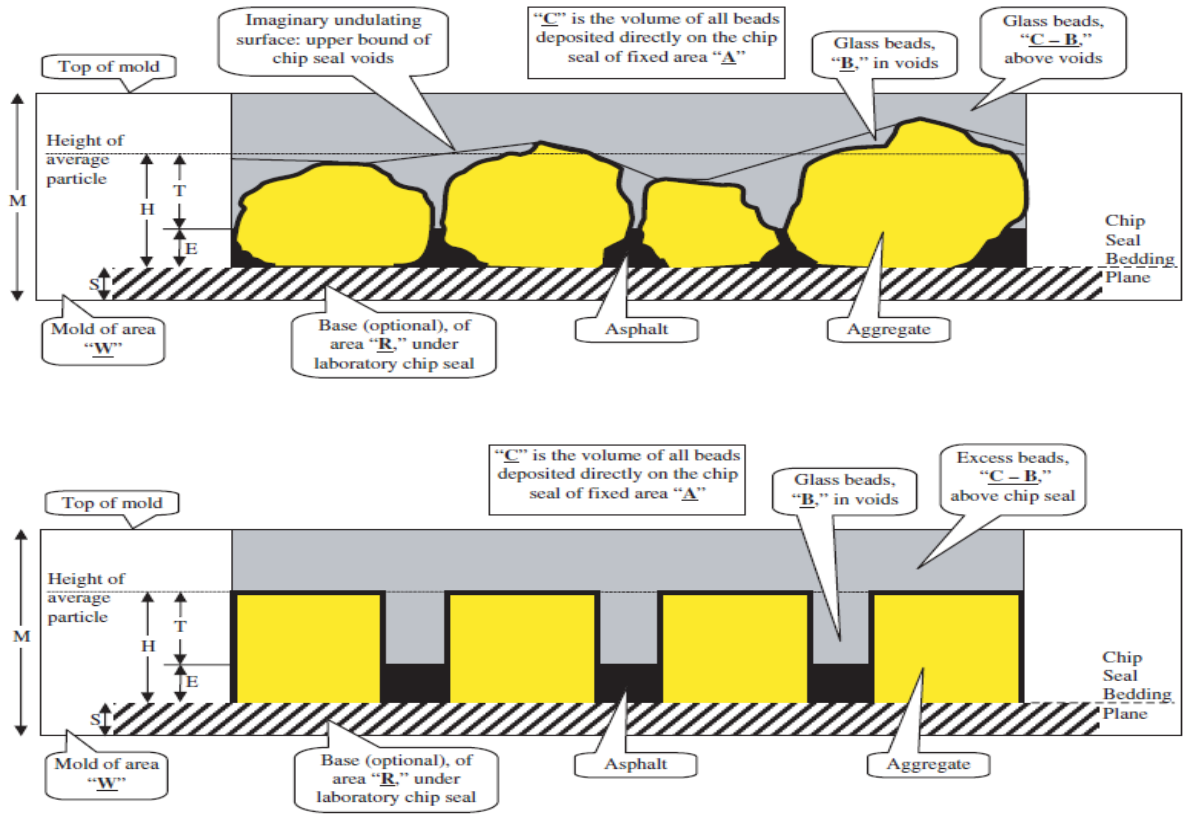

Figure 2.4: Normal and equivalent chip seal (Submerging method) (source: Schuler et al., 2011)

In the submerging procedure, it is important to subtract the excess volume of glass beads on the chip seal surface from the total glass beads volume for calculating texture height (T). Volume of glass beads filled only voids (B) is estimated by subtracting volume of excess glass beads on the chip seal surface from total volume of glass beads (C). Texture height is then calculated by dividing volume of glass beads filled only voids (B) by plan area of the beads using Equation 2.3. After calculation of texture height, percent embedment depth is estimated by using formulas 2.1 and 2.2.

$$B = C - [(M - S - H)\ x\ A\ ]\ and\ T = {}^{B}/_{A} \qquad [2.3]$$

where B = volume of glass beads only in the voids, C = total volume of glass beads, M = total height including excess volume of glass beads on the surface, S = base thickness, H = average particle height and A = plan area of the chip seal, T = texture height

Embedment depth estimation by using these methods (recommended by NCHRP Report 680) is easy and straightforward. However, aggregate embedment into the substrate is ignored. Also, substrate is considered to be perfectly straight and no binder leakage into the existing pavement is assumed.

2.3.2 Sweep Test of Bituminous Emulsion Surface Treatment Samples

The sweep test (ASTM D7000) is one of the laboratory test methods suggested by the NCHRP Report 680 (2011) for evaluation of the performance of asphalt chip seals in terms of aggregate loss. The components of the ASTM D7000 sweep test setup illustrated in Figure 2.5.

Figure 2.5: ASTM D7000 sweep test setup

Test procedure includes fabrication of asphalt chip seal samples, and testing by applying shear force to the surface of aggregates by using a nylon strip brush affixed to the mixer. Before and after testing, sample is weighted and percentage mass loss is calculated (ASTM D7000).

There is a controversial issue whether sweep test is a good indicator for assessing performance of chip seal in terms of development of bond between aggregate and asphalt bitumen. Wasiuddin et al. (2013) stated that performance evaluation of asphalt chip seal is better indicated by sweep test if the performance is investigated with respect to aggregate and binder type, aggregate gradation, moisture content of aggregates and pre-coating. However, Johannes et al. (2011) claimed that since inconsistent results were obtained after using different binder application rates, this test should not be used for a design tool. In addition, according to ASTM D7000, the goal of sweep test is to measure adhesive properties of the emulsion just after the construction, not to simulate traffic effect. In other words, this test method is designed to assess the curing characteristics of chip seals.

2.3.3 Other Test Methods

In addition to the two major methods recommended by NCHRP 680 (2011), there are several other methods exist. These test methods can be performed at laboratory, field or both. Performance criteria for asphalt chip seals vary according to test methods. Field and laboratory applicability as well as the properties measured by each test method are summarized in Table 2.2.

Table 2.2: Various other test methods used to evaluate asphalt chip seals

Test Methods	Applicability		Property measured
	Lab	Field	
Vialit Adhesion Test	x		% mass loss
Frosted Marble Test	x		% mass loss
Australian Aggregate Pull-out Test		x	Necessary pull-out force
Pennsylvania Aggregate Retention Test	x		% mass loss
British Pendulum Test	x	x	British Pendulum Number (BPN)
Locked Wheel Skid Test		x	Skid Number (SN)
Third Scale Model Mobile Loading Simulator (MMLS3)	x		% mass loss
Pneumatic Adhesion Tension Test	x		Pull-off adhesion strength achieved at failure

Vialit Adhesion Test

The Vialit Adhesion Test was first introduced in France to measure the effect of binder and aggregate type on performance. It consists of three components: metal base with the vertical rod, steel ball and metal test plates.

Jordan III et al. (2011) studied applicability of the Vialit test on surface seal treatments with respect to performance. In addition to the usual tray, they came up with a modified tray by changing the material to hot rolled steel from metal and modifying the surface texture (non-textured to textured) and changing the tray thickness. The authors concluded that results from the Vialit test are always questionable and it is not sufficient to make conclusions regarding performance of seal treatments. However, performance results based on only freezing time and freeze thaw with using modified tray were distinguishable. Another study from Epps et al. (2001) also suggested that results from the Vialit test are so inconsistent that they cannot differentiate between good and poor performance of the seal treatments.

Frosted Marble Test

Frosted marble test (FMT) was first introduced by Benedict (1990). FMT is aimed to look at binder adhesion by applying torque to marbles fixed with the binder. FMT setup is illustrated in the Figure 2.6. Test setup consists of torque wrench, hooked foot for applying shear and tray on which binder is spread and marbles are placed, respectively.

Howard et al. (2009) made a modification to the FMT setup by including temperature control using an environmental chamber. They also modified the curing procedure. Howard et al. (2009) stated that, even though the results from the FMT seem to be valuable for evaluating performance of binder adhesion and curing, it is not enough by itself and other test methods should be used to make comprehensive evaluation. Also, they concluded that the testing variability is another issue of the FMT, primarily because of the hooked foot position and marble positions on the tray of the test.

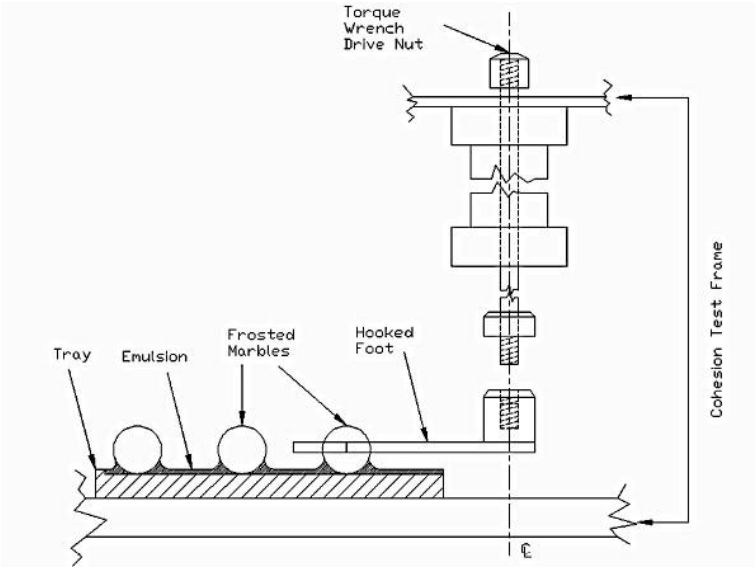

Figure 2.6: Frosted marble test setup (source: Howard et al. 2009)

Australian Aggregate Pull-out Test

This test method was developed for finding necessary pull-out force to separate aggregates from the asphalt bitumen material in seal surface treatments. After seal surface treatment is prepared, embedded aggregates are fixed by a crocodile clip and 20 g/sec pull-out rate is applied to the stone until it is detached and during this procedure, load measurements are taken continuously (Queensland Department of Transport and Main Roads 2012).

One of the uses of this test method is to determine the duration of traffic control after construction. In addition, coated average area of the binder on the aggregate can be observed visually to correlate with the peak tensile stress needed to pull out the aggregate. (Senadheera et al. 2006).

Pennsylvania Aggregate Retention Test

Pennsylvania aggregate retention test (PART) (illustrated in Figure 2.7) was first developed by National Center for Asphalt Technology Auburn University (Kandhal and Motter 1991). The test simulates the effect of traffic on the seal surface treatments by using the 'Mary Ann Laboratory Sieve Shaker'. Surface seal treatment sample is prepared within the pan and after compression and curing process, initial aggregate loss is obtained by turning upside down. Then, the pan is placed in the sieve shaker upside down at an inclination of 45^{o}. After 5 minutes of shaking, aggregate loss is measured and calculated as a percentage.

Figure 2.7: Sample Fabrication and Mary Ann Sieve Shaker (source: Kandhal and Motter 1991)

British Pendulum Test

The British Pendulum Test (BPT) is one of the tools used for measuring surface frictional properties. The measurement values obtained from the British Pendulum Test are scaled as BPN (British Pendulum Number), which represents frictional properties by measuring the energy loss when rubber slider slips over the sample (ASTM E303-93, 2013). The British Pendulum Test is illustrated in the Figure 2.8.

Figure 2.8: British Pendulum Test

The primary advantage of BPT is its applicability to both field and laboratory testing. However, Lu et al. (2006) stated that since BPT is capable of applying low speed to the surface (6 mph), the test only can measure the skid resistance due to microtexture of the surface. Higher speed is required to obtain the effect of macrotexture. In addition to the speed problem, the ASTM standard (ASTM E 303-93) does not have any temperature correction. The British standard (BS 7976-2) includes temperature factors only up to 35^{o}C. Therefore, temperature factor for BPT is an issue for the places having warmer climate.

Third Scale Model Mobile Loading Simulator

The third scale model mobile loading simulator (MMLS3) is one of accelerated pavement testing devices for determining performance of different kinds of pavements by simulating traffic effect in a determined scale. Lee (2003) first introduced the MMLS3 to measure the hot mix asphalt (HMA) performance with respect to fatigue cracking and rutting.

This test machine consists of 4 bogies, 1 axle per bogie and 1 wheel/tire per axle (Bhattacharjee et al., 2004). Each wheel has a diameter of 80 mm and is capable of applying max 800 kPa pressure, and between 1.9 kN and 2.7 kN load. Since the MMLS3 has an environment chamber around itself, desired temperature can be sustained. The MMLS3 test setup is illustrated in Figure 2.9.

In addition to applicability of MMLS3 to HMA pavements, this test is also applicable to seal surface treatments. Lee (2007) came up with design modification for Hanson design method for asphalt seal surface treatments by stating reference voids content after MMLS3 tests for lightweight and granite aggregate type.

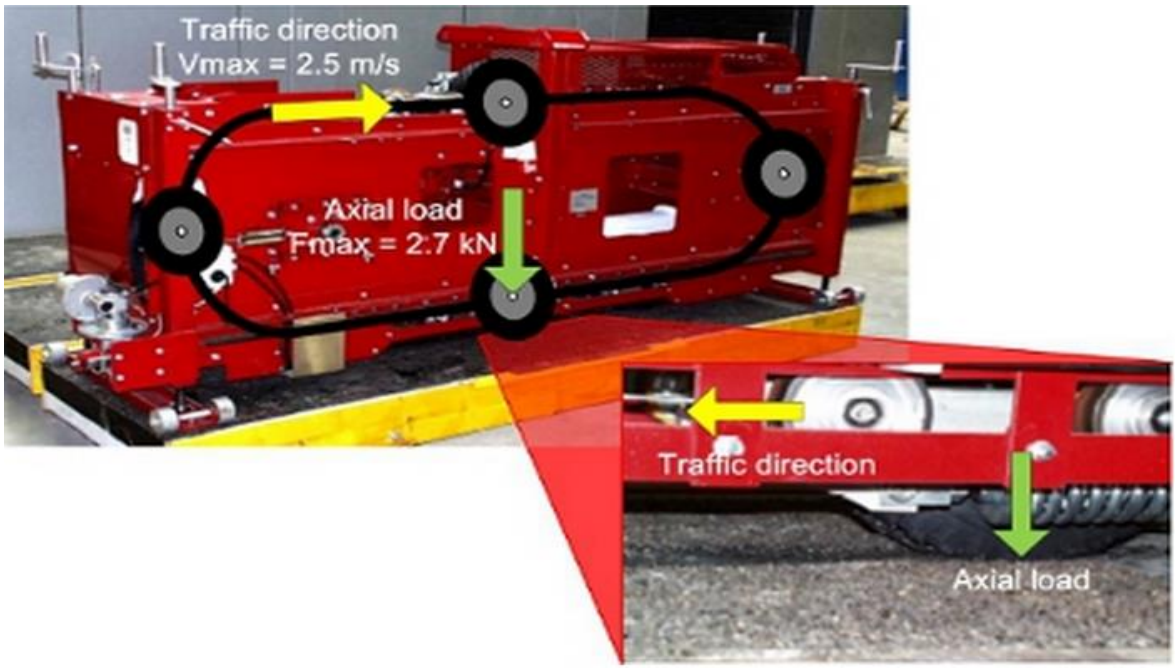

Figure 2.9: The Third Scale Model Mobile Load Simulator (MMLS3)

Pneumatic Adhesion Tension Test

Pneumatic adhesion tension testing instrument (PATTI) (illustrated in Figure 2.10) is used for evaluating bond strength of an asphalt binder by applying direct tension. Unlike the direct tensile bond test according to ASTM D7234 "Standard Test Method for Pull-Off Adhesion Strength of Coatings on Concrete Using Portable Pull-Off Adhesion Testers", same pulling rate can be applied to each test sample (Zhou et al. 2014).

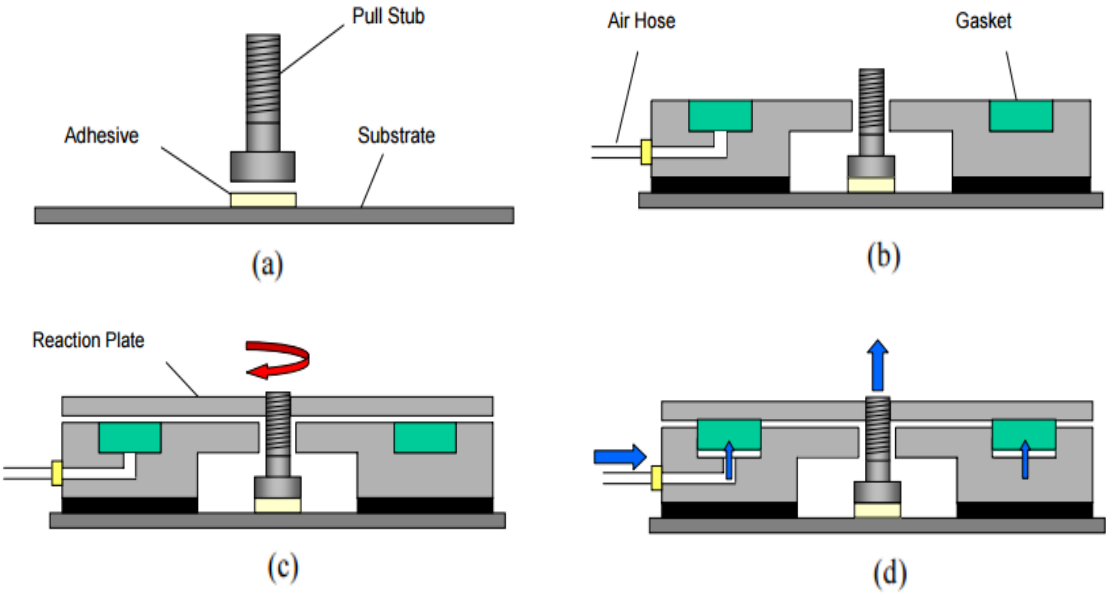

Figure 2.10: Pneumatic Adhesion Tensile Tester (source: Vickey 2007)

2.3.4 Image Processing Techniques for Performance Evaluation of Chip Seals

In literature, there are several studies regarding performance measurements by using image analysis techniques. Kim et al. (2008) used image analysis techniques to quantify texture differences in chip seals compacted using different rolling patterns. Chip seal cores were taken before and after the different rolling procedures, then cores were sliced and images were obtained by using a scanner. Macrotexture profiles were obtained by using MATLAB-based algorithms and the root mean square roughness of the chip seal profiles were estimated (ASME 2002). Then rolling effectiveness was investigated by looking roughness values derived from the chip seal profiles. One drawback of this method comes from the imaging technique. Kim et al. (2008) also stated that some of the aggregates seemed to be flying on the image since they

attached to surface at different place. Therefore, the algorithm was not always able to compute the profile accurately.

An extensive study was conducted by Kodippily (2013) to investigate the flushing mechanism of chip seals. In this study, the effect of volumetric and distribution of air voids in chip seal samples was studied via analysis of X-ray Computed Tomography (X-ray CT) images and flushing models were developed. This study showed that X-ray CT imaging is a viable option for determining internal structure of chip seal surfaces in a non-destructive way. However, X-ray CT is not a practical method of obtaining images because of its cost and expertise necessary for its operation.

Wielinski et al. (2011) selected three different sections on the road and pictures were taken at these sections over time. With the help of image processing techniques, they differentiated aggregates and binder from the chip seal texture picture at different time periods, and then aggregate retention of this specific section was calculated. The main drawback of this technique is that dust on the binder in the field caused some problems during differentiation of binder and aggregate during image processing.

In general, literature review regarding image processing techniques on asphalt chip seal is about getting texture properties, or air void within the chip seal samples. None of the methods were able to provide percent embedment directly.

2.3.5 Numerical Studies on Asphalt Chip Seals

First attempt for developing a numerical model in order to evaluate the performance of asphalt chip seal was made by Huurman et al. (2004). This study showed the applicability of

finite element methods on seal surface treatments. Due to some deficiencies of modeling and meshing of aggregate particles and representing base layer in prototype model, an improved model was established as shown in Figure 2.11 (Huurman 2010). In the prototype model, asphalt bitumen was placed between aggregates; whereas, mastic like (bitumen-rich) layer was defined below the aggreagtes due to embedment of aggregate into the existing pavement. In order to determine aggregate shape and size, a random number generator was used by using a multiplication factor for each node. Tire load was applied to each stone individually and vertical, lateral and longitudinal stress values were calculated by considering axle load and pressure, tire speed and distunguieshed shape functions proposed by Groenendijk (1998). Aggregate was assumed to be linear elastic, whereas the bitumen was assumed to follow the generalized Burger's viscoelastic model.

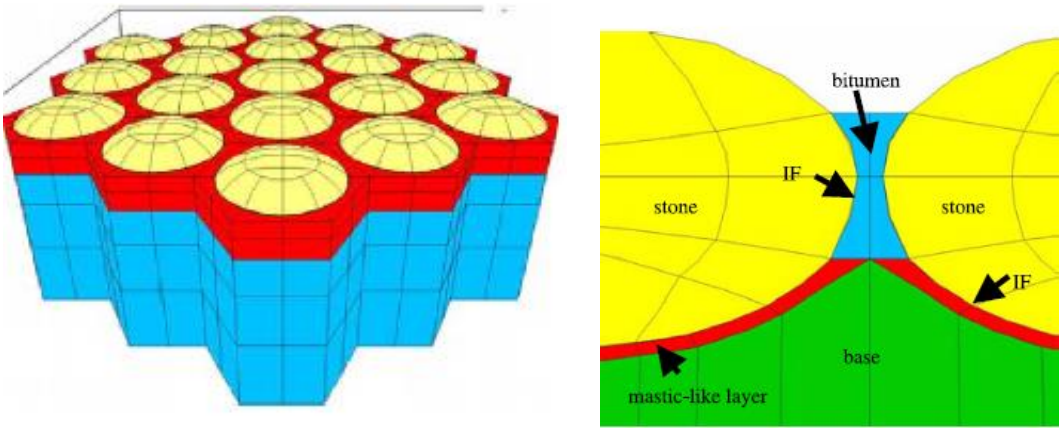

Figure 2.11: Chip seal finite element modeling (source: Huurman 2010)

Huurman's FEM study (Huurman 2010) included the evaluation of the performance of the chip seals by examining punching and aggregate rotation, fatigue cracking, low-temperature cracking, moisture damage and adhesion failure.

Henderson (2006) used real 2D chip seal slice images to develop a finite element model (FEM) to study the performance of chip seals. Due to limitations in computational time, aggregates were taken as rigid (instead of linearly elastic). Bitumen material behavior was modeled by using Prony series. Quadrilateral and triangular elements were used for aggregates and binder, respectively. Applied load was determined by study of de Beer (1994), which free rolling truck tire was simulated in the way that tire surface contacted all surface and rolled in or out of the page. The results with respect to stress and strain were determined. Two stress plots from this study is shown in Figure 2.12

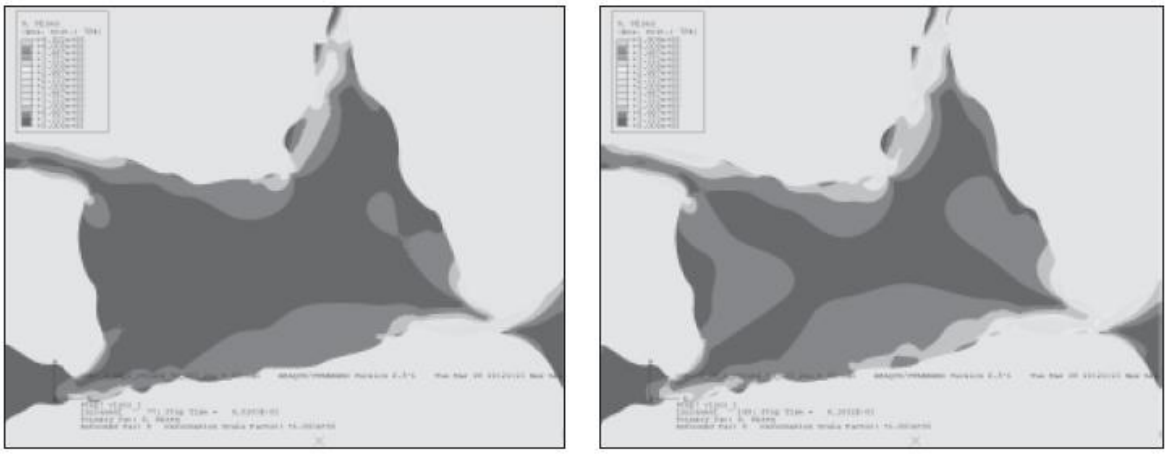

Figure 2.12: Stress distribution for chip seal modeling (source: Henderson 2006)

Although these studies give an insight into performance of chip seal surfaces under different conditions like using different size of cover aggregates and different type of binder, it is still so far away from giving actual results due to modeling chip seal in a perfect pattern. In other words, chip seal models in FEM analysis in current studies have been modeled in a perfect arrangement in terms of aggregate and binder position in the model. In that way, Henderson's study (2006) is much better to simulate actual chip seal performance by using slice images of the cores taken by the field. However, only 2D analysis of performance of chip seal was done.

2.4 Synthesis of Previous Work and Motivation for the Current Study

It can be concluded from the literature review that aggregate embedment depth into the binder plays a significant role for prevention of distresses (e.g., aggregate loss and bleeding) in chip seals. Most of the design methods mentioned in this Chapter recommended a desired percent embedment depth right after the construction and after certain traffic. However, all these recommendations were based on the observations and field experiences. There is no study that directly developed relationship between embedment depth and performance of the chip seals.

Methods such as the sand patch test (recommended by NCHRP Report 680) and texture scanning make certain assumptions while calculating the embedment depth. First, the existing pavement is assumed to be perfectly flat; therefore, pavement deteriorations on the surface are ignored. Aggregate embedment into the existing substrate is also neglected; however, aggregates do embed into the existing substrate in chip seal constructions when the existing pavement is relatively soft. In addition, binder seepage into existing substrate due to existing cracks on the surface is also ignored. These three assumptions have significant effects on the percent embedment depth; therefore, the current study focuses on developing a method of estimating embedment depth without making these assumptions.

The other test methods to measure the performance of chip seal applications are not related to the embedment depth. The target of these test methods is generally about adhesion properties of emulsion binder under different conditions. They do not include embedment depth concept as a performance criteria or one of the factors affecting the performance.

The work regarding image analysis techniques on chip seals done so far is not related to the embedment depth. Texture properties of the chip seals and air void existing in the chip seal were investigated through image processing techniques. Therefore, there is a need for developing image-based algorithms to directly estimate embedment depth of chip seals.

Numerical study of chip seals is relatively new topic. Modeling of chip seal in best way is still being investigated. Therefore, the effect of the embedment depth on performance is not studied in numerical studies on chip seals.

CHAPTER 3

CHIP SEAL SAMPLE ACQUISITION & FABRICATION

Chip seal samples used in this research project were either taken from the field or fabricated in the laboratory. Thirty (30) chip seal cores were taken from different chip seal sections of Michigan. In addition to field chip seal cores, forty (40) laboratory chip seal samples were fabricated.

3.1 Field Chip Seal Sample Acquisition

Chip seal samples initially were obtained by taking cores from the field. Thirty (30) chip seal cores were collected from 5 different sections in Michigan. The surface types of these chip seals were different. Chip seal cores collected from the field are summarized in Table 3.1.

Table 3.1: Summary of field chip seal cores

Section	Surface Types				Total
	Single Chip Seal	Double Chip Seal	Fog Sealed (Single Chip)	Fog Sealed (Double Chip)	
M-57 Near Clio	-	5	-	-	5
M-57 Near Pompeii	5	-	-	-	5
M-20	7	-	1	-	8
M-57 Near Carson City	4	-	-	-	4
M-33 From Alger to Rose City	-	-	8	-	8
Total	16	5	9	-	30

*Red: cannot be analyzed because of its nature - *Green: completed analyses

Among these 30 samples, twenty-one (21) single chip seal samples could be analyzed, because image analysis was not possible for the remaining 9 field chip seal (more details are given in Chapter 4). Chip seal samples from the M-57 Near Pompei, M-20 and M-33 from Alger to Rose city were sliced and their analyses were completed.

The aggregate and binder properties were not available for most of the sections. However, it can be assumed that contractors constructed the chip seal sections according to MDOT specifications for construction. Desired minimum aggregate physical requirements and emulsion chemical properties as well as application rate ranges are given in MDOT specifications in division 5 under chip seals section (2012). One of the most important parameters for aggregates affecting performance is size. According to MDOT specification (2012), 90 to 100% aggregates and 0 to 10% aggregates should pass through 3/8 inch sieve size and No.4 sieve size, respectively. Therefore, uniform one size aggregate gradation is targeted. The sizes of the aggregates were also verified using the image analysis procedure. Also, in MDOT's specification, the aggregate application range is from 20 to 24 lb/yd^2 (depending on the existing surface condition), and the binder application range is from 0.39 to 0.46 gal/yd^2.

3.1.1 Gradation of Aggregates from the Field

Contractors are responsible to use desired aggregate size for chip seal treatments based on MDOT chip seal specification (2012) in Michigan. The aggregates were collected only from the section on M-33 from Alger to Rose city. The size distribution of aggregates is shown in the Figure 3.1, which is based on the laboratory sieve analysis as well as the image processing techniques.

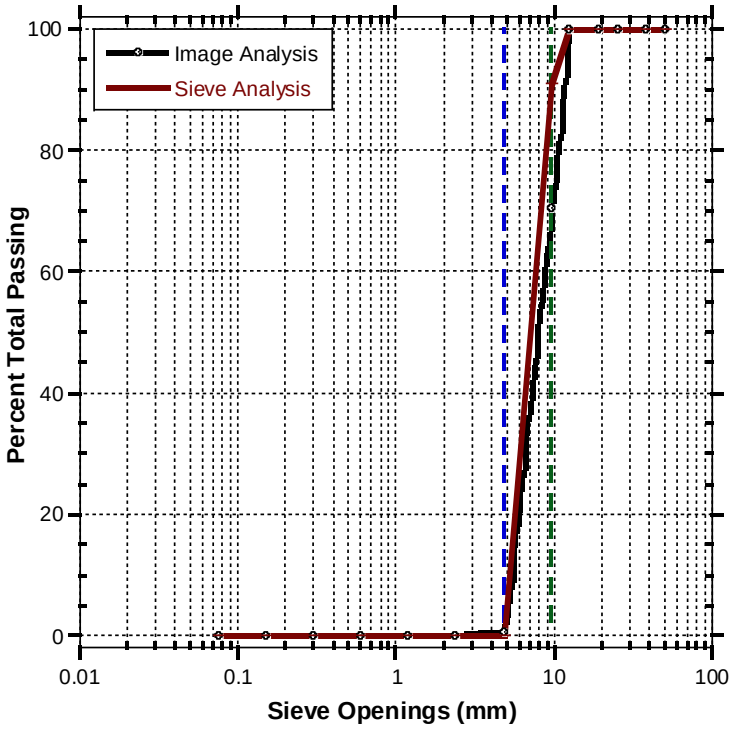

Figure 3.1: Gradation of the aggregates used in the field M-33 from Alger to Rose City

The size distribution for aggregates was determined using image-based algorithm developed by following the recommendations of Kumara et al. (2012). The 2-D images were used and areas of the particles were estimated with some assumptions. The gradation was obtained by using area of an ellipse, which is calculated by using the following formula:

$$A = \pi\, x \left(\frac{a}{2}\right) x \left(\frac{b}{2}\right) \qquad [3.1]$$

where A = area of the aggregate, a = the length of long axis, and b = the length of the intermediate axis.

From the 2-D images, a and b values were directly obtained from image-based algorithms. The percentage passing through a sieve was calculated by using the formula 3.2:

$$Percent\ Passing = \frac{\sum_i^p (A_i x b_i)}{\sum_i^n (A_i x b_i)}\ x\ 100\% \qquad [3.2]$$

where A = area of the aggregate, b = intermediate axis length p = number of aggregate passing through the grain size, and n = total number of particles

The procedure for computing gradation of aggregates by image-based algorithms is as follows:

- The aggregates are placed on the light table and pictures are taken by a document camera (see the Figure 3.2(a)).
- Aggregates are obtained separately (see the Figure 3.2(b)) and long and intermediate axis properties are taken from the algorithm. The resolution is calculated as mm/pixel.
- Area of each aggregate is calculated and percent passing through each grain size is obtained by using Equation 3.2.

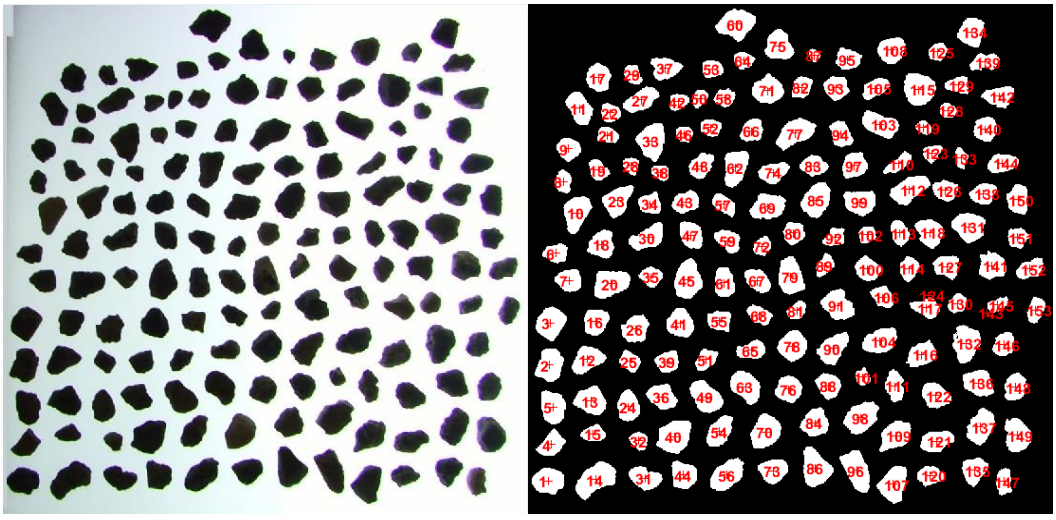

Figure 3.2: (a) Original image obtained from a document camera (b) Aggregate determination

3.1.2 Chip Seal Collection from the Field

Chip seal samples were collected with the help of MDOT crew. The field sections were selected by the MDOT crew and the care was made to select newly constructed chip seal sections. Before taking cores from the chip seal sections, MDOT crew performed both sand patch test and laser texture scanning to measure texture depth of corresponding section. Then, chip seal samples were taken by a coring machine. The procedure for collecting chip seal core samples from the field is illustrated in Figure 3.3.

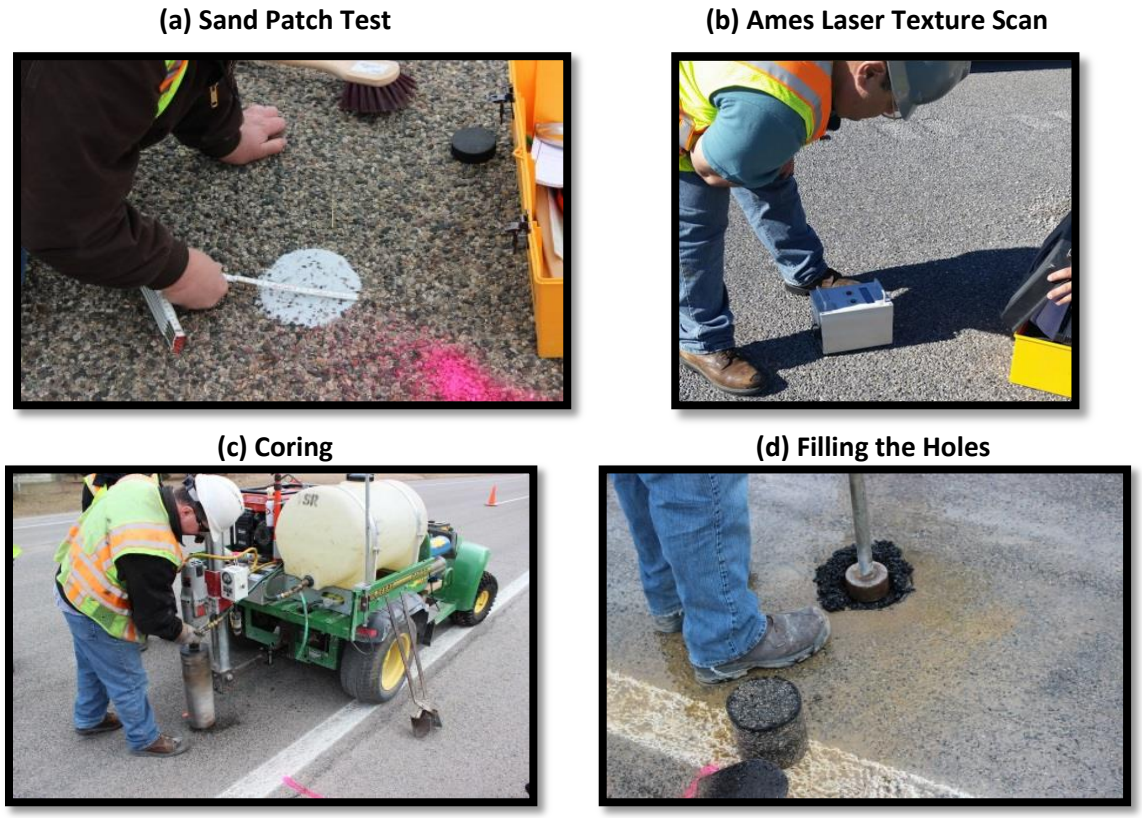

Figure 3.3: Procedure for taking cores from the field

3.2 Laboratory Chip Seal Sample Fabrication

In this section, the physical properties of aggregates, chemical properties of emulsion and procedure for fabricating chip seal samples in the laboratory are discussed. Total 40 laboratory samples were fabricated. These 40 samples can be divided into two groups:

- **Group 1:** This group included 8 chip seal samples. The goal was to investigate the effect of binder and aggregate application rate on percent embedment depth. For that purpose, 8 chip seal samples were fabricated by using the lowest and highest binder and aggregate application rates specified in the MDOT specification for construction (2012). Each set consisted of 2 replicates, and 4 different sets (8 samples) are summarized in Table 3.2:

Table 3.2: Summary of group 1 samples

Set No.	Binder App. Rate (gal/yd^2)	Aggregate App. Rate (lb/yd^2)
1	0.39	20
2	0.39	24
3	0.46	20
4	0.46	24

- **Group 2:** This group consisted of thirty-two (32) chip seal samples. The aim was to investigate the effect of sweep test on percent embedment and surface coverage area. Sixteen (16) sets of chip seal samples were prepared, and two replicates were prepared for each set (32 total chip seal samples were tested). Eight (8) sets were analyzed without performing sweep test, and remaining eight (8) of them were analyzed after sweep test was performed on

the samples. Both sets of chip seal samples were fabricated with the same binder and aggregate application rates shown in Table 3.3.

Table 3.3: Summary of group 2 samples

Sample No.	Binder App. Rate (gal/yd^2)	Agg. App. Rate (lb/yd^2)
1	0.39	20
2	0.40	20
3	0.41	20
4	0.42	20
5	0.43	20
6	0.44	20
7	0.45	20
8	0.46	20

3.2.1 Gradation of Aggregates and Sieve Analysis

The aggregates used for fabricating chip seal samples were selected according to MDOT Specification for Construction (2012). The size distributions of the aggregates obtained using laboratory sieve analysis and image based algorithms are shown in the Figure 3.4. As shown, uniformly graded aggregates were used to fabricate the chip seal samples. Two-dashed line represents 3/8 inch (9.75mm) and No.4 (4.75 mm) sieve size, from left to right respectively. It can clearly be seen that the aggregates satisfied the condition of 90 to 100% passing 3/8" sieve and 0 to 10% passing #4 sieve in accordance with the MDOT Specification for Construction (2012). In addition to the gradation, relatively round aggregates were used during chip seal fabrication.

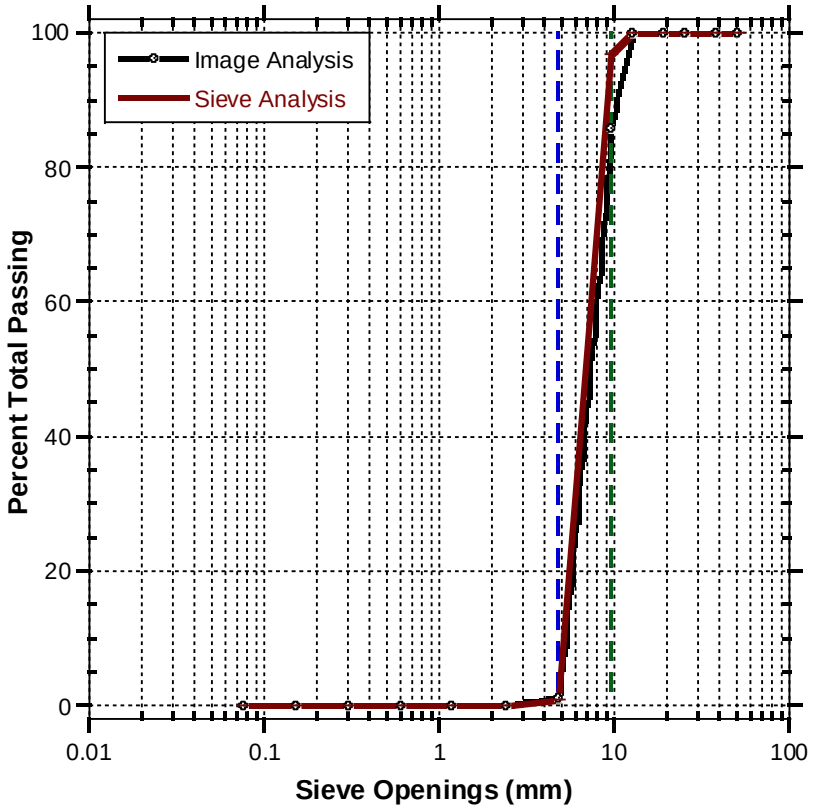

Figure 3.4: Gradation of the aggregates used in the laboratory

3.2.2 Emulsion Binder

Emulsion binder used for laboratory chip seal was obtained from Ergon Asphalt & Emulsions, Inc. Emulsion type was CRS-2, which is a cationic rapid setting type emulsified asphalt. Rapid setting emulsions are very conveniently used for chip seal constructions (NCHRP Report 680, 2011). Compositions on ingredients of emulsion are summarized in Table 3.4:

Table 3.4: Composition/ information on ingredients

Chemical Name	% in the Composition
Asphalt	50 - 70
Water	20 – 40
Hydrochloric Acid	< 1

3.2.3 Procedure for Chip Seal Sample Fabrication

Chip seal fabrication procedure can be divided into 3 steps: (i) binder application, (ii) aggregate application and (iii) compaction. Before preparing chip seal samples, hot mix asphalt samples with height of 40 mm were fabricated by gyratory compactor in order to simulate existing pavement condition.

Emulsion Binder Application

Emulsion binder on the hot mix asphalt surface was applied as follows: (1) required mass of emulsion binder mass was calculated by using the information of specific gravity for emulsion and surface area. (2) Emulsion binder was placed in the oven with 80^{o}F for an hour. (3) A tape was used to make a barrier around the HMA edge to prevent emulsion from spilling over the HMA sides (Figure 3.5a). (4) Desired emulsion binder mass poured onto the HMA surface and made the emulsion binder cover all surface by rotating sample (Figure 3.5b).

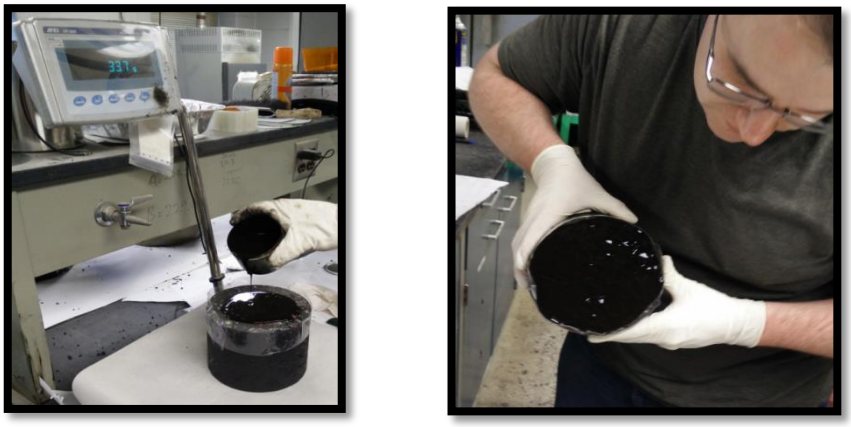

Figure 3.5: Binder application process: (a) pouring emulsion on the sample, and (b) spreading the binder by gravity & rotation

Aggregate Application

Aggregate application on HMA specimens was performed by using an aggregate spreader designed and manufactured in MSU's Advanced Asphalt Characterization Laboratory (AACL). The working principle of aggregate spreader based on the study of Howard et al. (2013). A sketch of the components of the aggregate spreader is shown in Figure 3.6.

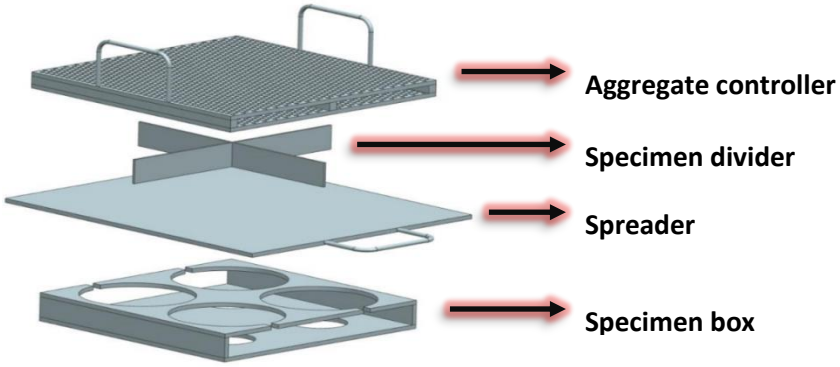

Figure 3.6: Sketch of the components of the aggregate spreader

Using the spreader, aggregate application on four HMA specimens can be performed at the same time and uniform aggregate spread can be sustained. Steps of aggregate spreading are summarized as follows: (1) cylindrical HMA mixtures are placed in the box of the aggregate spreader, (2) desired mass of aggregate (according to application rate) is placed on the spreader sheet, (3) aggregate controller, which consists of bolts for making aggregates one-thick size pattern and uniform, is placed on the top of the aggregate spreader, (4) spreader plate which holds the aggregates is pulled off to drop the aggregates on the HMA surface. This general procedure is illustrated in Figure 3.7.

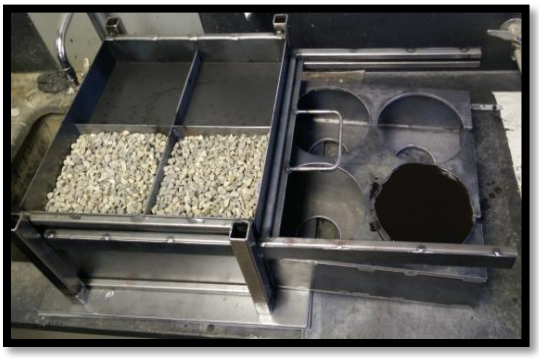

(1&2)

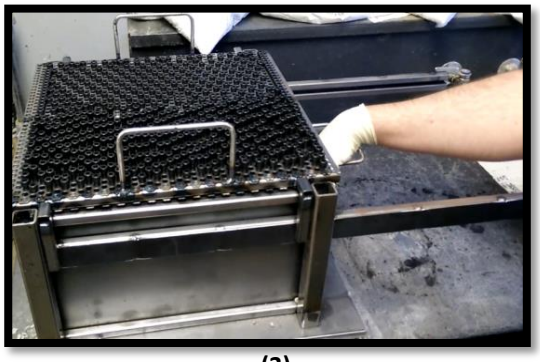

(3)

(4)

Figure 3.7: Procedure for using aggregate spreader

Compaction

Compaction of the chip seal was conducted by using both sweep test compactor and a material testing system (MTS). Also, a rubber sheet was placed on the top of the chip seal surface to simulate effect of rubber tire roller. In addition to the sweep test compactor, chip seal asphalt sample was compacted by MTS machine. About 600±18 kPa pressure (2383±70 pound-force for 6 inch diameter sample) was applied in stress controlled cyclic haversine mode at a frequency of 0.1 Hz for 25 cycles. The pressure was taken from the AASHTO T312 (2015), which is the procedure for preparing hot mix asphalt samples by gyratory compactor. Compaction procedure is illustrated in Figure 3.8.

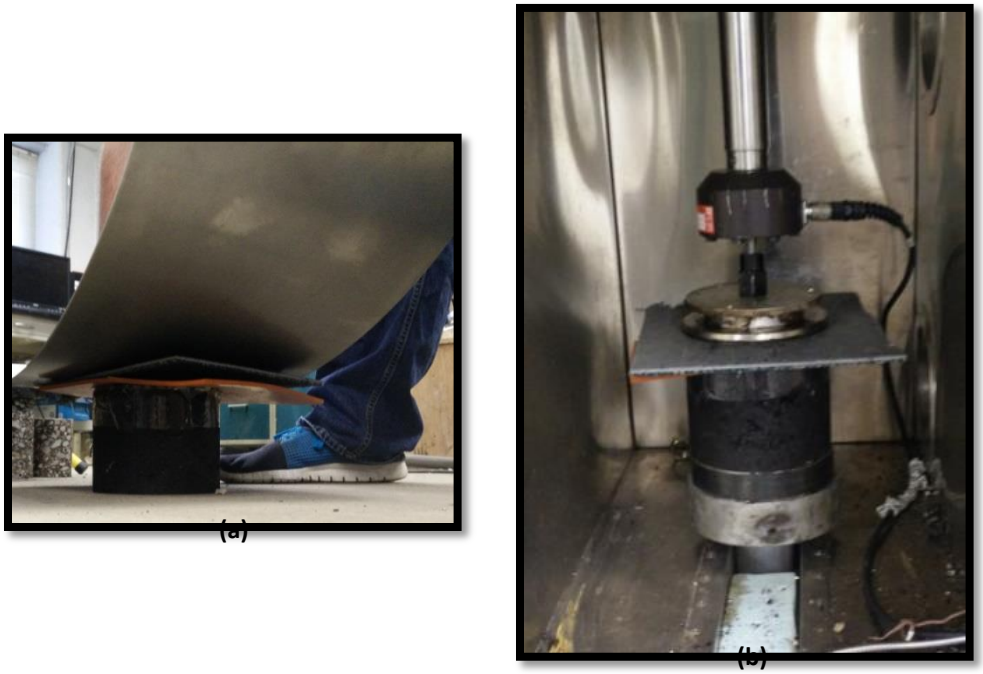

Figure 3.8: Sweep test compactor and compaction using the MTS: (a) Sweep test compactor and (b) compaction with MTS

CHAPTER 4

IMAGE ACQUISITION PROCEDURE AND IMAGE PROCESSING ALGORITHMS

In this chapter, sample preparation procedures for image acquisition, and the algorithms that are capable of calculating embedment depth (ED) and aggregate surface coverage (ASC), are introduced.

4.1 Sample Preparation and Image Acquisition

As shown in Figure 4.1, the chip seal samples are first sliced vertically to form a clean vertical face that the different phases (aggregate and chip seal binder) are distinctly visible and clear. Then, the digital images are captured using a document camera.

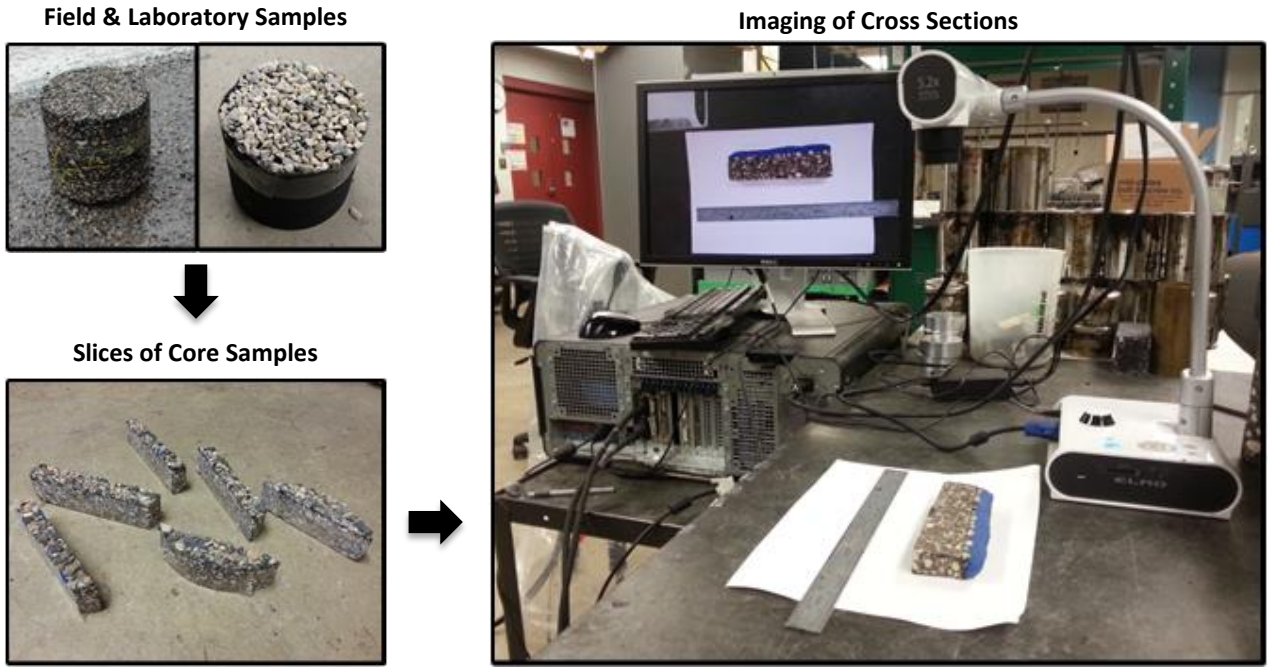

Figure 4.1: Illustration of sample preparation and image acquisition

There are two steps applied for cutting chip seal core samples in order to slice them properly (Figure 4.2). First step was a horizontal cutting procedure to make the core sample height smaller. The height of shortened chip seal cores ranged from 3 to 4.5 cm. Primary reason for the 'shortening' was to be able to fit the cores into the sweep test setup. Second cutting operation was vertical slicing.

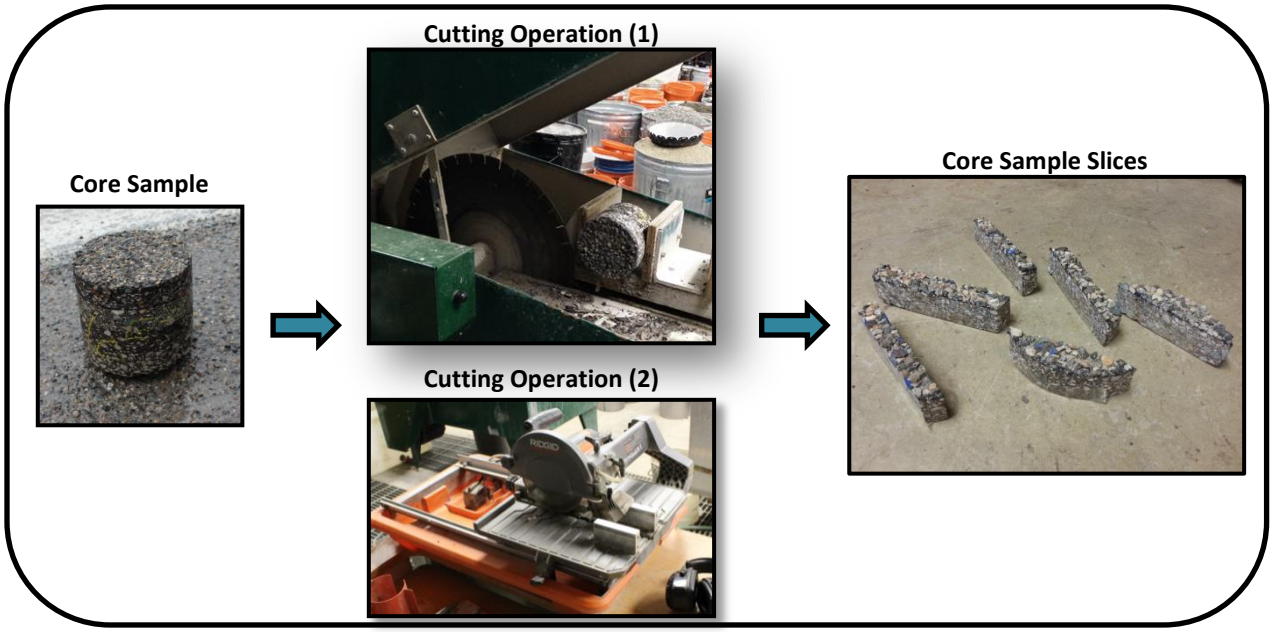

Figure 4.2: Sample cutting procedure

After obtaining cross sections from the chip seal cores, cross section pictures were taken by using a document camera. There are some important sample preparation criteria that are necessary for algorithms to work properly. These criteria are listed as follows:

- The top of the chip seal surface should be covered with a distinctly colored substance. Blue playdough was used to cover the top of the chip seal during imaging.
- Good color contrast between the aggregate and binder is necessary.

- There should be no light reflection on the binder or the aggregates during imaging. Several imaging techniques had been tried before getting good imaging results. Practicing for taking pictures with professional camera at different light conditions was done. However, a document camera (Brand: Elmo) with indoor white lightening was found to be the best option for imaging (See Figure 4.3).

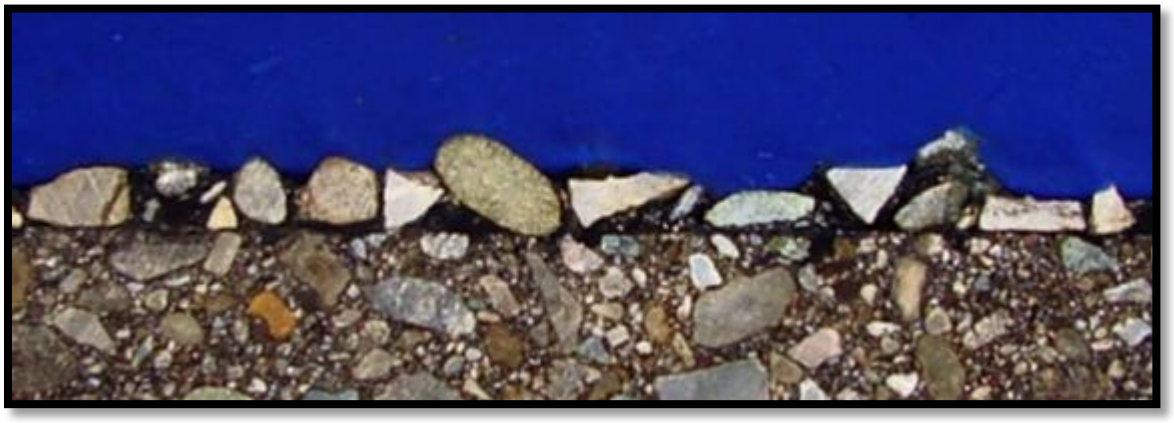

Figure 4.3: Desired cross section image

- Another issue for most of the cores from the field was the type of aggregates used. The aggregates had a lot of holes on their surface, because of being blast furnace slag. Contractors use iron blast furnace aggregates in chip seal constructions due to their availability and low cost. However, this kind of aggregate has a lot of holes, which prevents the image-based algorithms to work properly. Another difficulty with the blast furnace slag aggregates was their dark color. Since color contrast between aggregate and binder is poor; it is very difficult to analyze these images without improving the cross section surface for imaging. Figure 4.4 illustrates an example problematic cross section.

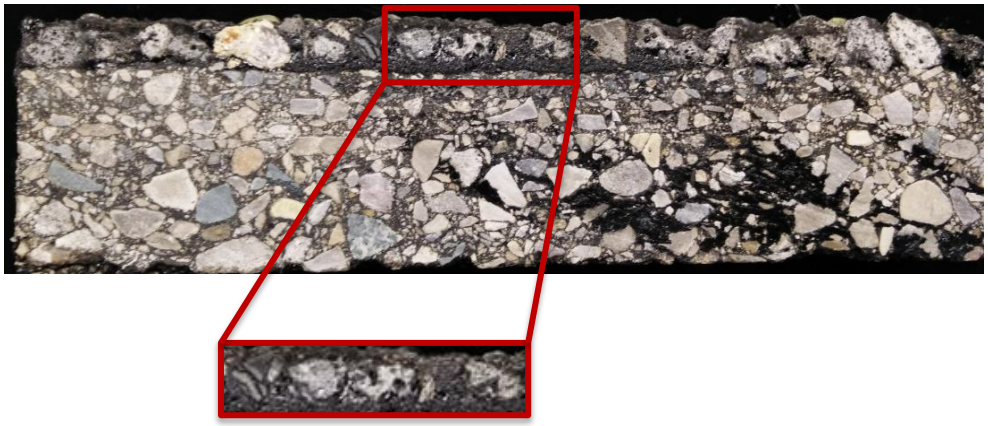

Figure 4.4: Image-based problems from cross sections

- After several trials for improving cross section, painting aggregates using a fine tip white pen was found to be promising. The aggregates were painted by using fine tip board marker and the holes on the aggregate surface were filled. This method appeared to be successful after cross section images were analyzed by using image-based algorithms. The Figure 4.5 illustrates the field chip seal cross section before and after modification. This modification was performed on all the field cross sections having iron blast furnace aggregates.

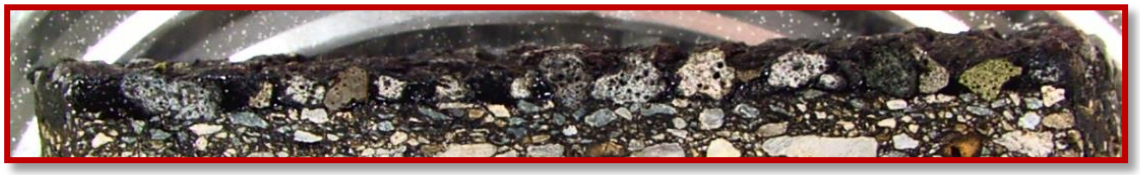

(a) Cross section before the painting

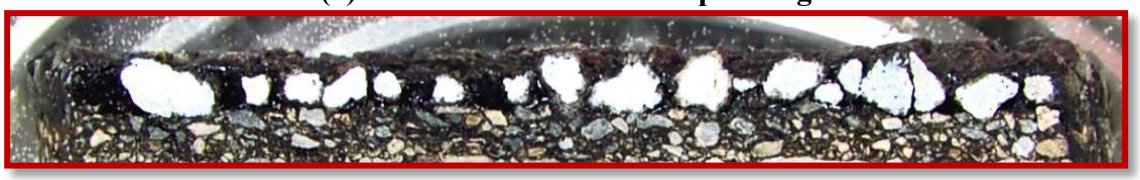

(b) Cross section after the painting

Figure 4.5: The effect of painting on cross section image

4.2 Image Adjustments

Before processing chip seal cross-section images, some further adjustments were necessary. First, since some cross sections were not aligned horizontally in the images, they were rotated until the substrate surface is horizontal (See Figure 4.6). Then, the images were cropped such that only desired portion of the image, chip seal area, is visible. This also prevented the algorithms from being computationally expensive. All these adjustments were made through a MATLAB graphical user interface (GUI) algorithm, developed as part of this study.

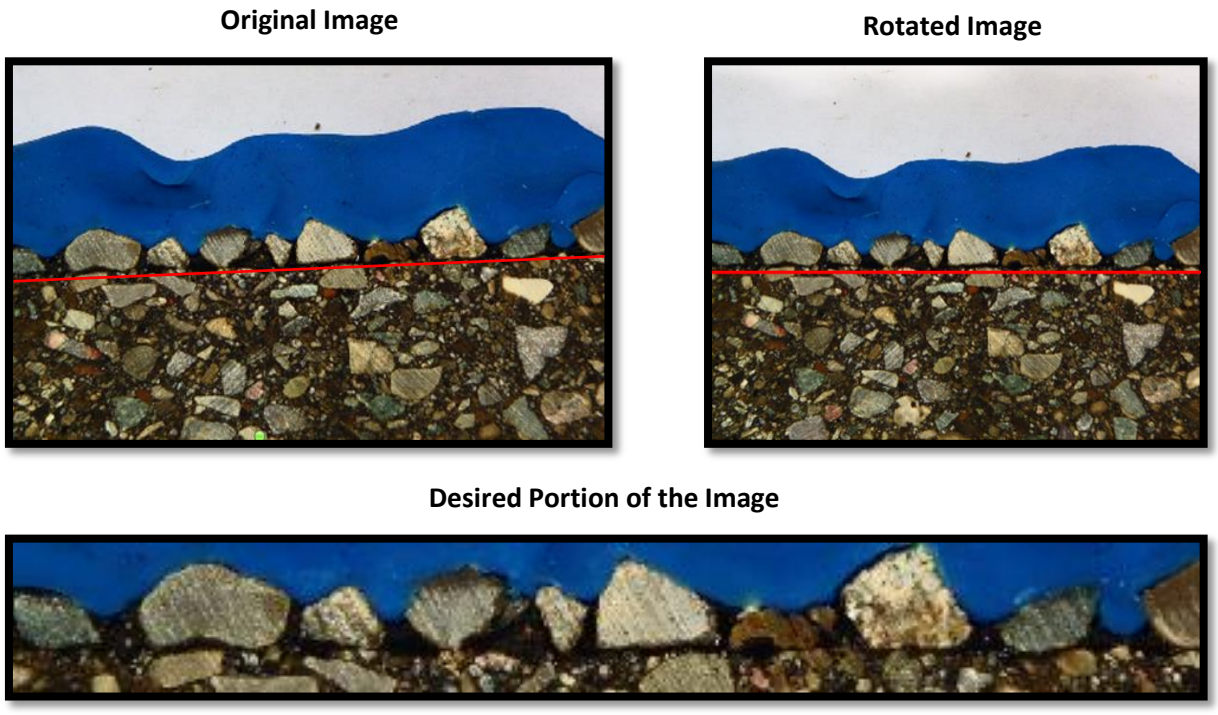

Figure 4.6: Rotated and cropped image

One of the other important adjustments was to find existing pavement underlying chip seal (i.e., substrate). For that purpose, certain points were initially set on the existing pavement manually in the algorithm (as input). These points were placed just below the emulsion of chip seal and care was taken to select sharp changes of color as shown in Figure 4.7.

Figure 4.7: Selecting points on the existing pavement

The algorithm drew lines between these points and formed a discrete curve (red line shown in Figure. 4.8a) consisting of multiple straight lines. Another parallel line (blue line shown in Figure. 4.8a) was automatically drawn 15 pixels above the red curve. Then, colored image was converted to grayscale image by applying some of the filtering techniques, including the Gaussian filter and image sharpening (see Figure. 4.8b). These filtering techniques were used to get rid of noise in the grayscale image. Then, for each x-coordinate, the intensities of the pixels located between blue line to red line were plotted as a profile (see Figure 4.8c). The direction of going the way was blue to red. The pixel locations, which had normalized pixel value smaller than 0.2, were determined. The last pixel value less than 0.2 was found, and was taken the transition point between existing pavement and chip seal surface emulsion. For instance, in Figure 4.8c, pixel values are taken from top to bottom at a specific x-coordinate. The last pixel value less than 0.2 (see plot in Figure 4.8c) is the transition point.

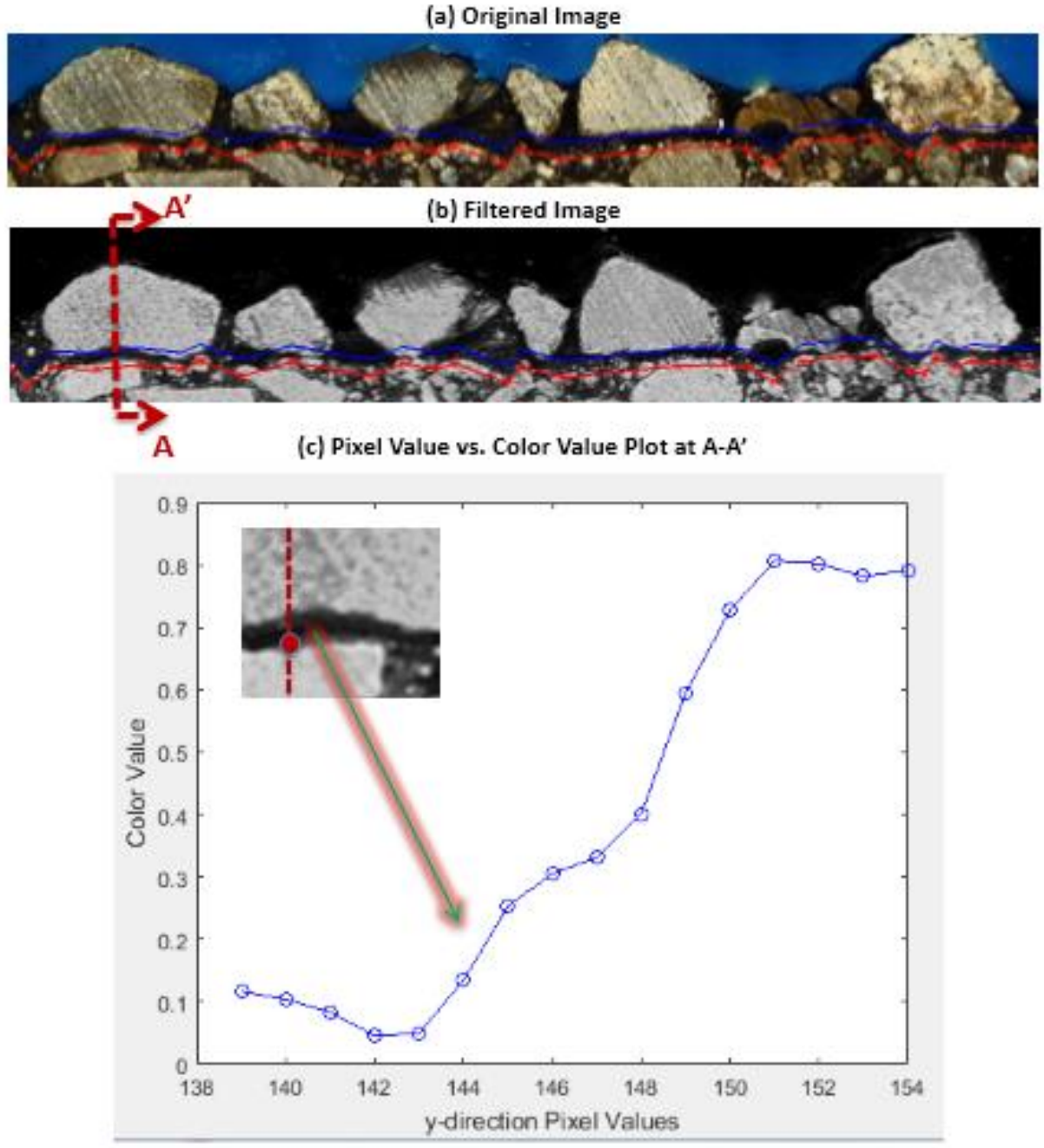

Figure 4.8: Procedure for finding existing pavement

4.3 Algorithms for Percent Embedment Depth Calculation

4.3.1 Method 1: Peak & Valley Method

In this method, first, the chip seal surface is determined by using color contrast between the blue play dough and aggregates (Figure 4.9). Chip seal surface can be thought as a line (green line in Figure 4.9) and local maxima and minima values are found on this line. Peak values (red-color points in Figure 4.9) are assumed as maximum aggregate height and valley values (pink-color points in Figure 4.9) are assumed as maximum binder height. Since all local maxima and minima values are found on the line, a user-defined threshold value (defined as delta in the algorithm) is used to limit number of peak and valley points. The steps of the algorithm for limiting the number of peak and valley points are as follows:

(1) All peak and valley values are found.

(2) The algorithm looks the height difference between two adjacent points (peak and valley points) (illustrated in fig. 4.9).

(3) If the height difference between these points is smaller than the delta value we defined, second point from left to right respectively is ignored until the condition is satisfied.

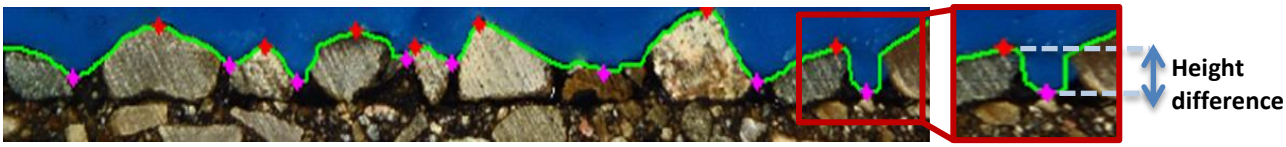

Figure 4.9: Finding peak and valley points

The average y-coordinate of existing pavement (found in a previous step) is taken and used as existing pavement substrate line (Figure 4.10b). One of the aggregate heights is calculated by subtracting existing pavement line height from peak height corresponding

aggregate. Same procedure is applied for calculating binder height by using valley points (Figure 4.10c). Then, averages for aggregate and binder heights are estimated and the ratio of binder height to aggregate height times 100 gives percent embedment depth.

$$P_e(\%) = \frac{h_b}{h_s} x100 \qquad [4.1]$$

where P_e = percent embedment depth, h_b = average binder height, h_s = average aggregate height

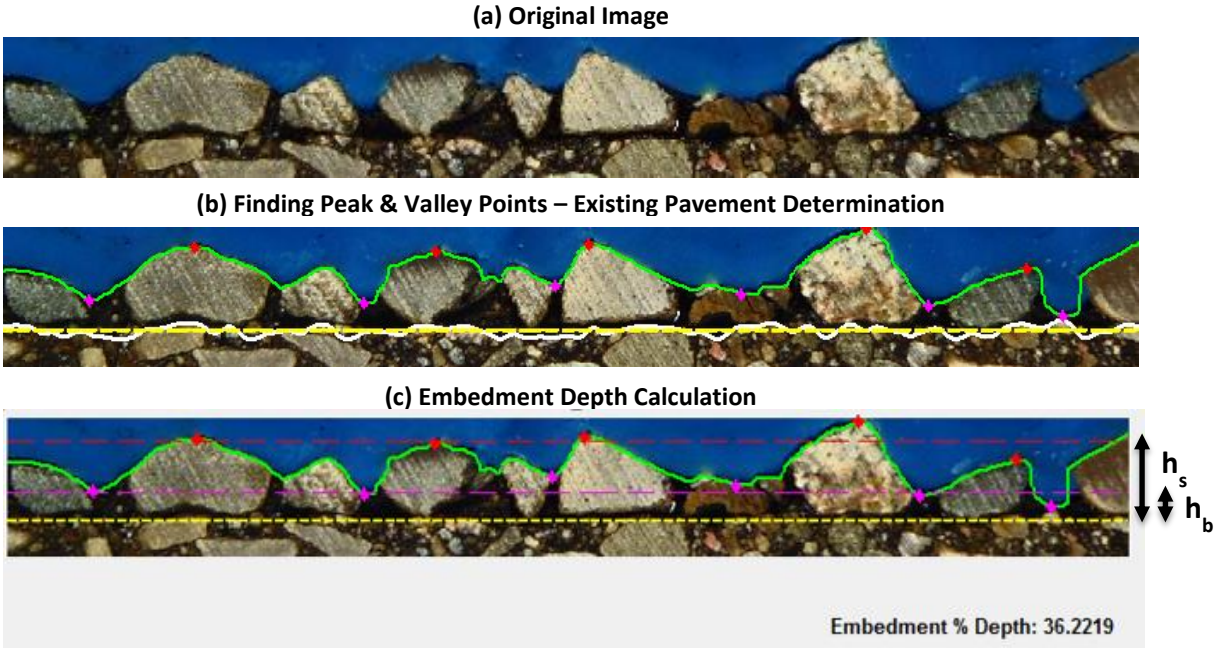

Figure 4.10: Illustration of steps of Method 1

4.3.2 Method 2: Area Method

The second method developed for calculating embedment depth is area method. In this method, embedment depth is estimated with the help of using aggregate areas, binder area and the total chip seal area. The aggregates are found by the algorithm separately to estimate aggregate area. In order to do so, colored chip seal image is converted into black and white image by using a user-defined normalized intensity threshold (I_t) value. Since this threshold

value is significant for getting aggregates properly, the algorithm takes the threshold value as an input. The importance of threshold value is illustrated in Figure 4.11.

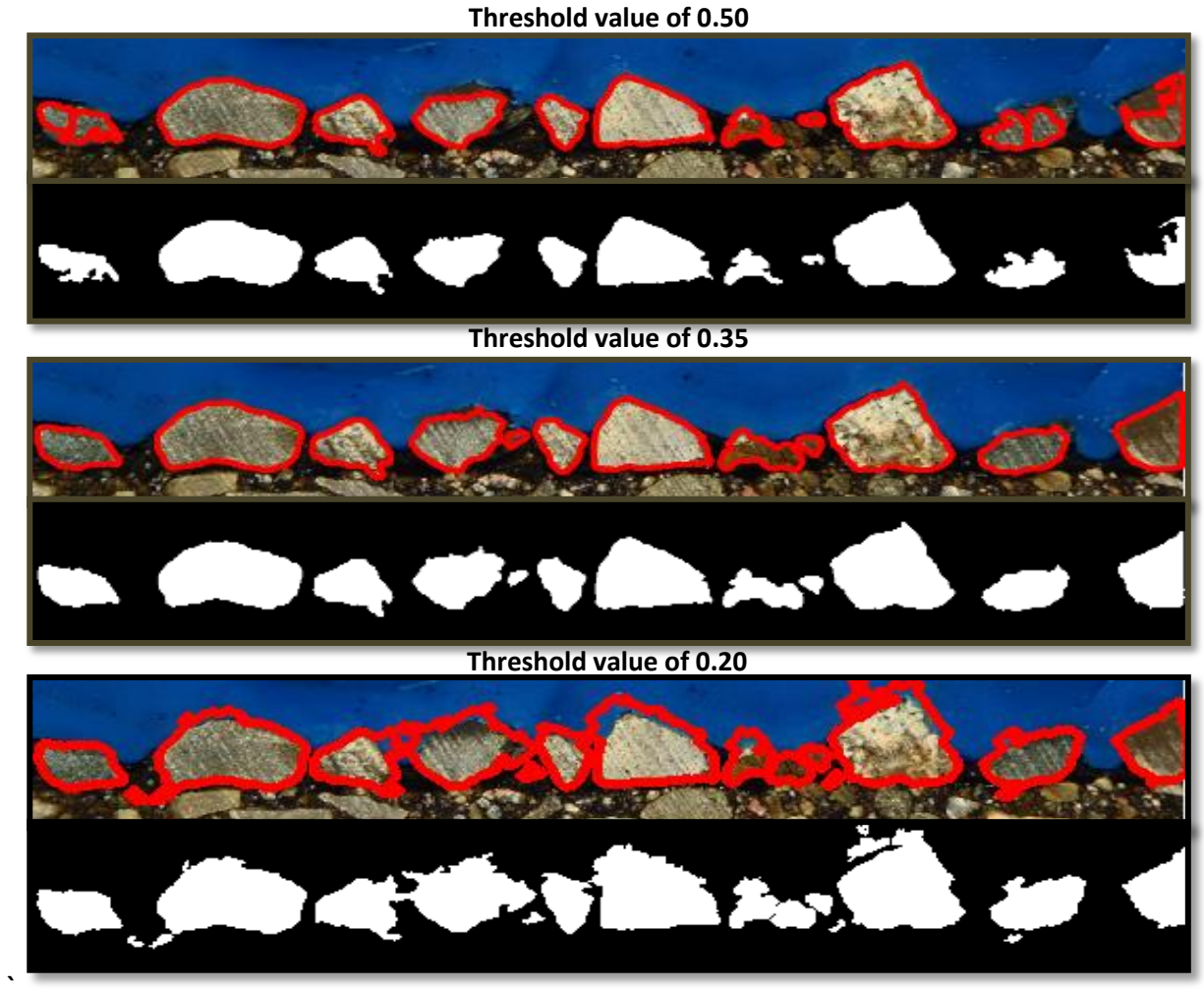

Figure 4.11: Different threshold values: (a) I_t = 0.5, (b) I_t = 0.35, (c) I_t = 0.20

As shown, too low threshold leads to too much noise especially around aggregate surface and aggregates are not selected properly (see Figure 4.9c). Also, too high threshold leads to disappearance of either aggregate itself or part of the aggregates (see Figure 4.9a). Every image has own threshold value because of the color and light properties of the image. Therefore, I_t = 0.35 is the best value for this image, as shown in Figure 4.9b.

The algorithm for this method works as follows:

- Total chip seal area is determined after getting existing pavement surface line and chip seal surface line.
- Total aggregate area is determined after getting all aggregates separately. The algorithm behind finding each aggregates separately is as follows:
    - All pixels under the existing surface is converted to black color in order to remove irregularities on the existing pavement (see Figure 4.12(a)).
    - True color (RGB) image is sharpened. This makes the features of the image such as edges to look sharper. After the sharpening of the image, the image is transformed to grayscale image by manipulating red, green and blue color indexes of the image so that aggregates become lighter color and remaining parts including blue playdough dark (see Figure 4.12(b)).
    - Grayscale image is then modified by applying 2-D median filtering (see Figure 4.12(c)). This modification removes the irregularities (noises) on the image and this filtered image is converted into black and white image. Then a series of dilation and contraction operations were performed to fill the holes on the aggregate surface (see Figure 4.12(d) and Figure 4.12(e)).
    - Finally, watershed transformation is performed to separate the aggregates that appear to sticking to each other (see Figure 4.12(f)).

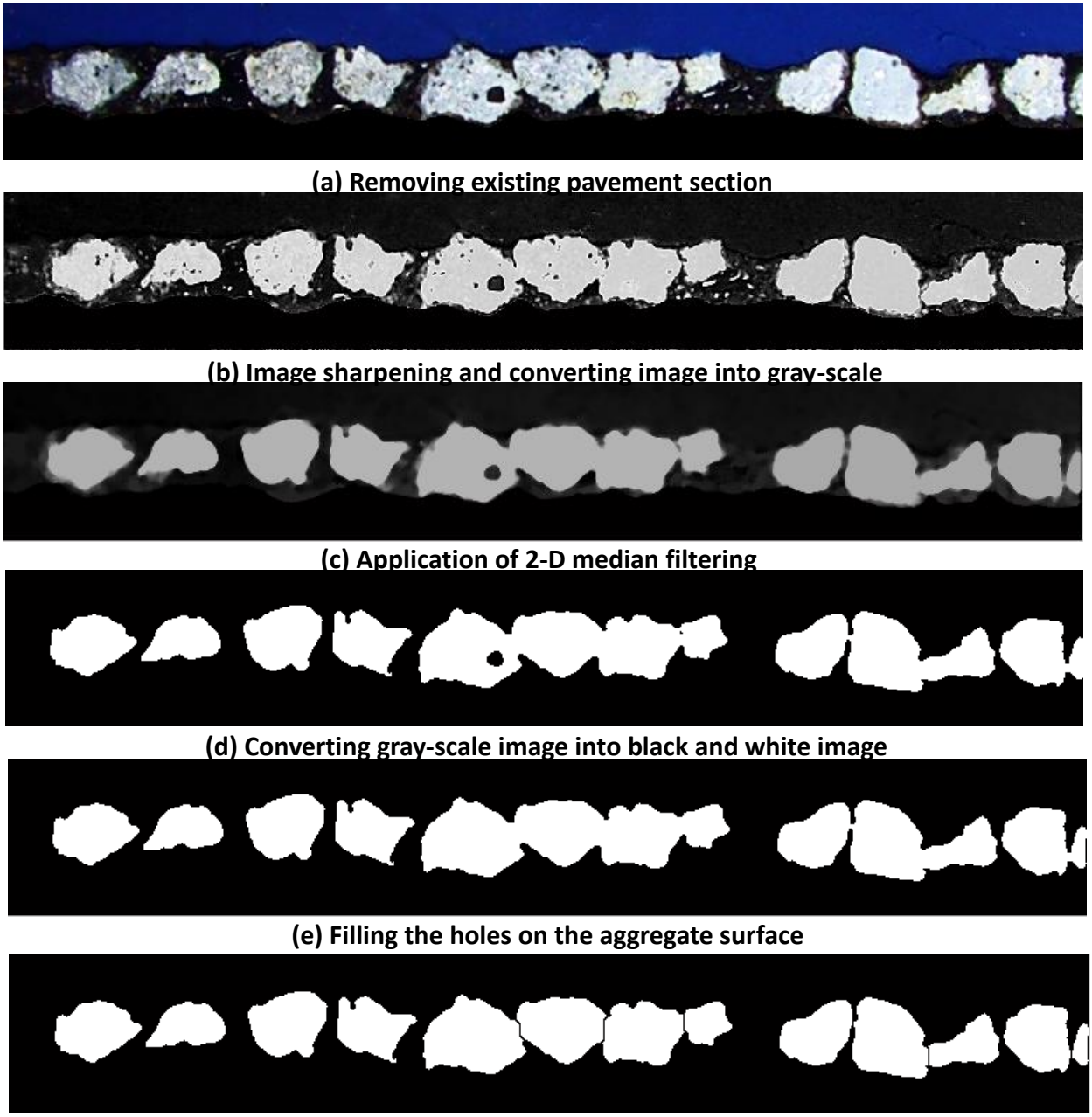

Figure 4.12: Algorithm for identifying aggregates separately

- Binder area is estimated by subtracting total aggregate area from total chip seal area. Then, binder height is obtained as dividing total binder area to length of image.

$$\boldsymbol{A_B} = A_C - \sum_i (A_A)_i \quad [4.2]$$

$$\boldsymbol{h_B} = \frac{\boldsymbol{A_B}}{L} \quad [4.3]$$

where A_B = binder area, A_C = chip seal area, A_A = aggregate area, h_B = average binder height and L = length of the image (See in Figure 4.13).

- Aggregate image properties such as x and y coordinates are available after getting all aggregates separately. Average of maximum y-values of each aggregate gives the average height.
- Embedment depth is calculated by dividing binder height to aggregate height.

$$\boldsymbol{P_e}(\%) = \frac{h_b}{h_s} x100 \quad [4.4]$$

where P_e = total percent embedment depth, h_b = binder height, h_s = aggregate height

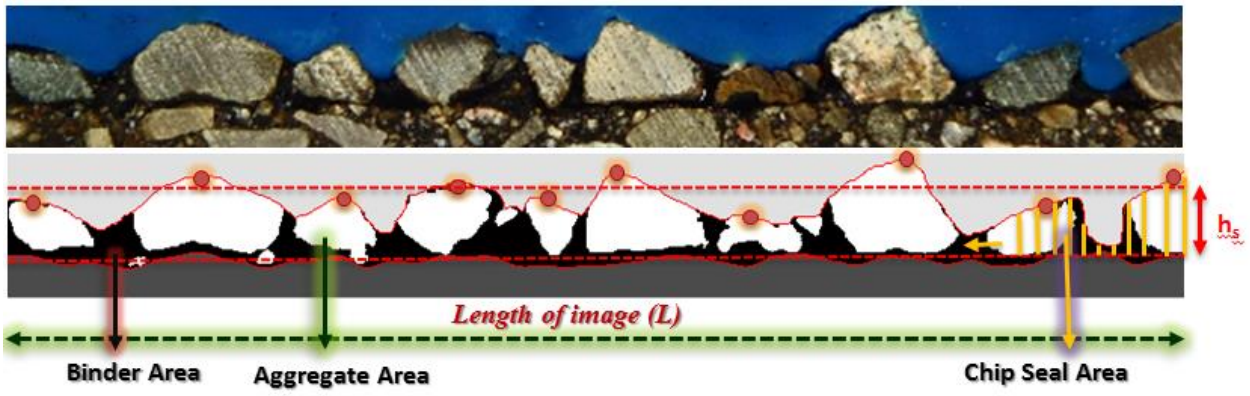

Figure 4.13: Illustration of embedment depth calculation by area method

4.3.3 Method 3: Embedment of Each Aggregate

In addition to these two algorithms, a new algorithm for estimating embedment depth is developed. This new algorithm is aimed at finding the percent embedment of each aggregate separately, followed by a statistical analysis to compute the distribution of percent embedment. The algorithm steps for this method are as follows:

- In order to determine binder peak points, chip seal surface coordinates determined from method-1 (peak/valley method) and each aggregate coordinates obtained from method 2 (area method) are used. Intersection between chip seal surface line and aggregate perimeter is determined as shown in Figure 4.14(a).
- Left and right end points of intersection lines for each aggregate are assumed to be peak binder heights.
- Binder height for each aggregate is average of two binder peak points from the base (lowest y-coordinate) of corresponding aggregate (see Figure 4.14(b)).
- Each aggregate height is calculated by subtracting lowest y-coordinate from highest y-coordinate of corresponding aggregate (see Figure 4.14(b)).
- Embedment depth for each aggregate is calculated by dividing binder height to aggregate height.

$$\mathbf{P_{e1}}(\%) = \frac{h_{b1}}{h_{s1}}\, x\, 100 \qquad [4.5]$$

where P_{e1} =single aggregate embedment depth, h_{b1} = binder height for the corresponding aggregate, h_{s1} = corresponding aggregate height.

- Total embedment depth is estimated by taking average of all embedment depths.

$$\mathbf{P_e}(\%) = \frac{\sum_i P_{e(i)}}{N} \qquad [4.6]$$

where P_e = total embedment depth, $P_{e(i)}$ = aggregate embedment depth, N = number of aggregate for that particular cross section

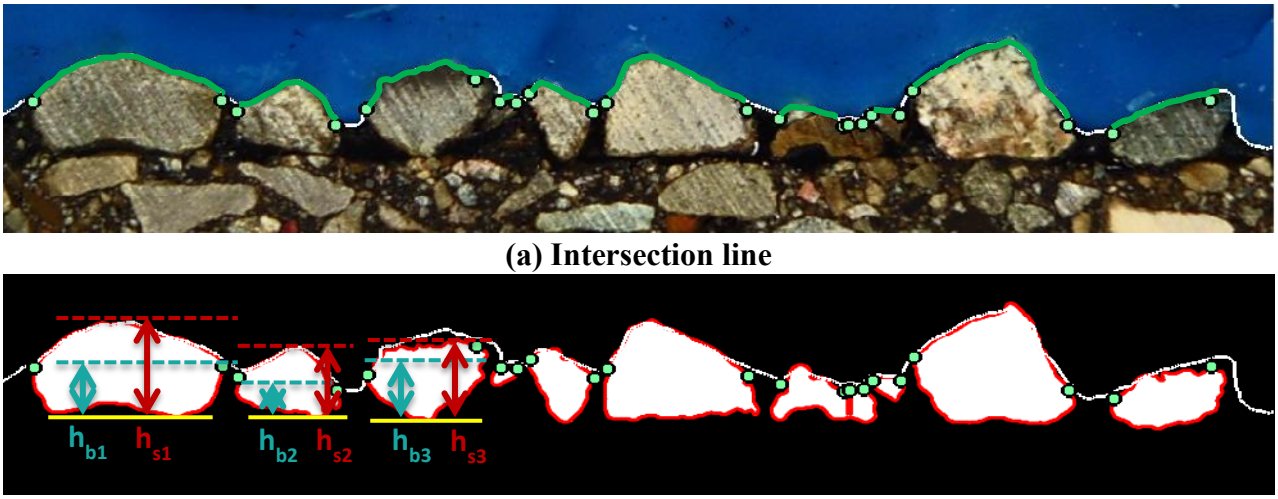

(a) Intersection line

(b) Embedment depth calculation

Figure 4.14: Method 3 – Embedment of each aggregate

4.4 Algorithm for Aggregate Surface Coverage Area

Another concept that may be considered as one of the performance criteria is aggregate surface coverage (ASC) by the binder. Adhesion between binder and aggregate prevents aggregate from being pulled out. Therefore, it is hypothesized that as the percentage of aggregate surface covered by the binder increases, the probability of aggregate loss decreases.

The algorithm detects binder around each aggregate and calculates percent surface coverage area for each aggregate. Average of these coverage areas gives general aggregate surface coverage area.

$$A_S = \frac{\left(\sum_i (\frac{(A_{BS})_i}{(A_{PS})_i} x100)\right)}{N} \quad [4.7]$$

where A_S = aggregate surface coverage, A_{BS} = binder coverage around the aggregates, A_{PS} = aggregate surface perimeter, and N = total number of aggregates.

Surface percent coverage area is illustrated in Figure 4.15.

Figure 4.15: Aggregate surface coverage

The steps of the algorithm are as follows:

- Each aggregate coordinates as well as perimeter pixels are computed the same way as the method 2.
- Aggregate surface coverage are examined one by one. For each aggregate, center coordinates (x and y coordinates) are calculated from perimeter. Starting from one of the perimeter coordinate, the direction from the center to that perimeter coordinate is obtained. Five (5) pixel goes outside from that perimeter coordinate through the direction obtained. If algorithm does not detect any blue color, it accepts that perimeter coordinate as binder and this procedure is repeated for all perimeter coordinate of corresponding aggregate as shown in Figure 4.16.

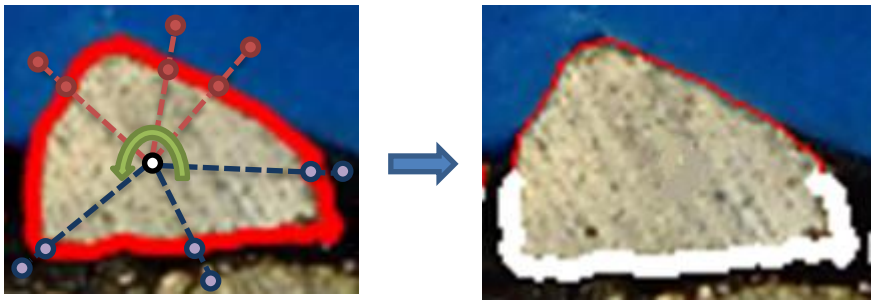

Figure 4.16: Finding surface coverage area

4.5 Validation of the Algorithms

In order to check whether the algorithms work properly, an idealized chip seal image is prepared as shown in Figure 4.17. After processing this idealized image, both percent embedment depth (for 3 methods) and surface coverage area are expected to produce 50%. Embedment depth using method 1 (Peak and Valley method), embedment depth using method 3 (each aggregate) and surface coverage area with binder gave 50%, 50% and very close to 50%, respectively. However, the area method did not give the 50% embedment depth. The reason why this method gives different embedment depth is related to how the binder height is determined. The binder height in this method is found from the total binder area. If the gap between the aggregates increases, since more binder volume fills the 50% heights, this method would produce different magnitudes. Therefore, it is recommended not to use this parameter.

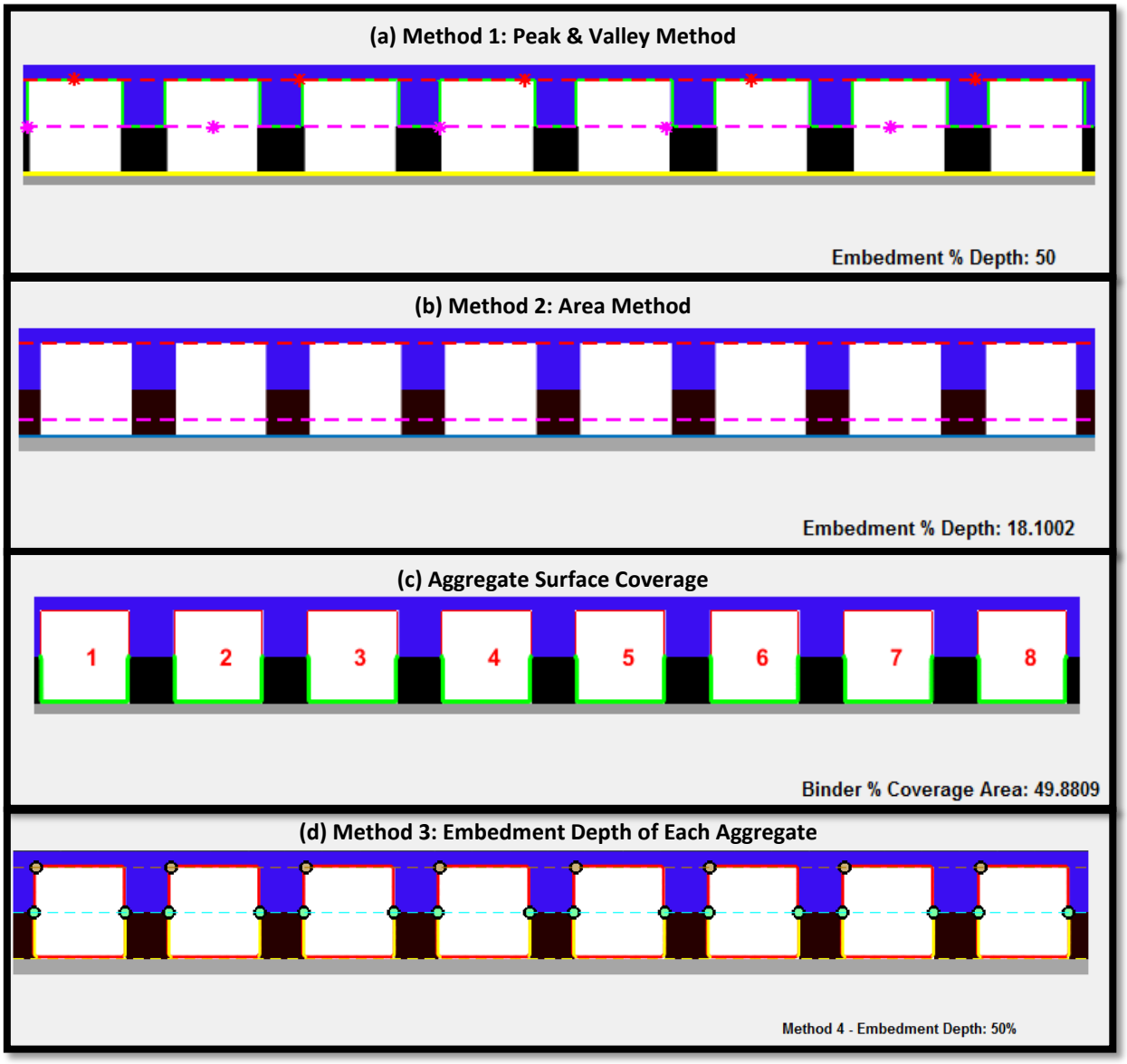

Figure 4.17: Idealized image analysis

CHAPTER 5

LABORATORY TESTING

This section includes two alternate methods used in the laboratory for calculating embedment depth and one laboratory test (sweep test) was performed to measure performance of chip seal samples in terms of aggregate mass loss.

5.1 Sand Patch Test

One of the common methods used both in the field and the laboratory to calculate the road surface texture is the sand patch test. The result of a sand patch test is not sufficient to calculate the embedment depth. The mean texture depth obtained from sand patch test and average aggregate height are used together to calculate the embedment depth.

For this project, sand patch test was performed on both field samples and laboratory samples. The "spreading method" was used to determine mean texture depth. In this method, fixed (known) volume of glass beads are used to cover all voids between aggregates. While performing the sand patch test in the laboratory, following steps were carried out:

- Ottawa sand were spread on the chip seal surface so that all voids between particles were filled and mass of Ottawa sand was measured by using Equation 5.1. This step was repeated 3 times and mass values were noted.

$$M_O = M_{SO} - M_s \quad [5.1]$$

where M_O = mass of Ottawa sand, M_{SO} = mass of sample with Ottawa sand, M_S = mass of specimen itself.

- Since density of the glass beads was known, volume of the glass beads used for sand patch test was computed by using mass obtained from previous step.
- With the information of the diameter of Ottawa sand covering the surface and their volume, mean texture depth was calculated by using the following formula:

$$(\boldsymbol{MTD}) = \frac{4\ x\ V_{GS}}{\pi\ x\ (D)^2} \quad [5.2]$$

where MTD = mean texture depth, V_{GS} = volume of glass beads, and D = diameter of the surface

- Mean texture depths obtained from 3 repeated measurements were averaged.

Aggregates typically tend to lie on their flattest side after compaction or due to the effect of traffic (Mcleod et al. 1969). Therefore, average least dimension of the aggregates was estimated by using the following formula (Wood et al. 2006):

$$H = \frac{M}{1.139285 + (0.011506)x(FI)} \quad [5.3]$$

where H = average least dimension (inches), M = median particle size (inches), and FI = percent flakiness index (in percent).

Percent embedment depth is calculated by using the following formula:

$$\%\ Embedment\ Depth = \frac{H - MTD}{MTD}\ \ x\ 100 \quad [5.4]$$

where H = average least dimension (inches), MTD = mean texture depth (inches) (shown in Figure 5.1).

Figure 5.1: Embedment depth calculation according to NCHRP 680

5.2 Ames Laser Texture Scanner

Another way to estimate chip seal surface texture is the use of a laser texture scanner. In this project, Ames laser texture device was used to measure the macro texture of the chip seal surfaces. With this device, it is easy to perform scanning both in the field and at the laboratory. After scanning, the scanner estimates and displays mean profile depth (MPD), texture profile index (TPI), estimated texture depth (ETD). Also, the raw scanning data can be extracted as a *.csv file format. Ames laser texture device can scan an area with a length of 107.95 mm and width of 72.01 mm.

Ames laser texture cannot directly calculate the mean texture depth. It initially measures the mean profile depth, and then converts it into estimated texture depth according to ASTM E1845-15.

$$\boldsymbol{ETD} = 0.2 + 0.8\,x\,MPD \qquad [5.5]$$

where ETD = estimated texture depth (in mm), MPD = mean texture depth (in mm).

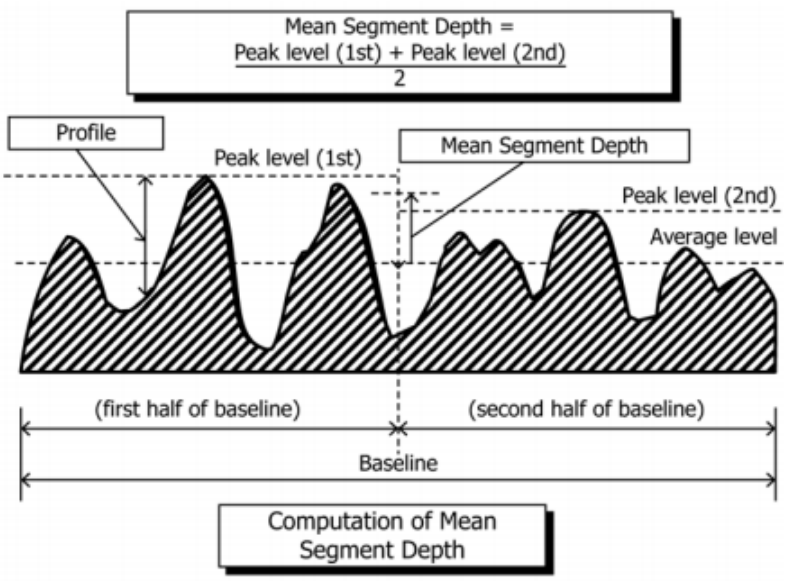

Figure 5.2: Procedure for computation of mean profile depth (source: ASTM E1845)

In order to calculate mean profile depth (MPD), profile is divided into 100 mm length baselines. Two peak levels are determined for first and second half of the baseline as shown in Figure 5.2. The difference between peak levels and average height level is estimated and then averaged. This procedure is repeated for all baselines along the profile and the average is taken as mean profile depth (MPD), or mean segment depth. Estimated texture depth (ETD) is prediction of mean texture depth (MTD) by using MPD. Based on the Freitas et al. (2008) study, the MTD results acquired from sand patch test are consistent with the ETD results estimated from MPD.

Estimated texture depth was assumed to be equivalent to the mean texture depth (MTD) in the results and analysis section of this thesis. Estimated texture depth is obtained line-by-line depending on the selected resolution. Average of these estimated texture depths gives mean texture depth of the chip seal surface.

In this project, samples taken from the field and fabricated in the laboratory were scanned by using Ames laser texture device and estimated texture depths were utilized as shown in Figure 5.3.

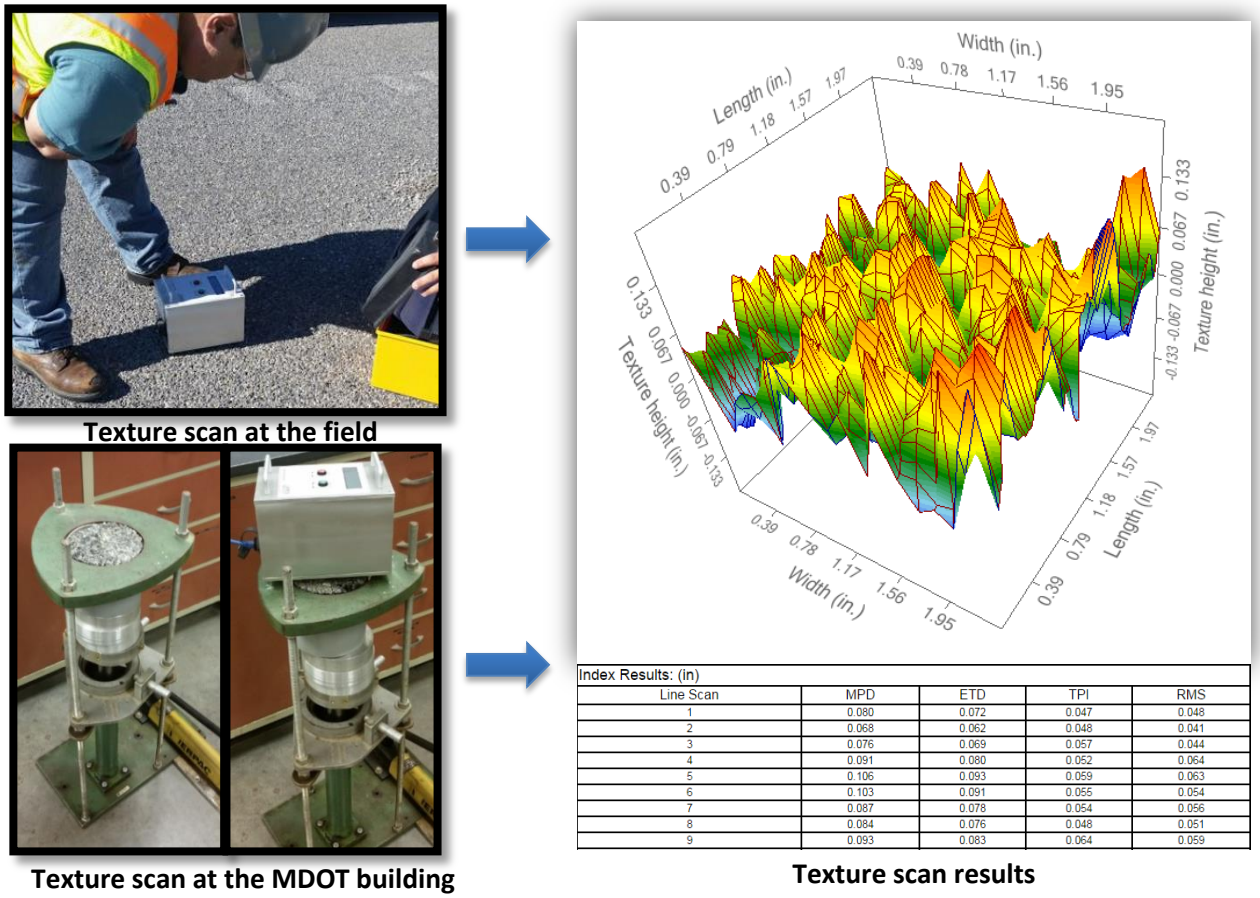

Index Results: (in)

Line Scan	MPD	ETD	TPI	RMS
1	0.080	0.072	0.047	0.048
2	0.068	0.062	0.048	0.041
3	0.076	0.069	0.057	0.044
4	0.091	0.080	0.052	0.064
5	0.106	0.093	0.059	0.063
6	0.103	0.091	0.055	0.054
7	0.087	0.078	0.054	0.056
8	0.084	0.076	0.048	0.051
9	0.093	0.083	0.064	0.059

Figure 5.3: Procedure for Ames laser texture scan

5.3 Sweep Test

Sweep test was performed on chip seal samples fabricated in the laboratory (see Figure 5.4). Sweep test apparatus was the same specified in ASTM D7000 except the mixer type. Specification suggests Hobart A120 mixer to use; however, Hobart N50 mixer, which is equivalent of A120 model, was used for sweep test due to the fact that A120 model is no longer

available. Sweep test procedure was performed according to the ASTM D7000 "Standard Test Method for Sweep Test of Bituminous Emulsion Surface Treatment Samples" and steps followed applied during test can be summarized as follows:

- Chip seal samples were conditioned at 35^{o}C in 30% of relative humidity for an hour.
- Chip seal sample weight measured before sweep test (A).
- Sweep test was performed with setting #1 (0.83 gyrations per second) for 1 minute.
- Chip seal sample weight was measured after the test (B).

Note that hot mix asphalt (HMA) weight below the chip seal was measured before chip seal fabrication (C). Percent mass loss was calculated by using formula 5.5.

$$\%\ \boldsymbol{Mass\ Loss} = \frac{A - B}{A - C}\ x\ 100 \qquad [5.6]$$

where A = chip seal sample weight before the test, B = chip seal sample weight after the test, and C = HMA weight below the chip seal surface.

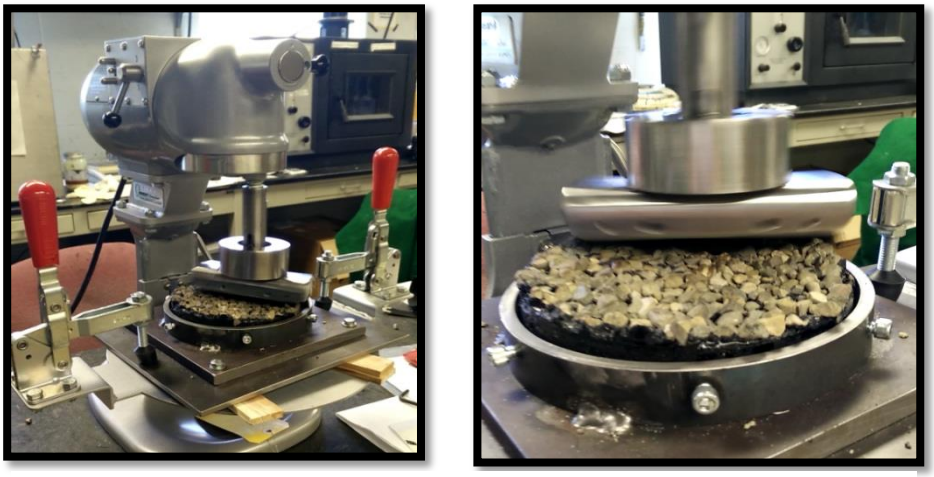

Figure 5.4: Sweep test procedure on chip seal surface

CHAPTER 6

RESULTS: FIELD & LABORATORY SAMPLES

6.1 Field Samples

Thirty (30) chip seal samples were collected from different sections of Michigan with the help of Michigan DOT crew. However, twenty-one (21) of them could be analyzed through imaging techniques. Cross sections obtained from the remaining chips seal sample cores had the following issue:

- It was almost impossible to find an existing pavement surface for double chip seal cross sections. In addition, even though the type of chip seal was stated as double chip seal, it was not a uniform double chip seal. Lastly, there was too much binder leakage into the substrate. All these problems can be seen in the Figure 6.1, which is a double chip, seal cross section obtained from field core samples.

Figure 6.1: Double chip seal cross section

Twenty-one (21) chip seal samples taken from the M-57 highway near the Pompei, M-20 highway and M-33 from Alger to Rose city from Michigan were analyzed through image-based

analysis. In addition to analysis, sand patch test was conducted on all these field samples and also laser texture scanning was performed by using Ames laser texture device.

6.1.1 Field Samples from M-57 Highway near The Pompei

Five (5) chip seal samples taken from the M-57 highway near the Pompei from Michigan were analyzed through image-based analysis methods as well as the sand patch test. Also, embedment depth was obtained from Ames laser texture scanning for 3 samples. Results are tabulated in Table 6.1:

Table 6.1: Embedment depth results of M-57 field samples

Sample ID	Embedment Depth - Peak/valley	Aggregate surface coverage	Embedment Depth - Each Aggregate	Sand Patch Test	Ames Laser Texture Scan
040215-7 - RWP	53.94	50.07	80.779	60.65	
040215-8 - LWP	46.7	51.87	83.65	50.2	68
040215-9 - CL	60.1	52.41	78.166	61.24	
040215-10 - RWP	57.5	52.82	81.77	58.1	72.8
040215-11 - LWP	47.6	48.26	84.872	53.4	67.8

Note: RWP = right wheel path, LWP = left wheel path and CL = center line

As shown in the Figure 6.3, Ames laser texture scanning gives higher percent embedment as compared to sand patch test. The reason can be due to empirical relationship between mean profile depths, output of the Ames laser texture; and mean texture depth. Also, Kim et al. (2013) stated that there is limited data used in developing correlation between mean texture depth and mean profile depth.

Although the results from the Ames laser texture are higher than the sand patch, their trends are similar for the 3 samples. The relationship between image-based embedment depth and the embedment depth obtained from sand patch test are also similar. Also, trends for both methods are also consistent to each other. The method for embedment depth of each aggregate gives higher than the embedment depth obtained from peak and valley method. Higher results can be derived from the fully-embedded aggregates which are considered during embedment depth calculations.

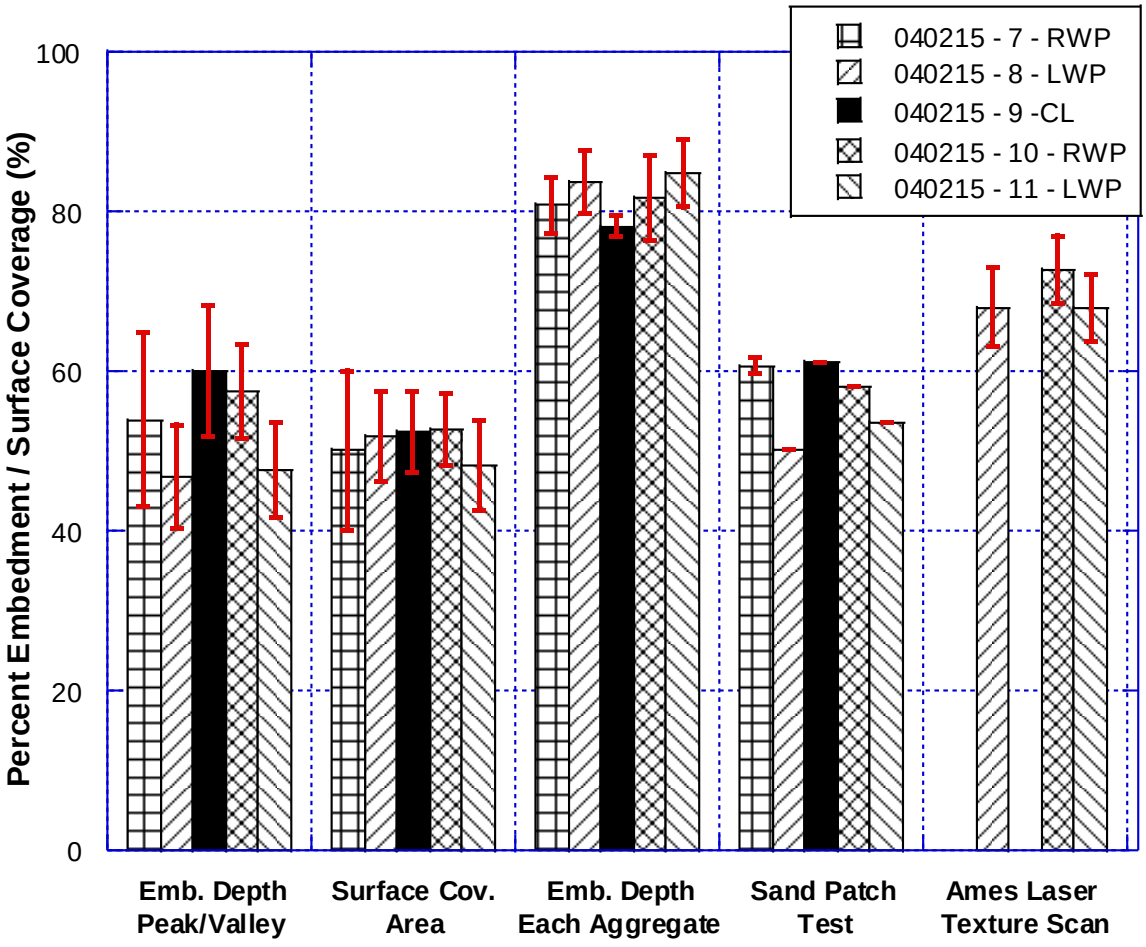

Figure 6.2: Comparison of different methods for M-57 Highway Near Pompei

6.1.2 Field Samples from M-20 Chip Seal Section

Eight (8) chip seal samples taken from the M-20 highway chip seal section from Michigan were analyzed through image-based analysis methods. In addition to image-based algorithms, embedment depth was obtained from sand patch test and Ames laser texture scanning for 8 samples. Results are tabulated in Table 6.2:

Table 6.2: Embedment depth results of M-20 field samples

Sample ID	Embedment Depth - Peak/valley	Aggregate surface coverage	Embedment Depth - Each Aggregate	Sand Patch Test	Ames Laser Texture Scan
M20 - 1	63.77	62.09	78.03	55.25	71.73
M20 - 2	71.42	62.89	79.54	56.68	71.91
M20 - 3	58.68	59.04	78.48	58.58	73.68
M20 - 4	67.1	61.1	78.84	57.85	78.33
M20 - 5	67.53	67.02	83.09	55.05	68.5
M20 - 6	53.52	54.39	75.03	58.85	71.77
M20 - 7	61.61	60.71	78.38	58.92	71.54
M20 - 8	61.12	55.13	74.12	53.2	71.21

Percent embedment depth and surface coverage are represented with respect to different methods as shown in the Figure 6.3. Although embedment depth results from sand patch test and Ames laser texture are different, their trends are quite similar. The reason why the errors are higher for Ames laser texture scan results is the large differences between embedment depths based on the estimated texture depth obtained at every line scan defined by the user for one sample.

Similar to the results between sand patch test and Ames laser texture scan, the results for embedment depth calculation obtained from peak and valley method and each aggregate method are different but similar trends. One of the improvements for embedment depth calculation with each aggregate method is low variability comparing to embedment depth calculation estimated by the peak and valley method.

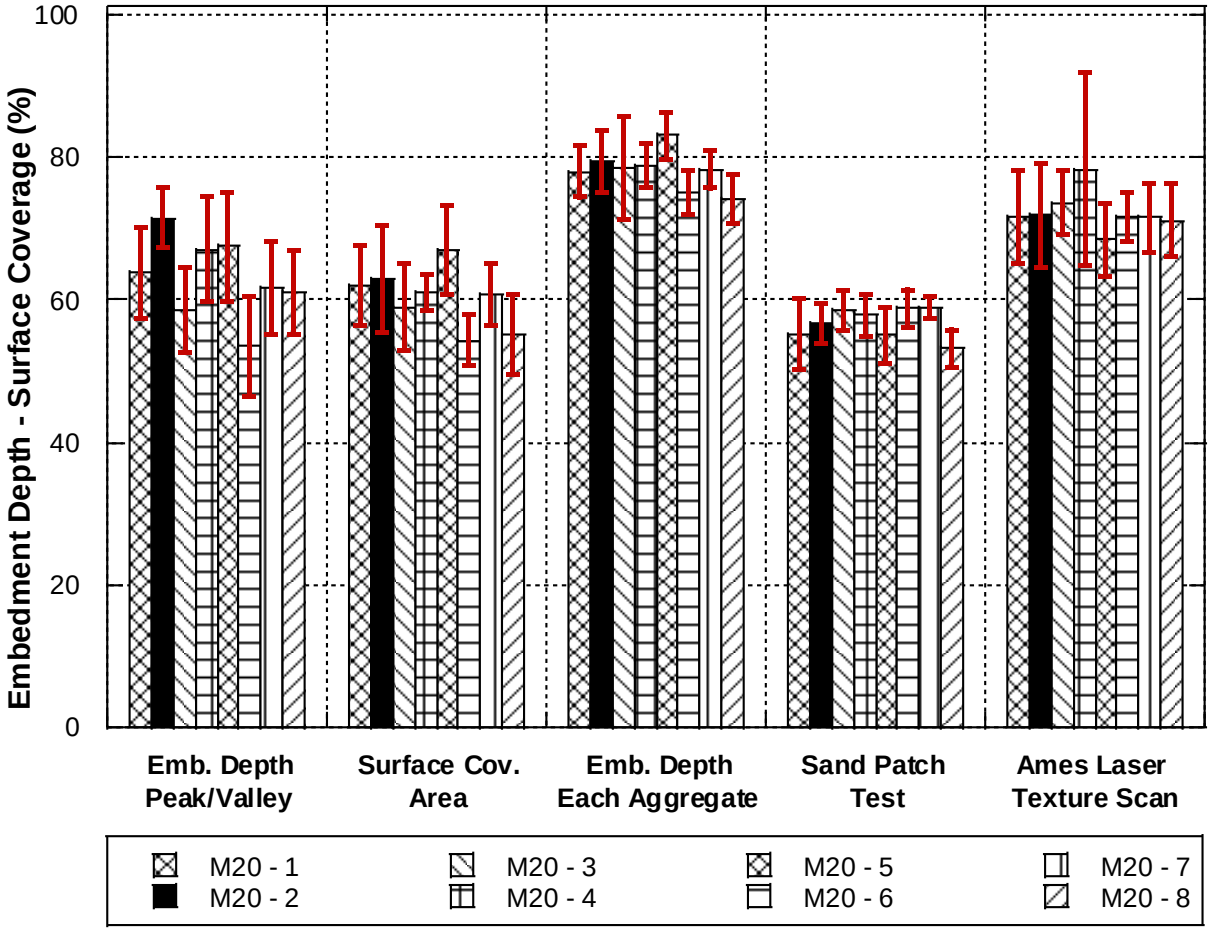

Figure 6.3: Comparison of different methods for M-20 Chip Seal Section

6.1.3 Field Samples from M-33 from Alger to Rose City

Eight (8) chip seal samples taken from the M-33 from Alger to Rose city chip seal section were analyzed in terms of percent embedment depth and surface coverage through image-based algorithms, sand patch test and Ames laser texture scan. Results are tabulated in Table 6.3:

Table 6.3: Embedment depth results of M-33 field samples

Sample ID	Embedment Depth - Peak/valley	Aggregate surface coverage	Embedment Depth - Each Aggregate	Sand Patch Test	Ames Laser Texture Scan
M33 - 1	75.26	65.86	82.7	48.98	62.41
M33 - 2	71.29	61.57	81.88	68.51	70.21
M33 - 3	68.75	60.79	77.91	72.26	73.71
M33 - 4	70.34	59.7	79.07	77.52	85.1
M33 - 5	57.87	55.97	72.98	70.96	78.81
M33 - 6	72.69	65.1	82.43	71.61	74.98
M33 - 7	70.51	60.27	79.22	48.98	62.72
M33 - 8	77.31	61.06	81.98	67.97	71.99

Like the results obtained from M-20 chip seal section, from the Figure 6.4, trends for sand patch and Ames laser texture scan results are quite similar; however, variability (errors) for laser scanning is higher than the sand patch test. The reason for low variability in sand patch results is that the estimated mean texture depths between repeated sand patch tests on the same sample are generally very similar. The relationship between two different methods to calculate embedment depth is similar to the results obtained from M-20 chip seal section as well. They both do not indicate similar embedment results but same trends. Percent embedment depth results obtained from each aggregate are higher than the peak and valley method. Normally, it is very difficult to say a relationship between embedment depth and surface coverage area, it is

seen similarities in trend-wise especially with embedment depth of each aggregate method. It can be due to the fully embedded aggregates that are considered at both methods.

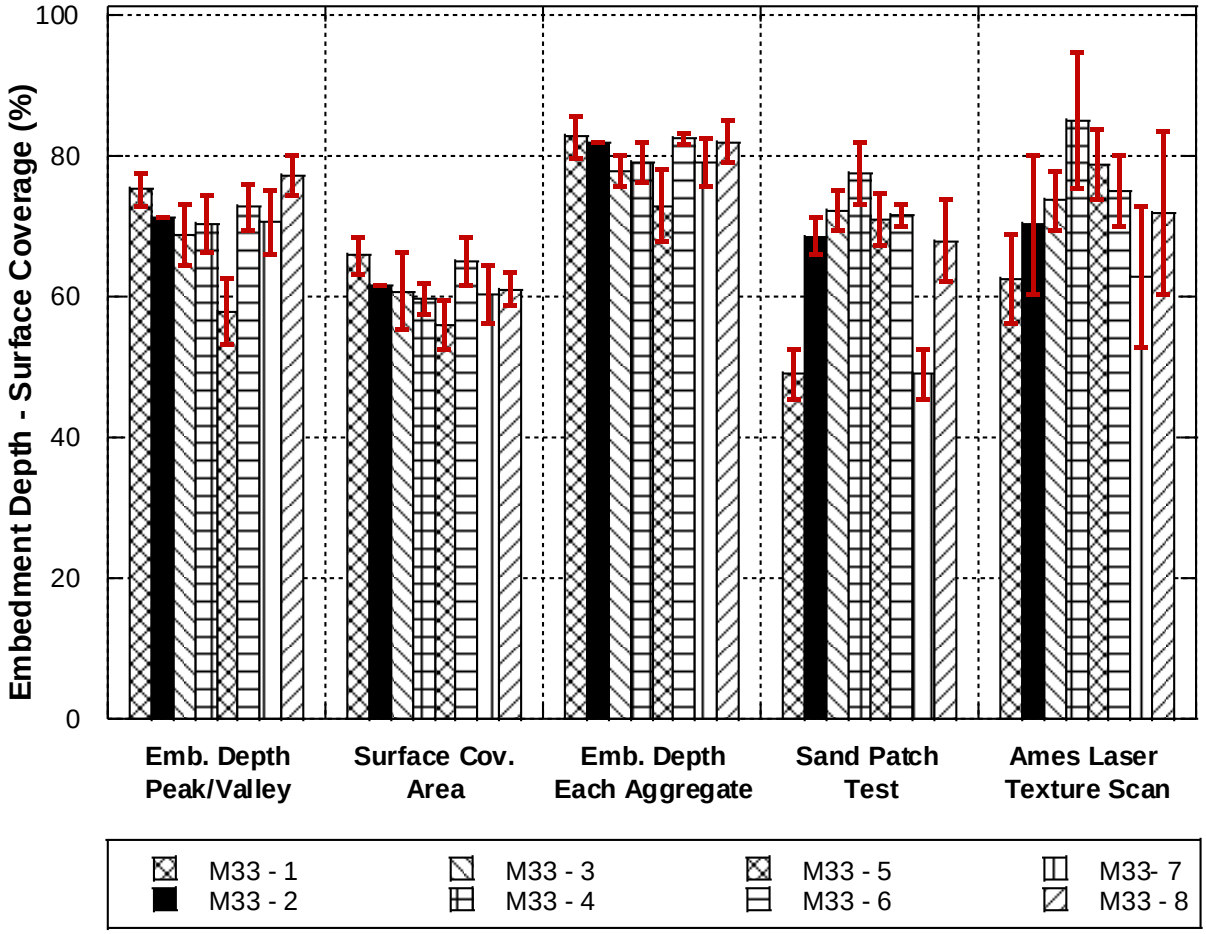

Figure 6.4: Comparison of different methods for M-33 Chip Seal Section

One of another result from the analyses for all field chip seal sample is that the embedment depth results obtained from the sand patch test gives the lowest results compared to other test methods. The reason for obtaining the lowest results for sand patch test is the assumption for the aggregates sitting perfectly on the ground. However, there is always binder under the chip seal aggregates and it increases the embedment depth obtained from the image based analysis. The effect of the binder under the aggregates on the percent embedment depth

can be seen in the Figure 6.5(b). The percent embedment depth (h_{e1}) calculated when aggregates sitting perfectly on the ground is less than the percent embedment depth (h_{e2}) while considering the binder under the aggregates.

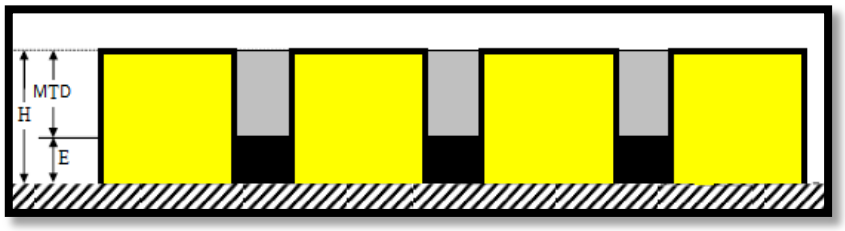

(a) Chip seal sketch for sand patch test

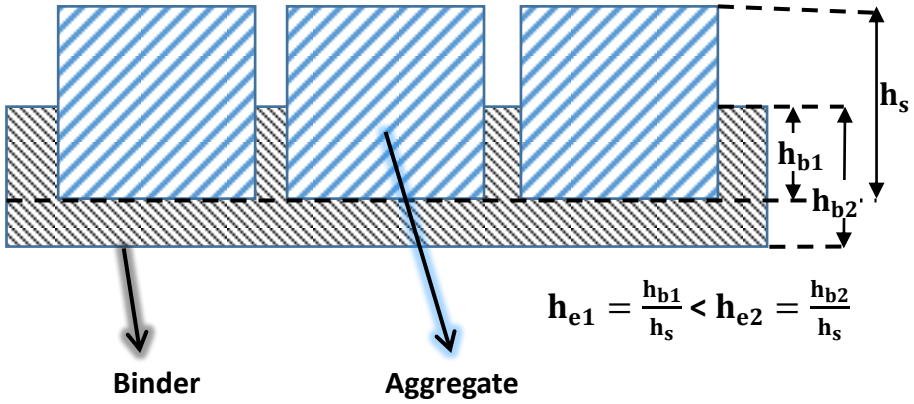

(b) Actual chip seal sketch

Figure 6.5: Sketches of the asphalt chip seals

6.1.4 Relationship Between the Image-based Algorithms and Other Methods

In addition to comparison of different methods for each field, the relationship between the embedment depth estimated from the image-based algorithms and the embedment depth measured from sand patch test and Ames laser texture scan was investigated. The embedment depth results calculated from method-1 and the embedment depth measured from sand patch test and Ames laser texture scanning are shown in the Figure 6.6. From the results, it can be concluded that there is no correlation between both method-1 vs. sand patch and method-1 and

laser texture scan except for the M-57 chip seal section. The reason can be the chip seal type for M-20 and M-33 which are fog chip seal. The glass beads which is used to calculate macrotexture depth could not fill the voids between aggregates because of fog sealing. Therefore, the embedment depth results measured from the sand patch and laser scanning can give wrong results for fog chip seal sections.

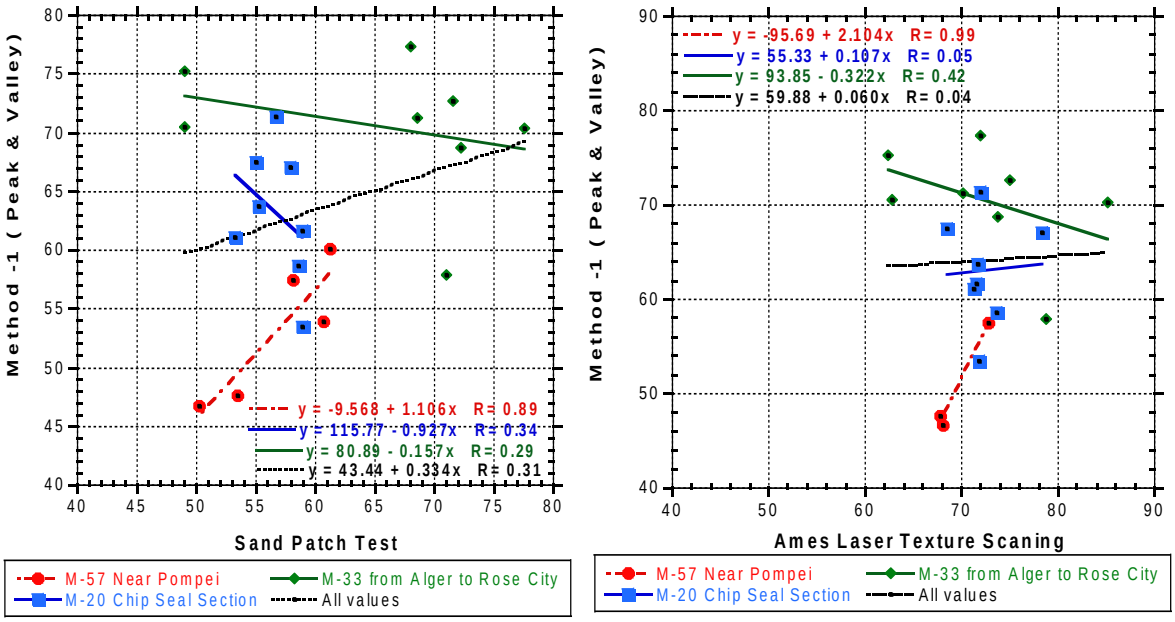

Figure 6.6: Method-1 relationship with sand patch and laser texture scanning

The rest of the combinations, method-3 vs. sand patch test and method-3 vs. Ames laser texture scanning, are available in the Appendix E. For the method-3, similar results were obtained as method-1. Also noted that since there is other factors affecting the embedment depth such as existing pavement condition (distresses), stiffness of the substrate, asphalt binder properties (viscosity); these factors can be considered in the correlation.

6.2 Laboratory Samples

As mentioned in the Chapter 4, forty (40) chip seal samples were fabricated in the laboratory and these 40 samples were separated into two groups.

6.2.1 Group 1 Samples

Eight (8) chip seal samples were categorized in group 1. The aim of testing this group was to investigate the effect of application rates (both aggregate and binder) on embedment depth and surface coverage area. Samples were prepared with upper and lower limits of both binder and aggregate application rates. For each combination, 2 replicates were tested. The plots in Figure 6.8 indicates that the embedment depth and surface coverage area do not seem to be affected by the aggregate application rate. Whereas, according to results illustrated in Figure 6.7, binder application rate has a greater influence on percent embedment and surface coverage area.

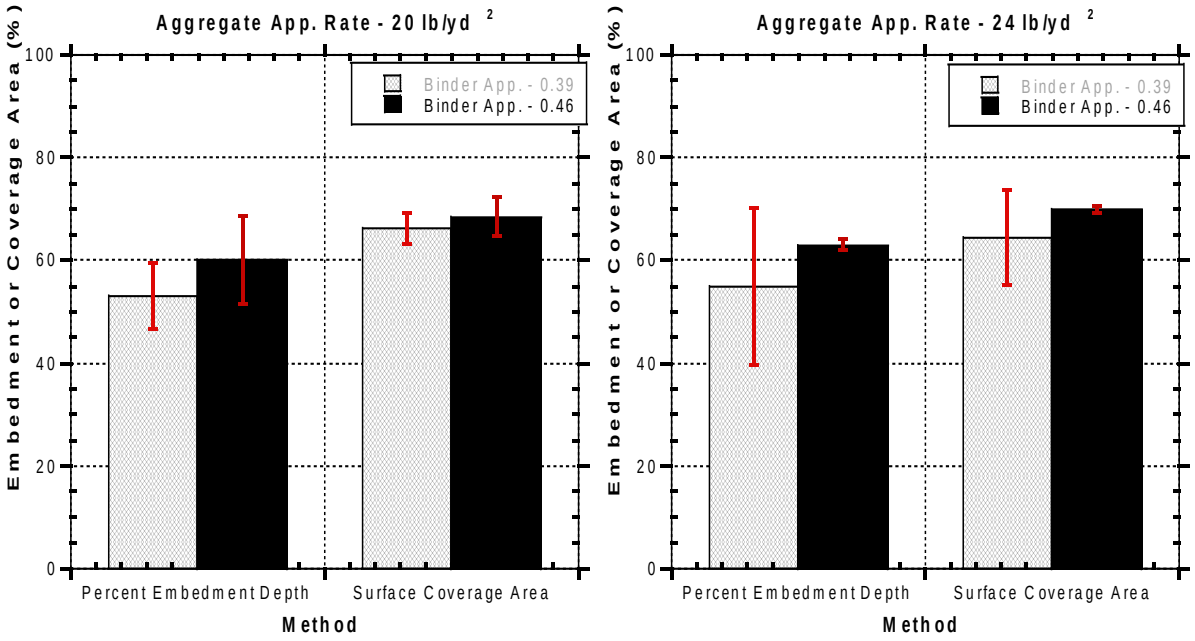

Figure 6.7: Effect of binder application rate

It is clearly seen from the Figure 6.7 that increases in the binder application rate leads to increase in the percent embedment depth and aggregate surface coverage. One of the reasons why aggregate application rate does not affect the results may be that there was already sufficient number of aggregate chips on the surface even after application of 20 lb/yd^2 rate. Excess aggregates were taken on the surface by brushing before cutting process. Therefore, since they would have similar aggregate application rates on the chip seal surface after brushing, embedment depths obtained by image-based algorithms were close to each other.

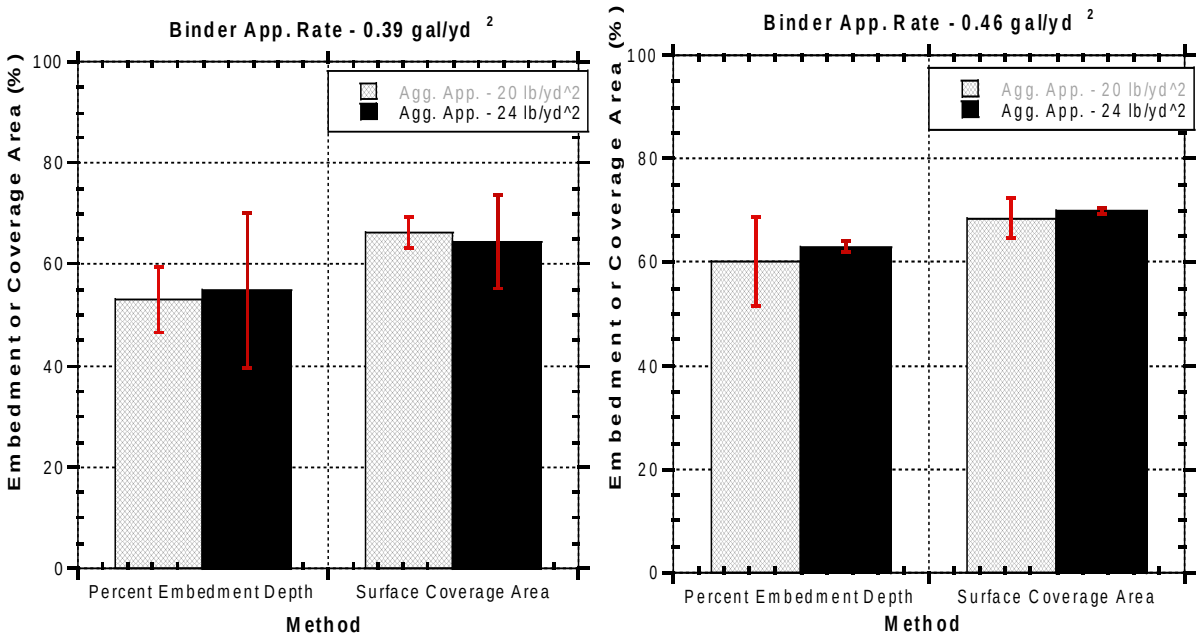

Figure 6.8: Effect of aggregate application rate

6.2.2 Group 2 Samples

Thirty two (32) chip seal samples were classified as group 2. Since aggregate application rate was found not to affect the embedment depth and surface coverage area for laboratory samples, aggregate application rate was kept constant, (20 lb/yd^2), and the binder application varied range between 0.39 gal/yd^2 and 0.46 gal/yd^2 with the increment of 0.1 gal/yd^2 was used as

binder application rates during preparing chip seal samples. Each aggregate-binder application rate set has 2 replicates and each set was prepared twice. One of them was for analysis without sweep testing; whereas, the remaining set was for analysis after sweep test had been performed. The goal of this group was to investigate performance of chip seals with embedment depth and surface coverage area by using sweep test.

The bar plot illustrated in the Figure 6.9 indicates the embedment depths by peak & valley method with changing binder application rates. Statistical independent t-test was done between pairs (non-sweep and sweep) to determine whether the samples are statistically different or not. The samples that had binder application rate of 0.39 gal/yd^2 and 0.42 gal/yd^2 were disregarded due to being statistically same samples without sweep and with sweep test.

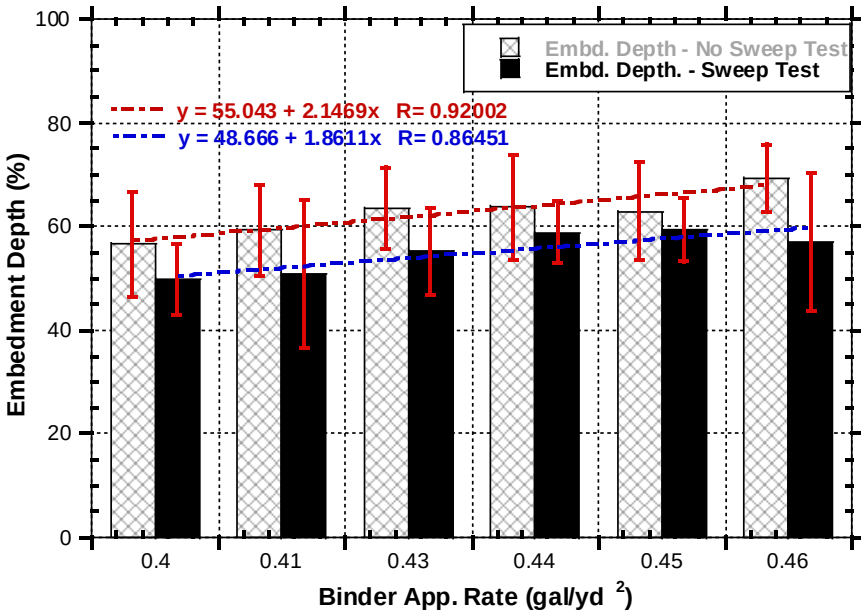

Figure 6.9: Embedment depth for different binder application rates

From this graph in the Figure 6.9, the effect of sweep test is visible. The difference in the embedment depth before and after the sweep test occurs because of two things: the first one is to take the aggregates off from the surface during brushing. The second reason is pulling the aggregates upward which decreases embedment depth. However, the difference in both embedment depth and surface coverage area as well as aggregate mass loss calculated after sweep test are actually not much and this situation is normal because we do not expect so much difference after sweep test. The goal of sweep test is to measure adhesive properties of the emulsion just after the construction, not to simulate traffic effect. Therefore, we can say that the emulsion that we used had good adhesive properties.

Another conclusion can be drawn from the plot in the Figure 6.9 is that the binder application range specified by MDOT meets the requirement exactly which is that percent embedment depth should be between 55 and 70 just after the construction.

Aggregate surface coverage was a new concept that was tried to understand effect on the performance. From the graph indicated in the Figure 6.10, there is a linear increase in surface coverage areas for both non-sweep and sweep performed test samples, and also, all surface coverage areas decreased after sweep test. After the traffic effect is simulated on the samples, this concept can be a good indicator of performance of chip seals.

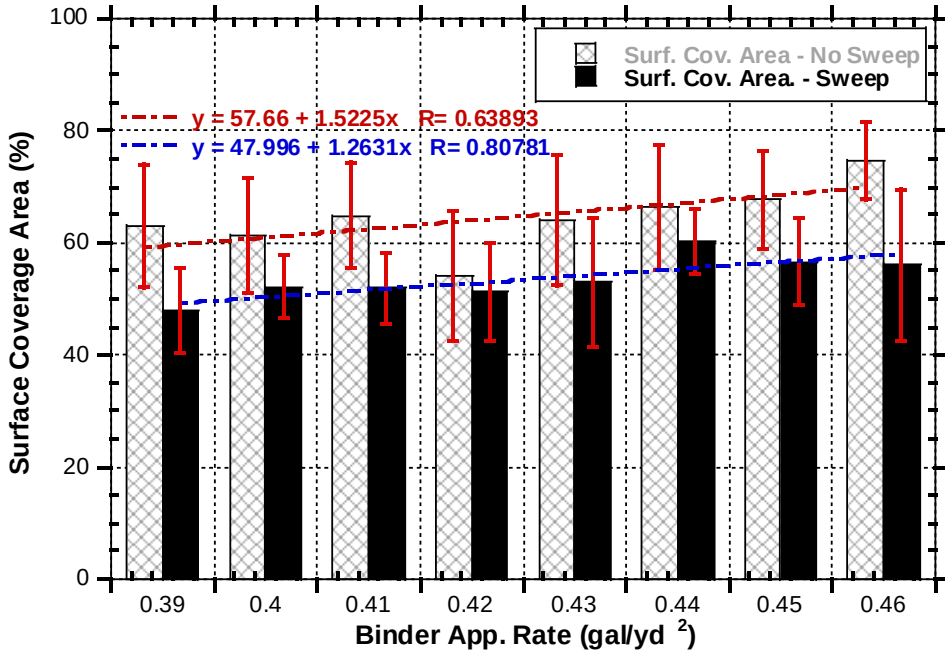

Figure 6.10: Surface coverage area for different binder application rates

CHAPTER 7

SUMMARY AND CONCLUSIONS

This research produced a novel methodology to directly measure percent embedment depth of chip seals using an image analysis procedure. The procedure involves extracting cores from the field, then obtaining vertical slices using a tile saw. Then, digital images of the vertical cut cross sections are captured and analyzed using an image analysis algorithm developed as part of this study. Major conclusions of this study can be summarized as follows:

- Procedure for chip seal sample acquisition by both taking cores from the field and fabricating in the laboratory seemed to be suitable for image processing techniques. However, since some of the aggregates shattered into multiple pieces under applied cyclic load during compaction in the laboratory, some modifications needs to be made in loading procedure of MTS machine to better simulate compacting.
- Among the image analysis algorithms, method 1 (peak & valley method) was found to be applicable for finding percent embedment depth of chip seal samples provided that appropriate peak and valley values are selected. The embedment depths obtained from the peak & valley method and sand patch method were close to each other because of the fact that both methods assumed that the existing pavement surface is perfectly straight, and there is no binder leakage and aggregate embedment into the substrate. However, more field samples should be collected and analyzed with both image-based algorithms and sand patch test method to obtain a better correlation. Method 2 (area method) for calculating embedment depth was found to be unsuitable for the chip seal analysis. Algorithm for calculating surface

coverage area seemed promising. It was able to detect binder coverage area as long as distinctly colored surface was sustained on the chip seal surface. In addition to these three algorithms, a new algorithm for estimating embedment depth is being developed. This new algorithm (method 3) is aimed at finding the percent embedment of each aggregate separately, then uses statistical analyses to present the distribution of percent embedment. Since embedment depth for each aggregate is considered and some of these aggregates are fully embedded into the binder, average embedment depth of these aggregates is higher than the average percent embedment depth obtained from method 1 (peak and valley method). One of the improvements for the method 3 is to improve the variability of chip seal samples. Variability of the embedment depth obtained from method 3 (each aggregate) is less than the embedment depth obtained from method 1 (peak/valley) for all field chip seal samples.

- The results of analyses for the chip seal samples taken from the field indicated that the method 1 (peak/valley) and method 3 (each aggregate) has same trends although they do not have similar results especially for the same type of chip seal samples (M-20 and M-33 chip seal sections). Therefore, the algorithms indicated consistency among them even if they were not supported with laboratory test methods indicating directly embedment depth due to being not available. In addition to image-based analyses, the results from sand patch test and Ames laser texture indicated that their trends are also similar. It is reasonable result since they both have same assumptions regarding the existing pavement surface condition.
- The results of analyses for the laboratory group-1 chip seal samples revealed that aggregate application rate limits of MDOT chip seal specification did not affect the percent embedment; whereas, the binder application rates of 0.39 gal/yd^2 and 0.46 gal/yd^2 played a significant role on embedment depth obtained from the image-based algorithm. For the

group-2 samples, it was observed that sweep test according to ASTM D7000 is not able to simulate the traffic effect on the chip seal surface. This was because the ASTM D7000 is designed to measure adhesion of the chip seal to the binder just after the construction, as stated in ASTM D7000. In addition to aggregate mass loss, although embedment depth and coverage surface area in percentage decreased after sweep test performed, the decay for all samples were relatively small to make a firm conclusion. Therefore, a new performance test simulating traffic effect on chip seal surfaces is required to assess embedment depth and surface coverage area concept with the performance.

- For further work, the chip seal samples indicating poor and good performance will be taken from the field and will be analyzed through image based algorithms to observe embedment depth variation under different distress types. In addition to field sample acquisition, chip seal samples will be fabricated with different types of aggregate in terms of size and shape in the laboratory so that the effect of aggregate properties can be observed on the embedment depth. The effect of binder application rates and different types of binder will also be investigated the relationship between performance of chip seals and embedment depth. Lastly, the aggregate embedment depth distribution obtained from method 3 (each aggregate embedment depth) over the sample can be studied and then statistical analyses to present the distribution of percent embedment can be used to investigate performance of the chip seal.

APPENDIX

Table A.1: Embedment depth and surface coverage area for cross sections of field samples of M-57 near Pompei Chip Seal Section

Sample ID	- file name	Average % Embedment Depth (Peak and Valley)	Average % Coverage	Average % Embedment Depth (Each Aggregate)
040215-8	1A	38.06	44.6	80.86
	1B	51.98	47.37	77.92
	2A	42.81	49.87	85.97
	2B	39.96	56.75	82.73
	3A	49.69	52.61	83.52
	3B	55.63	61.17	78.78
	4A	49.11	50.73	75.67
	Avg.	**46.75**	**51.87**	**80.78**
	Std Dev.	**6.55**	**5.62**	**3.57**
040215-10	1A	51.49	48.41	76.31
	1B	54.91	65.31	88.5
	2A	58.7	59.02	84.54
	2B	48.67	54.48	86.79
	3A	55.91	56.23	84.13
	3B	56.11	48.56	83.22
	4A	53.41	52.64	75.9
	4B	64.99	55.13	85.19
	5A	65.1	57.67	88.26
	5B	58.27	45.03	82.06
	Avg.	**57.49**	**52.82**	**83.65**
	Std Dev.	**5.97**	**4.51**	**4.01**
040215-11	1A	44.8	55.76	71.62
	1B	44.33	43.94	72.51
	2A	56.15	52.66	84.37
	2B	49.98	50.88	78.7
	3A	51.15	55.8	78.44
	3B	42.54	47.95	77.4
	4A	45.95	40.78	77.04
	4B	38.46	42.35	80.63
	5A	48.52	53.85	78.08
	5B	56.45	46.21	76.87
	Avg.	**47.58**	**48.26**	**78.17**
	Std Dev.	**5.91**	**5.63**	**1.29**

Table A.1 (cont'd)

Sample ID	- file name	Average % Embedment Depth (Peak and Valley)	Average % Coverage	Average % Embedment Depth (Each Aggregate)
040215-7	1A	53.44	55.36	86.04
	1B	24.38	51.93	82.07
	2A	40.56	47.96	80.57
	2B	38.62	38.3	70.68
	3A	55.83	56.41	86.57
	3B	57.5	45.42	82.12
	4A	63.81	60.15	84.34
	Avg.	**53.94**	**50.07**	**81.77**
	Std Dev.	**10.78**	**10.03**	**5.36**
040215-9	1A	57.6	53.92	88.56
	1B	63.94	47.47	76.54
	2A	56.88	56.04	87.29
	2B	45.33	49.73	85.27
	3A	64.48	59.35	84.16
	3B	73.7	52.46	86.19
	4A	60.67	43.69	81.26
	4B	57.87	56.62	89.71
	Avg.	**60.06**	**52.41**	**84.87**
	Std Dev.	**8.10**	**5.20**	**4.27**

Table B.1: Embedment depth and surface coverage area for cross sections of field samples of M-20 Chip Seal Section

Sample ID	Slice ID	Average % Embedment Depth (Peak and Valley)	Average % Coverage	Average % Embedment Depth (Each Aggregate)
M20 - CORE 1	1A	73.05	72.63	80.64
	1B	62.08	59.83	73.65
	2A	68.04	58.81	81.66
	2B	67.71	67.66	83.03
	3A	55.06	58.85	77.97
	3B	61.39	54.99	75.83
	4A	67.06	62.72	78.43
	4B	55.80	61.24	73.03
	Avg.	**63.77**	**62.09**	**78.03**
	Std Dev.	**6.31**	**5.61**	**3.67**
M20 - CORE 2	1A	71.70	77.61	86.39
	1B	71.65	69.03	81.93
	2A	70.85	64.00	77.55
	2B	68.25	66.57	82.79
	3A	76.73	57.45	75.67
	3B	71.21	62.28	82.16
	4A	69.67	49.44	71.17
	4B	78.45	63.35	81.86
	5A	63.34	60.31	79.03
	5B	72.30	58.90	76.87
	Avg.	**71.42**	**62.89**	**79.54**
	Std Dev.	**4.18**	**7.47**	**4.37**
M20 - CORE 3	1A	67.66	69.16	85.74
	1B	51.96	52.00	72.27
	2A	51.95	57.09	76.23
	2B	64.53	57.56	79.14
	3A	61.88	56.14	83.06
	3B	59.71	52.57	65.43
	4A	57.72	64.39	86.23
	4B	54.03	63.40	79.76
	Avg.	**58.68**	**59.04**	**78.48**
	Std Dev.	**5.85**	**6.05**	**7.07**

Table B.1 (cont'd)

Sample ID	Slice ID	Average % Embedment Depth (Peak and Valley)	Average % Coverage	Average % Embedment Depth (Each Aggregate)
M20 - CORE 4	1A	71.04	64.33	77.72
	1B	76.61	63.32	84.00
	2A	59.87	62.88	81.44
	2B	64.50	59.84	77.73
	3A	54.73	59.01	72.83
	3B	67.10	57.31	79.74
	4A	68.17	62.43	77.99
	4B	74.75	59.67	79.30
	Avg.	**67.10**	**61.10**	**78.84**
	Std Dev.	**7.35**	**2.47**	**3.25**
M20 - CORE 5	1A	75.60	67.50	77.00
	1B	60.38	57.73	79.72
	2A	64.73	61.31	84.89
	2B	66.84	68.52	82.32
	3A	56.19	62.17	84.11
	3B	64.90	69.22	84.08
	4A	77.35	76.32	87.92
	4B	74.24	73.42	84.68
	Avg.	**67.53**	**67.02**	**83.09**
	Std Dev.	**7.57**	**6.29**	**3.38**
M20 - CORE 6	1A	39.98	52.47	75.56
	1B	46.19	59.20	78.57
	2A	59.89	57.48	72.67
	2B	59.72	53.70	79.12
	3A	57.05	47.06	70.27
	3B	51.96	54.03	74.24
	4A	56.88	54.95	77.36
	4B	56.50	56.27	72.43
	Avg.	**53.52**	**54.39**	**75.03**
	Std Dev.	**7.08**	**3.67**	**3.18**

Table B.1 (cont'd)

Sample ID	Slice ID	Average % Embedment Depth (Peak and Valley)	Average % Coverage	Average % Embedment Depth (Each Aggregate)
M20 - CORE 7	1A	70.62	62.11	79.85
	1B	61.25	66.40	79.89
	2A	50.65	57.80	79.42
	2B	68.29	59.72	80.99
	3A	57.32	56.26	80.91
	3B	64.53	57.03	76.71
	4A	63.12	58.48	73.17
	4B	57.10	67.84	76.11
	Avg.	**61.61**	**60.71**	**78.38**
	Std Dev.	**6.50**	**4.36**	**2.77**
M20 - CORE 8	1A	60.40	47.41	71.48
	1B	65.28	51.27	71.34
	2A	70.11	56.99	80.26
	2B	64.31	55.30	69.65
	3A	62.72	53.34	76.84
	3B	59.62	64.26	73.71
	4A	53.57	50.87	74.92
	4B	52.93	61.56	74.77
	Avg.	**61.12**	**55.13**	**74.12**
	Std Dev.	**5.83**	**5.66**	**3.40**

Table C.1: Embedment depth and surface coverage area for cross sections of field samples of M-33 from Alger to Rose City

Sample ID	Slice ID	Average % Embedment Depth (Peak and Valley)	Average % Coverage	Average % Embedment Depth (Each Aggregate)
M33 - CORE 1	1A	66.51	60.01	78.24
	1B	69.77	56.40	78.88
	2A	74.55	60.92	75.05
	2B	63.84	67.62	80.81
	3A	74.72	68.83	80.11
	3B	70.19	59.38	75.20
	4A	63.05	61.16	78.40
	4B	67.40	52.00	76.57
	Avg.	**68.75**	**60.79**	**77.91**
	Std Dev.	**4.41**	**5.48**	**2.13**
M33 - CORE 2	1A	71.54	59.69	71.61
	1B	68.77	69.08	86.73
	2A	74.17	60.79	85.00
	2B	69.21	63.11	83.30
	3A	76.32	59.38	82.89
	3B	66.15	59.93	79.67
	4A	71.09	55.93	83.23
	4B	73.10	64.61	82.63
	Avg.	**71.29**	**61.57**	**81.88**
	Std Dev.	**3.25**	**3.99**	**4.61**
M33 - CORE 3	1A	65.80	57.68	74.14
	1B	75.42	63.86	82.77
	2A	75.31	67.29	84.99
	2B	69.98	55.39	77.56
	3A	62.84	56.26	76.48
	3B	70.94	62.43	79.99
	4A	69.75	58.77	79.05
	4B	74.02	60.44	78.78
	Avg.	**70.51**	**60.27**	**79.22**
	Std Dev.	**4.50**	**4.07**	**3.44**

Table C.1 (cont'd)

Sample ID	Slice ID	Average % Embedment Depth (Peak and Valley)	Average % Coverage	Average % Embedment Depth (Each Aggregate)
M33 - CORE 4	1A	78.77	65.53	82.07
	1B	75.92	66.84	81.03
	2A	74.57	68.62	86.55
	2B	76.06	63.3	86.72
	3A	73.64	62.32	80.32
	3B	76.42	69.52	82.99
	4A	71.47	64.91	79.22
	Avg.	**75.26**	**65.86**	**82.70**
	Std Dev.	**2.32**	**2.65**	**2.94**
M33 - CORE 5	1A	75.27	56.69	76.57
	1B	83.41	63.16	83.72
	2A	77.55	63.33	81.01
	2B	74.6	60.37	81.22
	3A	76.52	63.72	83.26
	3B	78.95	60.8	84.89
	4A	76.29	60.65	85.28
	4B	75.86	59.74	79.92
	Avg.	**77.31**	**61.06**	**81.98**
	Std Dev.	**2.81**	**2.34**	**2.90**
M33 - CORE 6	1A	74.95	63.25	81.88
	1B	69.22	63.59	81.46
	2A	73.53	65.13	83.28
	2B	78.17	65.85	81.56
	3A	69.76	62.55	83.55
	3B	72.56	62.54	82.88
	4A	74.23	73.07	82.39
	4B	69.11	64.83	82.41
	Avg.	**72.69**	**65.10**	**82.43**
	Std Dev.	**3.20**	**3.44**	**0.83**

Table C.1 (cont'd)

Sample ID	Slice ID	Average % Embedment Depth (Peak and Valley)	Average % Coverage	Average % Embedment Depth (Each Aggregate)
M33 - CORE 7	1A	54.66	61.71	80.8
	1B	62.71	53.24	71.8
	2A	55.66	51.01	64.57
	2B	50.36	52.43	69.31
	3A	63.44	58.99	77.15
	3B	57.5	56.92	76.11
	4A	63.24	56.47	71.44
	4B	55.35	57.01	72.63
	Avg.	**57.87**	**55.97**	**72.98**
	Std Dev.	**4.80**	**3.56**	**5.02**
M33 - CORE 8	1A	73.22	58.28	76.21
	1B	69.58	59.13	75.94
	2A	71.96	63.1	79.04
	2B	70.66	62.5	80.2
	3A	74.43	58.64	84.59
	3B	68.63	59.82	79.89
	4A	61.4	57.08	78.09
	4B	72.86	59.08	78.599
	Avg.	**70.34**	**59.70**	**79.07**
	Std Dev.	**4.10**	**2.07**	**2.71**

Table D.1: Embedment depth and surface coverage area for cross sections of group 1 laboratory samples

Sample ID	Side ID	Average % Embedment (Peak and Valley Method)	Average % Coverage	Sample ID	Side ID	Average % Embedment (Peak and Valley Method)	Average % Coverage
LS-1	1A	63.22	64.76	**LS-5**	1A	53.60	75.74
	1B	49.79	74.66		1B	66.66	72.17
	2A	47.08	53.19		2A	52.94	68.55
	2B	50.18	69.58		2B	57.34	66.27
	3A	49.05	72.47		3A	57.12	73.36
	3B	35.03	62.20		3B	53.96	57.75
	4A	46.56	60.31		4A	59.06	66.77
	4B	48.47	55.95		4B	61.50	66.51
LS-2	1A	63.16	74.47	**LS-6**	1A	64.73	58.34
	1B	44.52	72.13		1B	56.13	62.94
	2A	49.39	56.11		2A	70.41	70.52
	2B	60.09	72.32		2B	54.71	70.01
	3A	55.60	62.60		3A	77.06	78.21
	3B	50.96	74.58		3B	68.78	77.70
	4A	46.71	62.75		4A	64.25	79.28
	4B	62.40	51.04		4B	74.08	73.44
LS-3	1A	51.60	62.73	**LS-7**	1A	67.53	67.55
	1B	49.86	52.33		1B	55.02	61.53
	2A	38.74	51.13		2A	63.23	74.00
	2B	50.63	63.43		2B	64.92	67.11
	3A	28.08	57.15		3A	76.76	67.37
	3B	55.81	71.09		3B	72.73	75.13
	4A	20.94	62.27		4A	60.47	83.48
	4B	57.42	43.10		4B	65.04	72.00
LS-4	1A	42.19	72.18	LS-8	1A	59.88	70.83
	1B	50.61	46.39		1B	59.68	75.89
	2A	77.29	76.85		2A	59.29	63.38
	2B	69.02	69.11		2B	58.86	81.00
	3A	72.17	73.53		3A	75.15	72.29
	3B	61.67	76.89		3B	68.17	57.77
	4A	64.82	79.20		4A	48.95	66.99
	4B	72.00	69.79		4B	67.82	68.49

Table D.2: Embedment depth and surface coverage area for cross sections of group 2 laboratory samples

Sample ID	Side ID	Average % Embedment (Peak and Valley Method)	Average % Coverage	Sample ID	Side ID	Average % Embedment (Peak and Valley Method)	Average % Coverage
LS-9	1A	45.07	48.59	LS-14	1A	53.27	50.24
	1B	41.67	54.58		1B	54.49	52.50
	2A	44.68	37.48		2A	50.20	40.12
	2B	48.24	57.77		2B	57.55	50.32
	3A	33.27	52.11		3A	59.63	67.68
	3B	47.47	54.72		3B	55.88	52.84
	4A	50.85	66.97		4A	60.65	62.62
	4B	57.75	62.13		4B	69.54	76.86
LS-10	1A	38.59	42.00	LS-15	1A	62.90	45.53
	1B	48.33	50.56		1B	41.00	53.44
	2A	53.36	44.84		2A	61.29	62.09
	2B	54.88	67.83		2B	61.54	72.11
	3A	62.61	61.57		3A	52.91	69.71
	3B	70.34	60.22		3B	58.72	60.25
	4A	56.74	56.01		4A	60.73	45.25
	4B	59.40	50.44		4B	51.80	64.89
LS-11	1A	49.37	54.32	LS-16	1A	47.98	74.32
	1B	59.47	63.17		1B	59.77	62.66
	2A	59.24	79.30		2A	63.19	62.93
	2B	52.36	50.00		2B	64.82	63.46
	3A	45.64	53.78		3A	62.16	62.00
	3B	62.01	68.21		3B	74.55	64.55
	4A	74.94	66.77		4A	68.09	69.56
	4B	63.07	49.18		4B	59.83	50.32
LS-12	1A	49.49	43.86	LS-17	1A	67.99	68.83
	1B	57.61	42.42		1B	61.98	64.00
	2A	48.53	58.54		2A	64.57	78.68
	2B	47.18	43.23		2B	56.21	67.84
	3A	52.82	55.74		3A	73.57	80.61
	3B	67.34	57.03		3B	66.91	68.42
	4A	54.44	42.77		4A	78.09	79.91
	4B	55.23	43.10		4B	77.43	75.98

Table D.2 (cont'd)

LS-18	1A	61.54	69.57	**LS-22**	1A	67.50	76.07
	1B	39.24	74.94		1B	62.86	79.75
	2A	55.70	75.40		2A	73.98	72.26
	2B	53.67	70.17		2B	71.91	71.74
	3A	67.09	66.10		3A	73.78	66.59
	3B	53.73	70.60		3B	64.67	74.42
	4A	59.51	73.28		4A	73.41	65.76
	4B	58.35	73.61		4B	65.66	64.10
LS-19	1A	37.47	64.29	**LS-23**	1A	68.53	64.06
	1B	61.29	76.18		1B	68.19	66.98
	2A	59.34	78.44		2A	73.65	81.56
	2B	60.61	66.78		2B	74.05	80.69
	3A	60.45	62.96		3A	61.33	67.12
	3B	43.49	68.52		3B	79.75	77.74
	4A	68.05	66.04		4A	65.77	76.11
	4B	69.73	65.00		4B	77.91	74.00
LS-20	1A	49.72	65.10	**LS-24**	1A	68.47	69.84
	1B	65.62	61.40		1B	63.03	60.54
	2A	70.13	68.45		2A	65.10	65.26
	2B	44.95	64.36		2B	71.77	79.24
	3A	62.61	77.85		3A	60.08	72.00
	3B	62.76	75.26		3B	76.96	81.09
	4A	62.18	66.54		4A	38.75	62.56
	4B	65.31	74.76		4B	61.82	84.10
LS-21	1A	63.52	61.67	**LS-25**	1A	72.12	80.89
	1B	62.81	56.76		1B	70.23	84.60
	2A	70.73	57.37		2A	74.10	69.53
	2B	70.06	75.91		2B	66.65	73.81
	3A	55.96	65.03		3A	74.73	75.73
	3B	51.60	56.59		3B	77.37	81.25
	4A	51.60	71.29		4A	62.40	81.16
	4B	46.99	33.89		4B	65.55	63.20

Table D.2 (cont'd)

LS-26	1A	52.80	47.33	**LS-30**	1A	65.53	75.77
	1B	39.72	46.57		1B	49.52	57.30
	2A	54.84	59.62		2A	67.36	71.59
	2B	54.09	49.09		2B	44.65	53.71
	3A	47.44	45.72		3A	46.98	55.56
	3B	39.45	44.70		3B	50.72	46.87
	4A	58.75	42.15		4A	62.97	65.49
	4B	40.65	57.86		4B	59.97	45.27
LS-27	1A	4.58	51.53	**LS-31**	1A	58.55	54.98
	1B	58.68	65.16		1B	46.13	61.99
	2A	61.08	50.31		2A	65.73	63.53
	2B	43.95	52.37		2B	51.47	58.65
	3A	50.69	41.62		3A	53.28	60.31
	3B	41.30	51.61		3B	57.88	51.03
	4A	51.59	50.84		4A	64.24	64.47
	4B	50.48	61.08		4B	57.12	58.76
LS-28	1A	60.61	55.04	**LS-32**	1A	62.58	55.27
	1B	56.18	45.84		1B	47.58	47.12
	2A	42.90	35.81		2A	62.54	55.86
	2B	58.55	60.56		2B	58.80	49.29
	3A	56.55	54.74		3A	59.67	56.22
	3B	4.45	49.22		3B	52.87	43.64
	4A	61.13	63.29		4A	58.16	54.77
	4B	63.54	54.41		4B	46.12	44.08
LS-29	1A	73.89	71.00	**LS-33**	1A	40.67	27.69
	1B	72.54	60.94		1B	22.78	31.17
	2A	52.32	43.10		2A	47.24	47.73
	2B	64.20	57.37		2B	49.66	62.87
	3A	55.59	48.21		3A	68.14	63.29
	3B	42.95	48.88		3B	54.19	55.23
	4A	54.54	42.30		4A	46.47	51.16
	4B	50.74	34.71		4B	57.11	62.09

Table D.2 (cont'd)

LS-34	1A	59.47	55.22	**LS-38**	1A	51.13	51.98
	1B	58.46	56.86		1B	56.59	54.45
	2A	52.10	44.63		2A	55.94	52.29
	2B	43.47	54.20		2B	35.51	42.17
	3A	56.37	43.54		3A	62.68	44.62
	3B	47.17	55..26		3B	58.16	28.51
	4A	62.40	41.17		4A	56.08	48.58
	4B	31.84	31.61		4B	60.14	53.18
LS-35	1A	58.82	49.98	**LS-39**	1A	60.55	49.12
	1B	41.12	52.17		1B	53.58	58.21
	2A	57.39	60.27		2A	58.71	65.18
	2B	61.30	49.97		2B	69.16	71.14
	3A	61.40	54.65		3A	64.38	65.38
	3B	53.85	47.03		3B	55.40	66.74
	4A	47.83	48.93		4A	64.50	57.86
	4B	51.70	47.97		4B	59.69	56.94
LS-36	1A	48.71	53.84	**LS-40**	1A	62.80	66.44
	1B	61.49	53.99		1B	58.75	59.03
	2A	62.50	54.04		2A	66.23	62.40
	2B	49.66	49.88		2B	65.06	58.73
	3A	43.35	49.03		3A	66.05	59.77
	3B	43.30	46.85		3B	61.77	60.53
	4A	56.33	52.74		4A	65.52	67.08
	4B	45.95	52.10		4B	54.87	67.14
LS-37	1A	51.28	51.90	**LS-41**	1A	74.76	81.92
	1B	51.74	49.87		1B	67.95	72.51
	2A	53.15	58.38		2A	59.81	56.84
	2B	57.79	54.58		2B	70.00	60.65
	3A	39.13	50.55		3A	59.81	47.77
	3B	51.48	42.07		3B	61.79	61.94
	4A	71.94	52.20		4A	59.73	58.01
	4B	58.55	54.61		4B	72.44	56.52

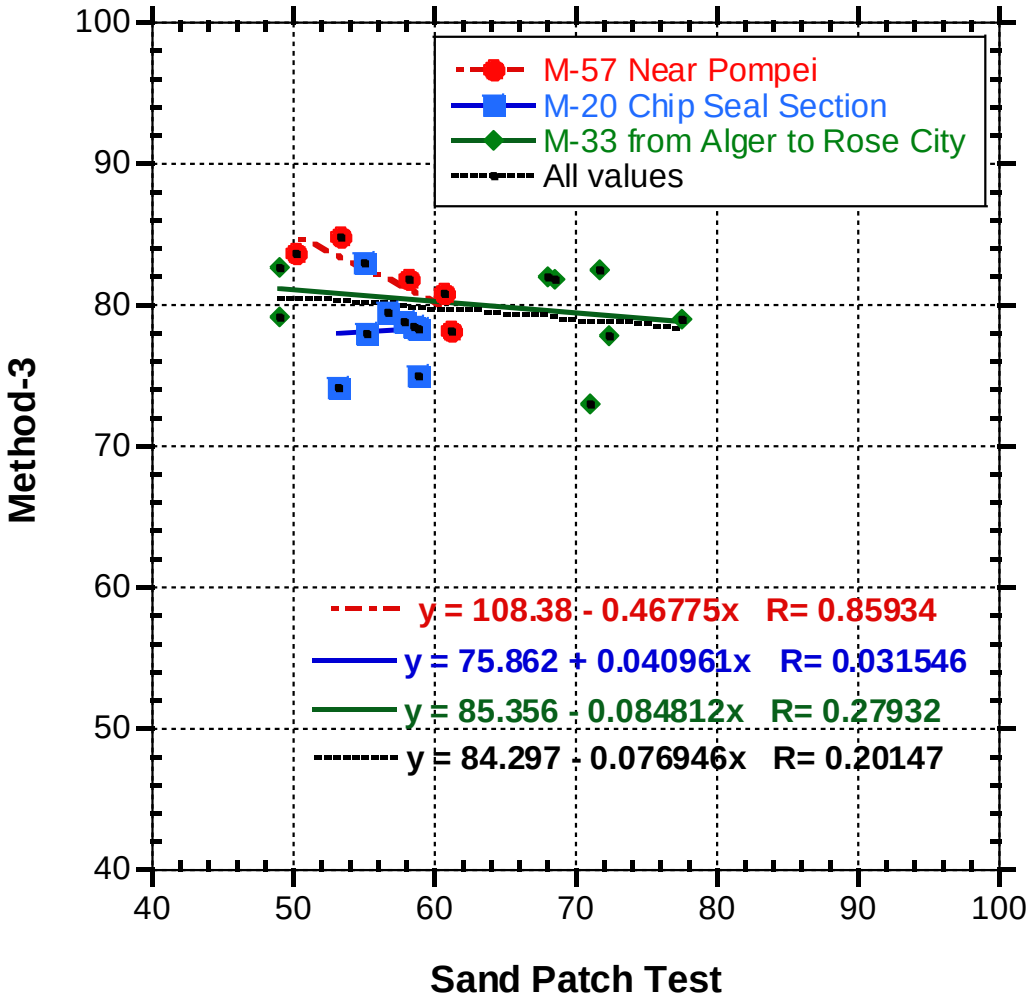

Figure 6.11: Comparison of method-3 and sand patch test

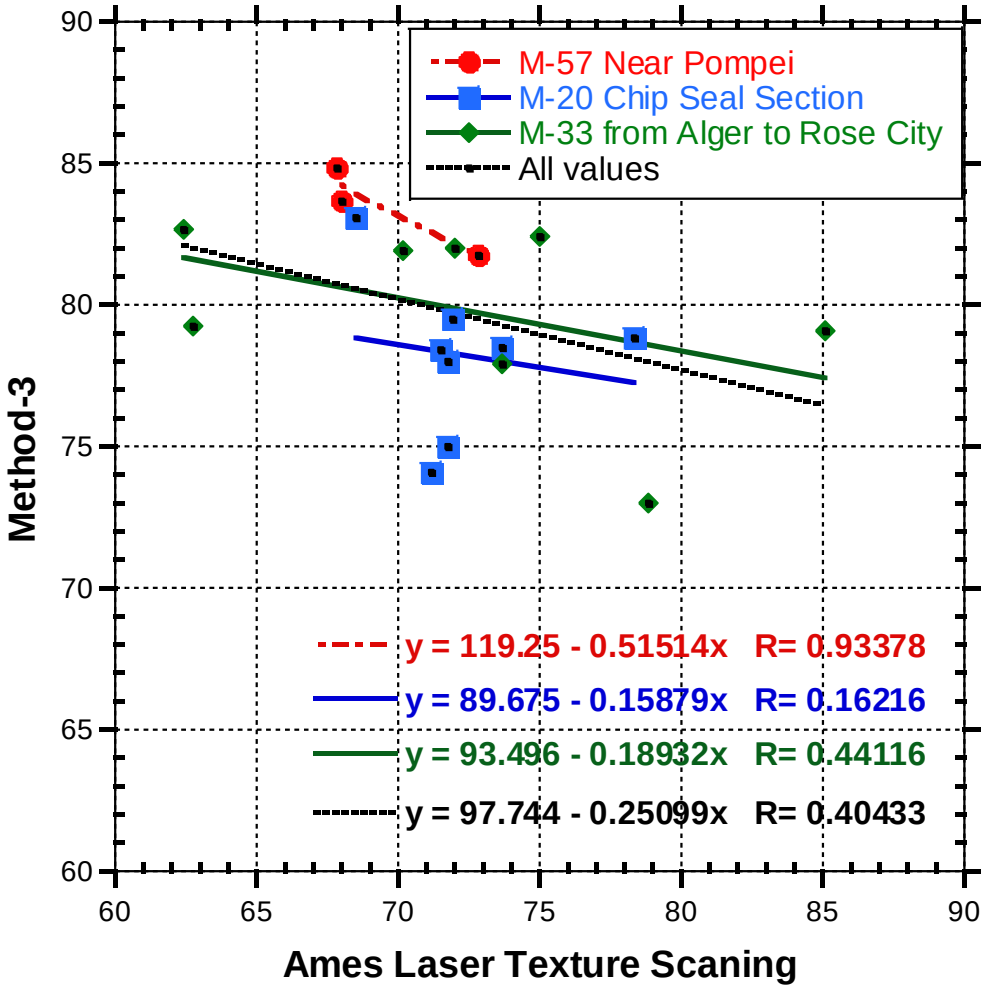

Figure 6.12: Comparison of method-3 and Ames laser texture scanning

REFERENCES

REFERENCES

AASHTO T 312-15 Preparing Hot-Mix Asphalt (HMA) Specimens by Means of the Superpave Gyratory Compactor, 2011, American Association of State Highway and Transportation Officials, Washington, D.C.

Abdul-Malak, M.U., Fowler, D.W. and Meyer, A. H. (1993) "Major Factors Explaining Performance Variability of Seal Coat Pavement Rehabilitation Overlays", *Transportation Research Record: Journal of the Transportation Research Board*, No. 1388, pp 140-149.

Ames Engineering, 2014. Ames Engineering Laser Texture Scanner User Manual Model 9300

American Society of Mechanical Engineers. (ASME) (2002) An American National Standard Surface Texture (Surface Roughness, Waviness, and Lay).

ASTM E 1845-15. (2015). Standard Practice for Calculating Pavement Macrotexture Mean Profile Depth, ASTM International, West Conshohocken, PA.

ASTM E 303-93. (2013). Standard Test Method for Measuring Surface Frictional Properties Using the British Pendulum Tester, ASTM International, West Conshohocken, PA.

ASTM D 7000. (2011). Standard Test Method for Sweep Test of Bituminous Emulsion Surface Treatment Samples, ASTM International, West Conshohocken, PA.

ASTM D 7234-12. (2012). Standard Test Method for Pull-odd Adhesion Strength of Coatings on Concrete Using Portable Pull-off Adhesion Testers, ASTM International, West Conshohocken, PA.

Bazlamit, S. M., and Reza F. (2005). "Changes in Asphalt Pavement Friction Components and Adjustment of Skid Number for Temperature", Journal of Transportation Engineering, ASCE, Vol. 131, No.6, 470-476

Benedict, C. R. (1990). Laboratory measurement of chip retention strength by the frosted marble modified ISSA cohesion tester. In Joint AEMA/ISSA Conference, Atlanta, GA.

Beer, M. D. (1996). Measurement of Tyre/Pavement Interface Stresses Under Moving Wheel Loads. International Journal of Heavy Vehicle Systems, 3(1-4), 97-115.

Bhattacharjee, S., Gould, J.S., Mallick, R.B. and Hugo, F. (2004). "Use of MMLS3 Scaled Accelerated Loading For Fatigue Characterization of Hot Mix Asphalt (HMA) In The Laboratory", 2nd International Conference on Accelerated Pavement Testing, Minneapolis, Minnesota

British Standard Institute BS 7976-2, 2002. Pendulum testers, London, UK.

BS EN 12272-1. (2002). Surface dressing. Test methods. Rate of spread and accuracy of spread of binder and chippings

Choubane, B., Holzschuher, C.R., and Gokhale, S. (2004). "Precision of Locked-Wheel Testers for Measurement of Roadway Surface Friction Characteristics", Transportation Research Record: Journal of the Transportation Research Board, No.1869, pp. 145-151

Colwill, D.M., John, M. and J. Clifford, N. (1995). "U.K Design Procedure for Surface Dressing", Transportation Research Record, 1507. Washington DC: Transportation Research Board, pp. 13–22.

Epps, J.A., Chaffin, C.W., and Hill, A.J. (1980) Research Report 214-25: "Field Evaluation of a Seal Coat Design Method", Research Report 83-2F,Texas Transportation Institute, Austin

Epps, J.A., and Gallaway, B.M. (1974) Research Report 83-1: "Synthetic Aggregate Seal Coats-Current Texas Highway Department Practices", Texas Transportation Institute, Austin

Epps, A. L., Glover, C. J., & Barcena, R. (2001). A performance-graded binder specification for surface treatments (No. FHWA/TX-02/1710-1,)

Freitas, E. F., Pereira, P. A., Antunes, M. L., & Domingos, P. (2008). Analysis of test methods for texture depth evaluation applied in Portugal. Seminário Avaliação das Características de Superfície dos pavimentos.

Gransberg, D. and James, D.M.B. (2005) Chip Seal Best Practices, NCHRP Synthesis 342, National Cooperative Highway Research Program, National Research Council, Washington, DC.

Groenendijk, J. (1998) Accelerated Testing and Surface Cracking of Asphaltic Concrete Pavements (Doctoral Dissertation). Retrieved From Delft University of Technology Institutional Repository

Hanson, F.M. (1934) Bituminuos Surface Treatment of Rural Highways, Proceedings of the New Zealand Society of Civil Engineers, pp. 189-220

Henderson, R., Herrington, P. and Patrick, J. (2006). "Finite-element Modelling of a Chip Seal Road Surfacing: A Preliminary Study", A Journal of Australian and New Zealand Research and Practice, Road & Transport Research, Vol. 15, No.3, pp. 3-18

Holmgreen, R. J., Epps. J.A., Hughes, C.H. and Gallaway, B.M. (1985) Research Report 297-1F: "Field Evaluation of The Texas Seal Coat Design Method", Texas Transportation Institute, Austin, 174p.

Howard, I. L., Hemsley Jr, M., Baumgardner, G. L., & Jordan III, W. S. (2009). Chip and scrub seal binder evaluation by frosted marble aggregate retention test. In Transportation Research Board 88th Annual Meeting (No. 09-1662).

Howard, I.L., Alvarado, A., and Floyd, W.C. (2013) Performance Oriented Guidance for Mississippi Chip Seals-Volume II, Final Report FHWA/MS-DOT-RD-13-211-Volume II, Mississippi Department of Transportation, Mississipi.

Huurman, M., Milne, T. I., ven de Ven, M.F.C and Scarpas, A. (2004) Development of a structural FEM for road surfacing seals, ICCES, Curfu, Greece

Huurman, M. (2010). "Developments in 3D surfacing seals FE modelling", International Journal of Pavement Engineering, Vol.11, No.1, pp. 1-12

Johannes, P.T., Mahmoud, E. and Bahia, H. (2011). "Sensivity of ASTM D7000 Sweep Test to Emulsion Application Rate and Aggregate Retention", Transportation Research Record: Journal of the Transportation Research Board, No. 2235, pp. 95-102, Washington D.C.

Jordan III, W.S. and Howard, I.L. (2011). "Applicability of Modified Vialit Adhesion Test for Seal Treatment Specifications", Journal of Civil Engineering and Architecture, Vol. 5, No.3 (Serial No. 40)

Kandhal, P.S. and Motter, J.B. (1991) Criteria For Accepting Precoated Aggregates for Seal Coats and Surface Treatments, Transportation Research Board, No. 1300, pp. 80-89, Washington D.C.

Kearby, J.P. (1953) Tests and Theories on Penetration Surfaces, Highway Research Board Proceedings, Vol.32, pp. 232-237

Kim, H. B., Lee, S. W., Hyun, T. J., & Lee, K. H. (2013). Measurement of Texture Depth of Pavement Using Potable Laser Profiler. Journal of the Eastern Asia Society for Transportation Studies, 10(0), 1576-1589.

Kim, Y. R and Lee, J. (2008) Research Report FHWA/NC/2006-63: "Quantifying the Benefits of Improved Rolling of Chip Seals", North Caroline Department of Transportation, Raleigh, NC

Kodippily, S. (2013). Modelling the Flushing Mechanism of Thin Flexible Surface Pavements (Doctoral Dissertation). Retrieved From The University of Auckland Libraries and Learning Services

Kumara, G. H. A. J. J., Hayano, K., & Ogiwara, K. (2012). Image analysis techniques on evaluation of particle size distribution of gravel. Int. J. Geomate, 3(1), 290-297.

Lee, S. (2003) Long-Term Performance Assessment of Asphalt Concrete Pavements Using The Third Scale Model Mobile Loading Simulator And Fiber Reinforced Asphalt Concrete (Doctoral Dissertation). Retrieved From North Carolina State University Libraries

Lee, J.S. and Kim, Y.R. (2008). "Understanding the Effects of Aggregate and Emulsion Application Rates on Performance of Asphalt Surface Treatments", Transportation

Research Record: Journal of the Transportation Research Board, No. 2044, pp. 71-78, Washington D.C.

Lu, Q., and Steven, B. (2006). Technical Memorandum UCPRC-TM-2006-10: "Friction Testing of Pavement Preservation Treatments: Literature Review", California Department of Transportation

McLeod, N.W., Chaffin, C.W., Holberg, A.E., Parker, C.F., Obrcian, V., Edwards, J.M., Campen and Kari, W.J. (1969) "A General Method of Design for Seal Coats and Surface", Journal of the Association of Asphalt Paving Technologists, Vol. 38, pp.537-628

Michigan Department of Transportation (2012). "2012 Standard Specifications for Construction"

New Zealand Roading Division, (1968) Manual of Sealing and Paving Practice. National Roads Board, New Zealand.

Queensland Department of Transport and Main Roads (2012). Materials Testing Manual, The State of Queensland, Department of Transport and Main Roads.

Roberts, C. and Nicholls J.C. (2008) Design Guide for Road Surface Dressing, Road Note RN39 Sixth Edition, Transport Research Laboratory

Roque, R., Anderson, D. and Thompson, M. (1991). "Effect of Material, Design, and Construction Variables on Seal Coat Performance", Transportation Research Record: Journal of the Transportation Research Board, No. 1300, pp. 108-115, Washington D.C.

Senadheera, S., Tock, R.Wm., Hossain, S., Yazgan, B. and Das, S. (2006) Research Report FHWA/TX-06/0-4362-1: "A Testing and Evaluation Protocol to Assess Seal Coat Binder-Aggregate Compatibility", Texas Department of Transportation, Austin

Schuler, S., Lord, A., Epps, A., and Hoyt, D. (2011) Manual for Emulsion-Based Chip Seals for Pavement Preservation, NCHRP Report 680, National Cooperative Highway Research Program, National Research Council, Washington DC.

Sprayed Seal Design Project Group (2001) Austroads Provisional Sprayed Seal Design Method Revision 2000, Austroads Project No. N.T.&E.9902, Austroads Incorporated Level 9

The South African National Roads Agency, (2007). Technical Recommendations for Highways. Technical Recommendations of Highways, Pretoria, South Africa.

Wasiuddin, N.M., Marshall, A., Saltibus, N.E., Saber, A., Abadie, C. and Mohammad, L.N. (2013) "Use of Sweep Test for Emulsion and Hot Asphalt Chip Seals: Laboratory and Field Evaluation", Journal of Testing and Evaluation, Vol. 41, No. 2, pp. 1-10

Wielinski, J.C., Brandenburg, J. and Wissel, H. (2011) The Monroe Michigan Chip Seal Case Study: An Evaluation of Multiple Chip Seals' Cold Weather Field Performance. Transportation Research Board 90th Annual Meeting, CD-ROM.

Wood, J., Thomas, Janisch, D.W., and Gaillard, F.S. (2006) Final Report: “Minnessota Seal Coat Handbook 2006”, Minnesota Department of Transportation, December 1998, Revised 2007

Zhou, F., Li, H., Chen, P. and Scullion T. (2014) Research Report FHWA/TX-14/0-6674-1: ”Laboratory Evaluation of Asphalt Binder Rutting, Fracture, and Adhesion tests”, Texas Department of Transportation, Austin